

International Ocean Discovery Program Expedition 397 Preliminary Report

Iberian Margin Paleoclimate

11 October-11 December 2022

David A. Hodell, Fatima F. Guedes Abrantes, Carlos A. Alvarez Zarikian, and the Expedition 397 Scientists

Publisher's notes

Core samples and the wider set of data from the science program covered in this report are under moratorium and accessible only to Science Party members until 11 June 2024.

This publication was prepared by the *JOIDES Resolution* Science Operator (JRSO) at Texas A&M University (TAMU) as an account of work performed under the International Ocean Discovery Program (IODP). This material is based upon work supported by the JRSO, which is a major facility funded by the National Science Foundation Cooperative Agreement Number OCE1326927. Funding for IODP is provided by the following international partners:

National Science Foundation (NSF), United States
Ministry of Education, Culture, Sports, Science and Technology (MEXT), Japan
European Consortium for Ocean Research Drilling (ECORD)
Ministry of Science and Technology (MOST), People's Republic of China
Australia-New Zealand IODP Consortium (ANZIC)
Ministry of Earth Sciences (MoES), India

Portions of this work may have been published in whole or in part in other IODP documents or publications.

Disclaimer

The JRSO is supported by the NSF. Any opinions, findings, and conclusions or recommendations expressed in this material do not necessarily reflect the views of the NSF, the participating agencies, TAMU, or Texas A&M Research Foundation.

Copyright

Except where otherwise noted, this work is licensed under the Creative Commons Attribution 4.0 International (CC BY 4.0) license (https://creativecommons.org/licenses/by/4.0/). Unrestricted use, distribution, and reproduction are permitted, provided the original author and source are credited.



Citation

Hodell, D.A., Abrantes, F., Alvarez Zarikian, C.A., and the Expedition 397 Scientists, 2023. Expedition 397 Preliminary Report: Iberian Margin Paleoclimate. International Ocean Discovery Program. https://doi.org/10.14379/iodp.pr.397.2023

ISSN

World Wide Web: 2372-9562

Expedition 397 participants

Expedition 397 scientists

David A. Hodell

Co-Chief Scientist

Department of Earth Sciences University of Cambridge

United Kingdom

dah73@cam.ac.uk

Fatima F. Guedes Abrantes

Co-Chief Scientist

Marine Geology and Georesources Division

Portuguese Institute of the Sea and Atmosphere (IPMA)

Portugal

fatima.abrantes@ipma.pt

Second affiliation:

Centre of Marine Sciences (CCMAR)

University of Algarve

Portugal

Carlos A. Alvarez Zarikian

Expedition Project Manager/Staff Scientist

International Ocean Discovery Program

Texas A&M University

USA

zarikian@iodp.tamu.edu

Hannah L. Brooks

Sedimentologist

Energy and Mineral Resources Group

RWTH Aachen University

Germany

hannah.brooks@emr.rwth-aachen.de

William B. Clark

Micropaleontologist (nannofossils)

Department of Geology

University of Alabama

USA

wclark15@crimson.ua.edu

Louise F.B. Dauchy-Tric

Paleomagnetist

Institut de Physique du Globe de Paris

Université Paris Cité

France

dauchy@ipgp.fr

Viviane dos Santos Rocha

Sedimentologist

Department of Earth, Atmosphere, and Environment

Northern Illinois University

USA

Z1932945@students.niu.edu

José-Abel Flores Villarejo

Micropaleontologist (nannofossils)

Department of Geology

University of Salamanca

Spain

flores@usal.es

Timothy D. Herbert

Physical Properties Specialist/Stratigraphic Correlator

Department of Geological Sciences

Brown University

USA

Timothy_Herbert@brown.edu

Sophia K.V. Hines

Inorganic Geochemist

Department of Marine Chemistry and Geochemistry

Woods Hole Oceanographic Institution

USA

shines@whoi.edu

Huai-Hsuan May Huang

Physical Properties Specialist/Stratigraphic Correlator

National Museum of Natural History

Smithsonian Institution

USA

huanghuaihsuan@gmail.com

Hisashi Ikeda

Sedimentologist

Geosphere Sciences

Yamaguchi University

Japan

Hisashi.0906@outlook.jp

Stefanie Kaboth-Bahr

Physical Properties Specialist/Stratigraphic Correlator

Institute for Geosciences

University of Potsdam

Germany

kabothbahr@uni-potsdam.de

Junichiro Kuroda

Physical Properties Specialist

Department of Ocean Floor GeoScience

University of Tokyo

Japan

kuroda@aori.u-tokyo.ac.jp

Jasmin M. Link

Sedimentologist

Institute of Environmental Physics

University of Heidelberg

Germany

jasmin.link@iup.uni-heidelberg.de

Jerry F. McManus

Sedimentologist

Lamont-Doherty Earth Observatory

Columbia University

USA

jmcmanus@ldeo.columbia.edu

Bryce A. Mitsunaga

Organic Geochemist

Earth, Environmental, and Planetary Sciences

Brown University

USA

bryce_mitsunaga@brown.edu

Lucien Nana Yobo Inorganic Geochemist

Department of Geology and Geophysics

Texas A&M University

USA

Lnanayobo@tamu.edu

Celeste T. Pallone Sedimentologist

Department of Earth and Environmental Sciences

Columbia University

USA

cpallone@columbia.edu

Xiaolei Pang

Sedimentologist

Centre for Ocean Research

Peking University

China

xiaolei.pang@pku.edu.cn

Marion Y. Peral

Micropaleontologist (planktonic foraminifera)

Environnements et Paléoenvironnements Océaniques et

Continentaux EPOC -UMR

Université de Bordeaux

France

marion.peral@vub.be

Observer

Emília Salgueiro

Observer/Sedimentologist

Marine Geology and Georesources Division

Portuguese Institute of the Sea and Atmosphere (IPMA)

Portugal

Second affiliation:

Centre of Marine Sciences (CCMAR)

University of Algarve

Portugal

emilia.salgueiro@ipma.pt

Outreach

Amy Mayer

Onboard Outreach Officer

USA

amyhmayer@gmail.com

Maya Pincus

Onshore Outreach Officer

Lamont-Doherty Earth Observatory

Columbia University

USA

maya.pincus@gmail.com

Saray Sanchez

Physical Properties Specialist

College of Earth, Ocean, and Atmospheric Sciences

Oregon State University

USA

sanchsar@oregonstate.edu

Komal Verma

Micropaleontologist (planktonic foraminifera)

Department of Geology

Banaras Hindu University

India

komal.geo@bhu.ac.in

Jiawang Wu

Inorganic Geochemist

School of Marine Sciences

Sun Yat-Sen University

China

jwwu@tongji.edu.cn

Chuang Xuan

Paleomagnetist

School of Ocean and Earth Science

University of Southampton

United Kingdom

c.xuan@soton.ac.uk

Jimin Yu

Sedimentologist

Research School of Earth Sciences

Australian National University

Australia

jimin.yu@anu.edu.au

Operational and technical staff

Siem Offshore AS officials

Jacob C. Robinson

Master of the Drilling Vessel

Mark RobinsonDrilling Supervisor

JRSO shipboard personnel and technical representatives

Alejandro Avila Santis

Marine Laboratory Specialist

Timothy Blaisdell

Applications Developer

William Cary

Applications Developer

Lisa Crowder

Laboratory Officer

Enrico De Pano

Marine Computer Specialist

Fabricio Ferreira

Marine Laboratory Specialist

Clayton Furman

Schlumberger Engineer

Randy Gjesvold

Marine Instrumentation Specialist

Kevin Grigar

Operations Superintendent

Sandra Herrmann

Marine Laboratory Specialist

Mark Higley

Marine Laboratory Specialist

Myriam Kars

Marine Laboratory Specialist

James Kowalski

Curatorial Specialist

Aidan Leetz

Marine Laboratory Specialist

Carel Lewis

Curatorial Specialist

Chang Liu

Marine Laboratory Specialist

Daniel Marone

Assistant Laboratory Officer

Aaron Mechler

Marine Laboratory Specialist

Beth Novak

Assistant Laboratory Officer

Jessica Riekenberg

Marine Laboratory Specialist

Daniel Rudbäck

Marine Laboratory Specialist

Alyssa Stephens

Publications Specialist

Steven Thomas

Marine Electronics Specialist

Garrick Van Rensburg

Marine Instrumentation Specialist

Abstract

During International Ocean Discovery Program Expedition 397, we recovered a total of 6176.7 m of core (104.2% recovery) at four sites (U1586, U1587, U1385, and U1588) from the Promontório dos Principes de Avis (PPA) (Figure F1), a plateau located on the Portuguese continental slope that is elevated above the Tagus Abyssal Plain and isolated from the influence of turbidites. The drill sites are arranged along a bathymetric transect (4691, 3479, 2590, and 1339 meters below sea level [mbsl], respectively) to intersect each of the major subsurface water masses of the eastern North Atlantic (Figures F2, F7). Multiple holes were drilled at each site to ensure complete spliced composite sections (Figure F3; Table T1), which will be further refined postcruise by a campaign of X-ray fluorescence core scanning.

At Site U1586 (4691 mbsl), the deepest and farthest from shore, a 350 m sequence was recovered in four holes that extend as far back as the middle Miocene (14 Ma), which is nearly twice as old as initially predicted from seismic stratigraphy. Sedimentation rates are lower (averaging 5 cm/ky in

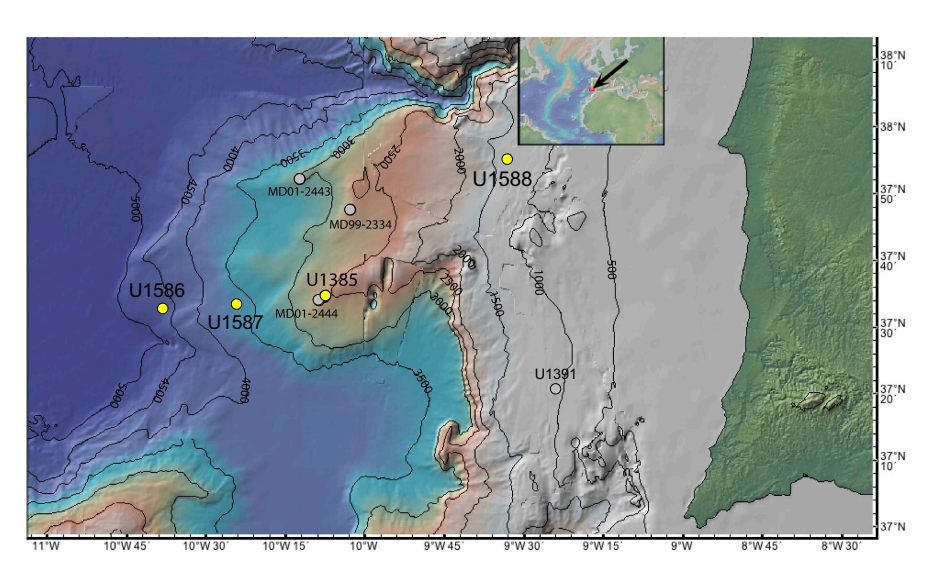


Figure F1. Bathymetry of the PPA showing the locations of the four sites (U1586, U1587, U1385, and U1588) drilled during Expedition 397, Marion Dufrense (MD) piston cores, and IODP Site U1391. Site U1385 was occupied previously during Expedition 339, as was Site U1391. The map is modified from Hodell et al. (2015) and was made with GeoMapApp (**www.geo-mapapp.org**) using the bathymetry of Zitellini et al. (2009).

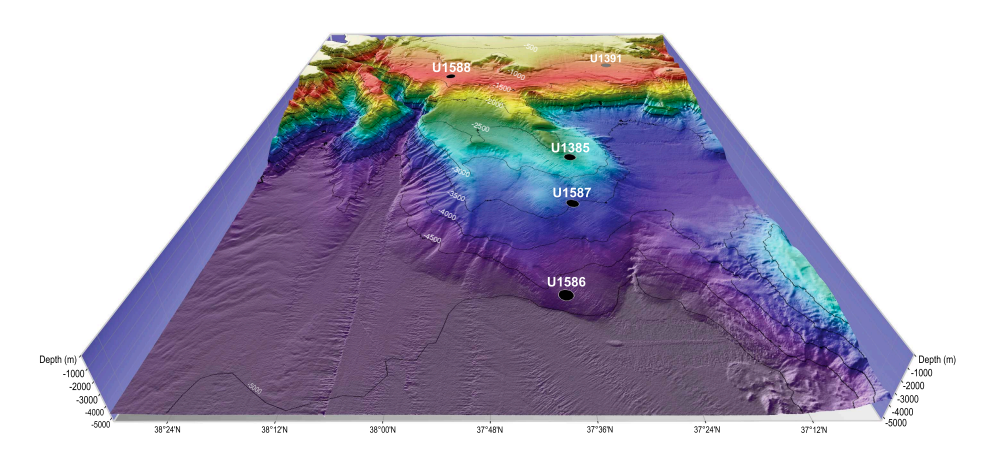


Figure F2. Depth distribution of Expedition 397 drill sites on the PPA looking onshore to the east. The sites are located on a bathymetric transect that intersects each of the major subsurface water masses of the North Atlantic. Depths range from 1339 mbsl (Site U1588) to 4691 mbsl (Site U1586). Expedition 339 Site U1391 is also shown. (Figure made by Helder Pereira using Mirone and iVew4D software.)

the Quaternary) at Site U1586 than other Expedition 397 sites (Figure F4), and a few slumped intervals were encountered in the stratigraphic sequence. Despite these limitations, Site U1586 anchors the deep end-member of the bathymetric transect and provides an important reference section to study deepwater circulation, ventilation and carbon storage in the deep eastern North Atlantic.

At Site U1587 (3479 mbsl), the second deepest site along the depth transect, we recovered a 567 m sequence of late Miocene to Holocene sediments that accumulated at rates between 6.5 and 11 cm/ky (Figure $\mathbf{F4}$). The high sedimentation rates and long continuous record at this site will permit climate reconstruction at high temporal resolution (e.g., millennial) for the past 7.8 My. A complete Messinian Stage (7.246–5.333 Ma) was recovered, which provides a valuable opportunity to study the Messinian Salinity Crisis in an open marine setting adjacent to the Mediterranean.

Site U1385 (Shackleton site) was a reoccupation of a position previously drilled during Integrated Ocean Drilling Program Expedition 339. Expedition 339 Site U1385 has yielded a remarkable record of millennial-scale climate change for the past 1.45 My (Marine Isotope Stage [MIS] 47) (Figure F6). During Expedition 397, we deepened the site from 156 to 400 meters below seafloor (mbsf), extending the basal age into the early Pliocene (4.5 Ma). Sedimentation rates remained high, averaging between 11 and 9 cm/ky throughout the sequence (Figure F4). The newly recovered cores at Expedition 397 Site U1385 will permit the study of millennial climate variability through the entire Quaternary and into the Pliocene, prior to the intensification of Northern Hemisphere glaciation.

Site U1588 is the shallowest, closest to shore, and youngest site drilled during Expedition 397 and is also the one with the highest sedimentation rate (20 cm/ky). The base of the 412.5 m sequence is 2.2 Ma, providing an expanded Pleistocene sequence of sediment deposited under the influence of the lower core of the Mediterranean Outflow Water (MOW). Together with other Expedition 339 sites, Site U1588 will be important for determining how the depth and intensity of the MOW has varied on orbital and millennial timescales. In addition, it also provides a marine reference section for studying Quaternary climate variability at very high temporal resolution (millennial to submillennial).

A highlight of the expedition is that sediment at all sites shows very strong cyclicity in bulk sediment properties (color, magnetic susceptibility, and natural gamma radiation). Particularly notable are the precession cycles of the Pliocene that can be correlated peak-for-peak among sites (Figure

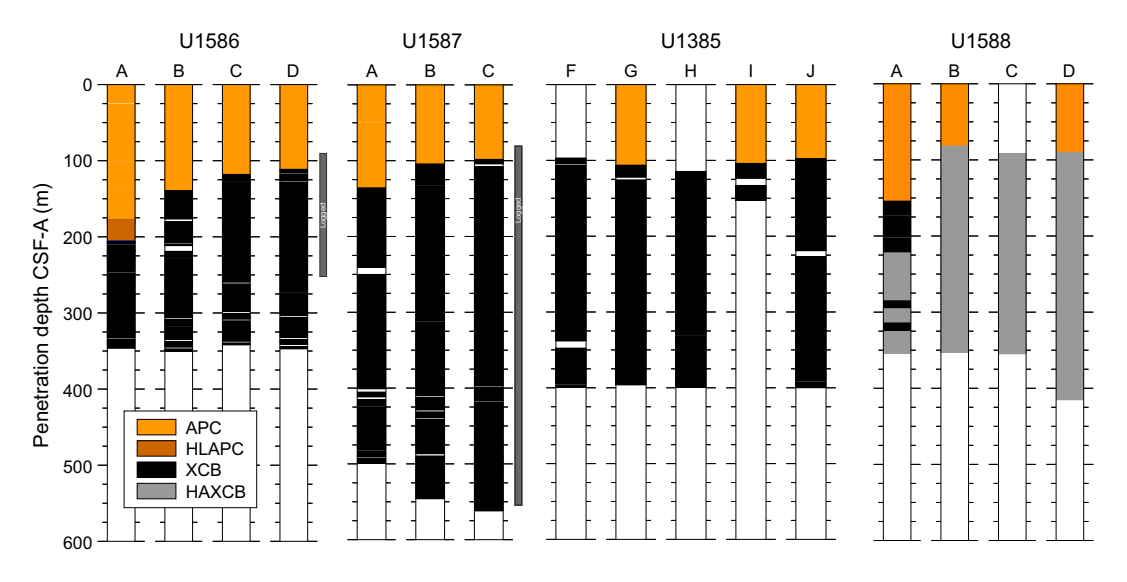


Figure F3. Core recovery for each hole drilled during Expedition 397. Holes U1385F, U1385H, and U1588C were washed down without recovery before XCB coring. HAXCB = half advance extended core barrel. Gray bar alongside Holes U1586D and U1587C = portion of the hole logged using the triple combo tool string.

F10). These cyclic variations will be used to derive an orbitally tuned timescale for Expedition 397 sites and correlate them into classic Mediterranean cyclostratigraphy.

The cores recovered during Expedition 397 will form the basis of collaborative postcruise research to produce benchmark paleoclimate records for the late Miocene through Quaternary using the widest range of proxy measurements. It will take many years to complete these analyses, but the records will lead to major advances in our understanding of millennial and orbital climate changes and their underlying causes and evolving contextuality.

Outreach during Expedition 397 was highly productive, reaching a record number of students and the general public across the world through several diverse platforms, including live ship-to-shore events, webinars, social media, videos, radio pieces, blog posts, and in-person activities.

Table T1. Hole summary, Expedition 397.

Hole	Latitude	Longitude	Water depth (m)	Total penetration (m)	Cored interval (m)	Recovered length (m)	Recovery (%)	Drilled interval (m)	Total cores (N)	APC cores (N)	HLAPC cores (N)	XCB cores (N)	XCB half-cores (N)
U1586A	37°37.3108′N	10°42.5987′W	4691.1	350.0	350.0	339.6	97.0		42	19	7	16	0
U1586B	37°37.3478′N	10°42.5506′W	4690.5	350.0	350.0	335.1	95.8		40	16	0	24	0
U1586C	37°37.2911′N	10°42.6216′W	4692.4	349.1	349.1	334.4	95.8		38	13	0	25	0
U1586D	37°37.2835′N	10°42.6289′W	4693.6	350.0	350.0	337.8	96.5		38	12	0	26	0
	Site U1586 totals:			1399.1	1399.1	1346.9	96.0		158	60	7	91	0
U1587A	37°34.8602′N	10°21.5400′W	3480.5	500.0	500.0	478.1	95.6		53	15	0	38	0
U1587B	37°34.8650′N	10°21.5314′W	3478.0	547.8	547.8	534.3	97.5		59	11	0	48	0
U1587C	37°34.8750′N	10°21.5205′W	3479.0	567.9	567.9	553.3	97.4		61	12	0	49	0
		Site U1587 totals:		1615.7	1615.7	1565.7	97.0		173	38	0	135	0
U1385F	37°33.9999′N	10°07.6587′W	2589.1	400.0	303.1	290.8	95.9	96.9	32	0	0	32	0
U1385G	37°34.0108′N	10°07.6656′W	2592.4	397.3	397.3	396.3	99.8		42	12	0	30	0
U1385H	37°34.0223′N	10°07.6641′W	2592.4	399.2	284.6	285.0	100.1	114.6	31	0	0	31	0
U1385I	37°34.0205′N	10°07.6505′W	2589.1	152.5	152.5	145.4	95.3		16	11	0	5	0
U1385J	37°34.0103′N	10°07.6513′W	2593.1	400.0	400.0	397.8	99.4		43	11	0	32	0
		Site U1385 totals:		1749.0	1537.5	1515.2	99.0	211.5	164	34		130	0
U1588A	37°57.6044′N	9°30.9961′W	1339.3	353.0	353.0	378.4	107.2		49	17	0	9	23
U1588B	37°57.6149′N	9°30.9956′W	1339.3	350.0	350.0	456.1	130.3		64	9	0	0	55
U1588C	37°57.6160′N	9°30.9814′W	1339.3	353.6	261.6	345.0	131.9	92.0	53	0	0	0	53
U1588D	37°57 60.23′N	9°30.9820′W	1338.5	412.5	412.5	569.4	138.1		76	11	0	0	65
		Site U1588 totals:		1469.1	1377.1	1748.9	127.0	92.0	242	37	0	9	196
		Expedition 397 totals:		6232.9	5929.4	6176.7	104.0	303.5	737	169	7	365	196

Hole	Date started (2022)	Start time UTC (h)	Date finished (2022)	End time UTC (h)	Time on hole (h)	Time on hole (d)
U1586A	16 Oct	1730	20 Oct	0830	87.12	3.63
U1586B	21 Oct	0900	25 Oct	1220	99.36	4.14
U1586C	25 Oct	1220	28 Oct	0345	63.36	2.64
U1586D	28 Oct	0345	1 Nov	0710	99.36	4.14
U1587A	1 Nov	1130	5 Nov	0250	87.36	3.64
U1587B	5 Nov	0250	10 Nov	1530	132.72	5.53
U1587C	10 Nov	1530	15 Nov	1000	114.48	4.77
1112055	16 Nov	0120	10 Na.	2225	02.26	2.00
U1385F		0120	19 Nov	2235	93.36	3.89
U1385G	19 Nov	2235	22 Nov	0200	51.36	2.14
U1385H	22 Nov	0200	23 Nov	2315	45.36	1.89
U1385I	26 Nov	0800	27 Nov	0215	18.24	0.76
U1385J	27 Nov	0215	30 Nov	0140	71.52	2.98
U1588A	30 Nov	0600	2 Dec	0145	43.68	1.82
U1588B	2 Dec	0145	3 Dec	2145	43.92	1.83
U1588C	3 Dec	2145	5 Dec	1550	42.00	1.75
U1588D	5 Dec	1550	8 Dec	0038	56.88	2.37

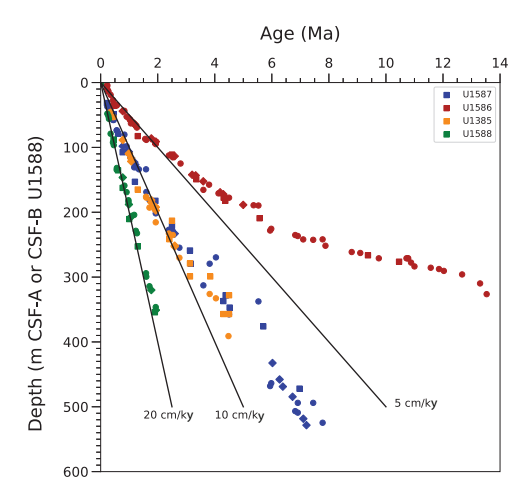


Figure F4. Age-depth points based on biostratigraphy and magnetostratigraphy for each Expedition 397 site. Sedimentation rates of 5, 10, and 20 cm/ky are shown for reference. Squares = planktonic foraminifera markers, circles = nannofossil markers, diamonds = magnetostratigraphic markers.

Plain language summary

From 11 October to 11 December 2022, International Ocean Discovery Program Expedition 397 took place off the coast of Portugal southwest of Lisbon. The main objective was to recover the exceptional sedimentary archive preserved beneath the seafloor on the Iberian margin to study past climate change at high temporal resolution. During the expedition, which carried 26 international scientists, four sites were drilled, recovering 6.2 km of marine sediments that accumulated rapidly, thereby providing a high-fidelity record of past climate change on timescales of hundreds to thousands of years and extending back millions of years ago. Climate signals from these marine sediment cores will be correlated precisely to polar ice cores from both hemispheres and with European pollen records, providing a rare opportunity to link oceanic, atmospheric, and terrestrial climate and environmental changes. The four drill sites are located at different water depths (1339, 2590, 3479 and 4691 m below sea level), permitting scientists to study how deep-ocean circulation and chemistry changed in the past, including its role in deep-sea carbon storage and atmospheric CO₂ changes. The sediment cores recovered during Expedition 397 will provide benchmark records of North Atlantic climate change at high temporal resolution from the late Miocene (about 8 million years ago) to present. This period includes the last 3 million years when changes in the Earth's orbit resulted in the growth and decay of large ice sheets in the Northern Hemisphere and a warmer world before this time when atmospheric CO₂ was similar to today. All cores recovered show strong changes in physical properties (such as color) that represent a response to known cyclic changes in Earth's orbit, which will aid in accurately dating the sediment. Many years of research will be needed to extract the detailed climatic signals from the kilometers of core recovered during Expedition 397, but the records to be produced will be vital for testing numerical climate models and understanding how the climate system works and how it might change in the future.

1. Introduction

The Iberian margin is a well-known source of rapidly accumulating sediment that contains a high-fidelity record of millennial climate variability (MCV) for the late Pleistocene. Previous studies have demonstrated that surface and deepwater climate signals from the region can be correlated precisely to the polar ice cores in both hemispheres. Shackleton et al. (2000) demonstrated that surface oxygen isotope and sea-surface temperature records mirror those of Greenland ice core records, whereas the deepwater signal follows the Antarctic ice core climate signal, thereby preserving a history of both polar ice cores in a single sedimentary archive (Figure F5). The relative timing of surface (Greenland) and deepwater (Antarctic) signals in the same core provides a means

to assess interhemispheric phasing of climate change (e.g., bipolar seesaw), which has been independently verified by methane synchronization of ice cores for the last glacial period (Blunier and Brook, 2001; WAIS Divide Project Members, 2015). Moreover, the narrow continental shelf off Portugal results in the rapid delivery of terrestrial material to the deep-sea environment, thereby permitting correlation of marine, ice core, and European terrestrial records (Margari et al., 2010, 2014; Naughton et al., 2019; Oliveira et al., 2016, 2017, 2018, 2020; Sánchez Goñi et al., 1999; Shackleton et al., 2003; Tzedakis et al., 2009, 2004).

The continuity, high sedimentation rates, and fidelity of the climate signals preserved in Iberian margin sediments make it a prime target for ocean drilling. A proof-of-concept, Site U1385 was drilled during Integrated Ocean Drilling Program Expedition 339 (Mediterranean Outflow) in late 2011 at a water depth of 2582 meters below sea level (mbsl) (Hodell et al., 2013b; Expedition 339 Scientists, 2013a). Five holes were cored using the advanced piston corer (APC) system to a maximum depth of ~155.9 meters below seafloor (mbsf). Immediately after the expedition, cores from all holes were analyzed by core scanning X-ray fluorescence (XRF) at 1 cm spatial resolution (Hodell et al., 2015). Ca/Ti data were used to accurately correlate hole-to-hole and construct a composite spliced section containing no gaps or disturbed intervals to 166.5 meters composite depth (mcd). A high-resolution oxygen isotope record confirms that Site U1385 contains a continuous record of MCV from the Holocene to 1.45 Ma (Marine Isotope Stage [MIS] 47) (Hodell et al., preprint) with sedimentation rates of $\sim 10-20$ cm/ky (Figure F6). Strong precession cycles in color and elemental XRF signals from Site U1385 were used to develop an orbitally tuned reference timescale that is independent of LR04 (Hodell et al., 2015). Although results are still emerging, Site U1385 demonstrates the great potential of the western Iberian margin to yield long, undisturbed records of millennial-scale climate change and land-sea comparisons.

Building on the success of Site U1385 and given the seminal importance of the Iberian margin for paleoclimatology and marine-ice-terrestrial correlations, International Ocean Discovery Program (IODP) Expedition 397 was designed to accomplish the following:

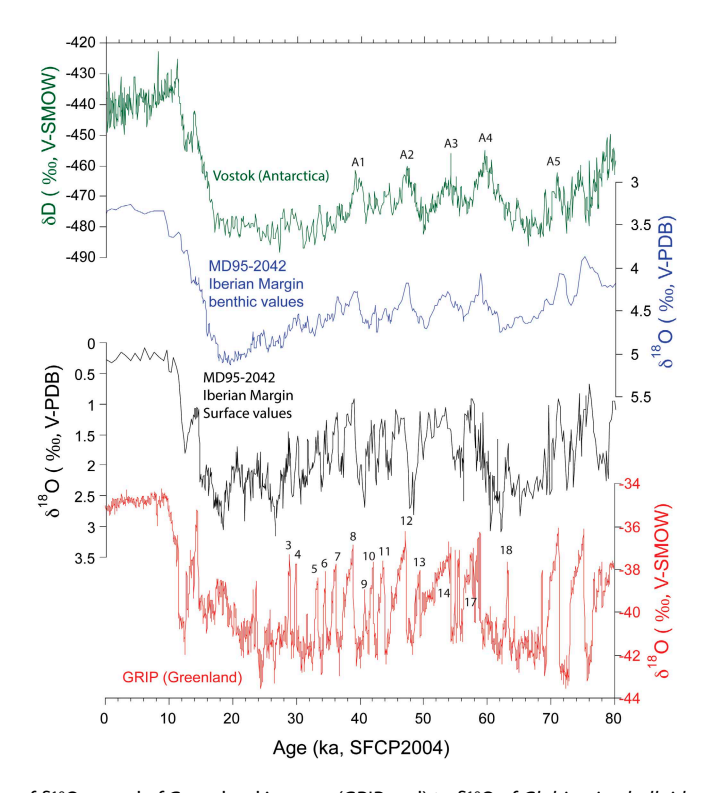


Figure F5. Correlation of δ^{18} O record of Greenland ice core (GRIP; red) to δ^{18} O of *Globigerina bulloides* (black) in Core MD95-2042 (Shackleton et al., 2000). Selected Dansgaard-Oeschger events are labeled in GRIP record and Antarctic isotope maxima (A1–A5) are labeled in Vostok. Timescale is SFCP2004 published by Shackleton et al. (2004). V-SMOW = Vienna standard mean ocean water, V-PDB = Vienna Peedee belemnite. From Hodell et al. (2013b).

- Extend the record beyond the base of Site U1385 (1.45 Ma) and recover the high-fidelity Iberian margin sedimentary archive for study of climate variability from the Quaternary through the late Miocene and
- Recover a bathymetric transect of sites from 1339 to 4691 mbsl that spans the range of the major subsurface water masses of the eastern North Atlantic (Figure F7).

The depth transect is designed to complement those sites drilled during Expedition 339 where sediment was recovered at intermediate water depths (560–1073 mbsl) under the influence of Mediterranean Outflow Water (MOW). Together, the Expedition 339 and 397 sites will constitute

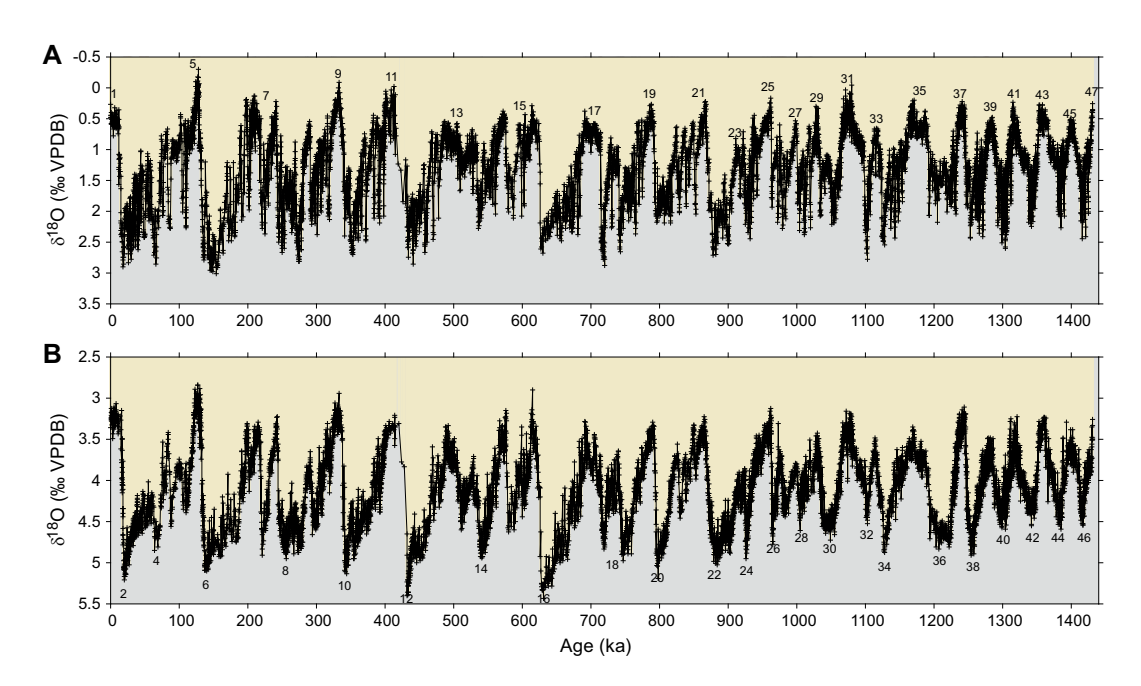


Figure F6. Oxygen isotope record of (A) *Globigerina bulloides* and (B) mixed benthic foraminifera species mostly consisting of *Cibicidoides wuellerstorfi*, spanning the last 1.45 My (to MIS 47) at Expedition 339 Site U1385. Marine isotope stages are numbered: interglacial in (A) and glacial in (B). Figure from Hodell et al. (preprint). VPDB = Vienna Peedee belemnite.

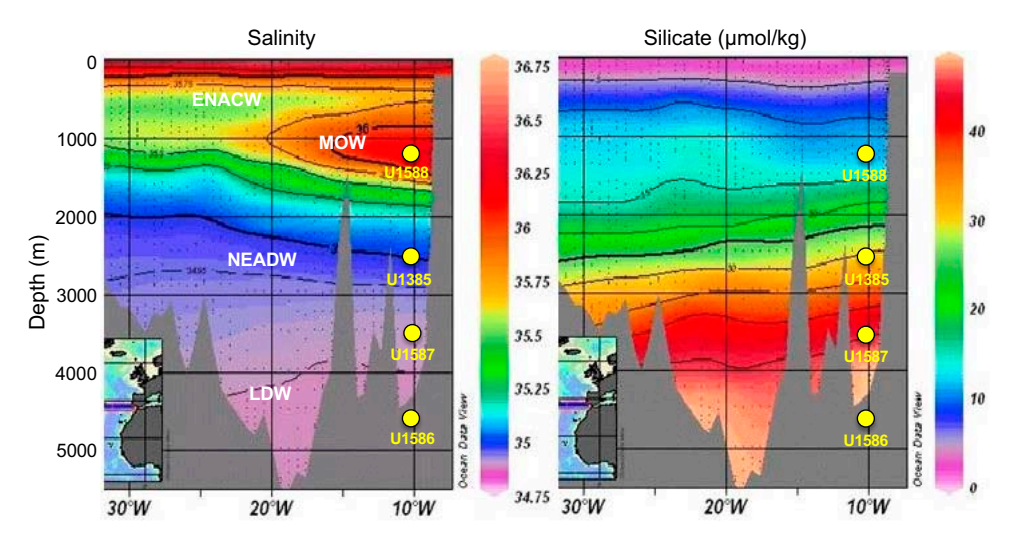


Figure F7. Salinity and silicate profiles on WOCE Line A03 (36°N) showing proposed site locations on the Iberian margin. Tongue of high salinity water between 600 and 1200 m is MOW. High Si (>35 mmol/kg) below 3000 m represents a contribution from LDW sourced from the Southern Ocean. Water masses do not have clearly defined boundaries but rather consist of a series of core layers bordered by transition (mixing) zones between adjacent layers. The positions of Expedition 397 sites are shown relative to each of the identified subsurface water masses.

a complete depth transect from 560 to 4691 mbsl with which to study past variability of all the major subsurface water masses of the eastern North Atlantic.

2. Preliminary scientific assessment

Expedition 397 accomplished almost all of its primary objectives and was a great success overall. We recovered 6176.7 m of sediment (104.2% recovery) at four primary sites (U1586, U1587, U1385, and U1588). Multiple holes were drilled at each site, and complete composite sections were constructed. Sites U1586 and U1385 were drilled to the planned depths of 350 and 400 mbsf, respectively. We recovered much older sediment (14 Ma) than anticipated at Site U1586, which extended the expedition objectives into the middle Miocene (Figure F8). At Site U1587, we sought and were granted permission from the Environmental Protection and Safety Panel (EPSP) to deepen the hole from 400 to 450 mbsf to ensure complete recovery of the Messinian Stage (7.246–5.333 Ma). Site U1588 could only be drilled to 412.5 mbsf out of the planned 500 mbsf because severe gas expansion of the sediment forced us to alter our strategy and drill half advances (4.8 m) with the extended core barrel (XCB) system, which significantly slowed the recovery rate.

The decision to use a polycrystalline diamond compact (PDC) bit and cutting shoe with the XCB system proved pivotal to the expedition's success, resulting in very high recovery and good quality XCB cores. The exceptional percent recovery (104%) was aided by half advances of the XCB system at Site U1588 that recovered a greater length of core than that drilled because of gas expansion.

A primary objective of Expedition 397 was to recover marine sequences that could be compared with existing and future polar ice core records. If the Beyond EPICA-Oldest Ice (BE-OI) Project and/or Center for Oldest Ice Exploration (COLDEX) are successful, the Antarctic ice core record

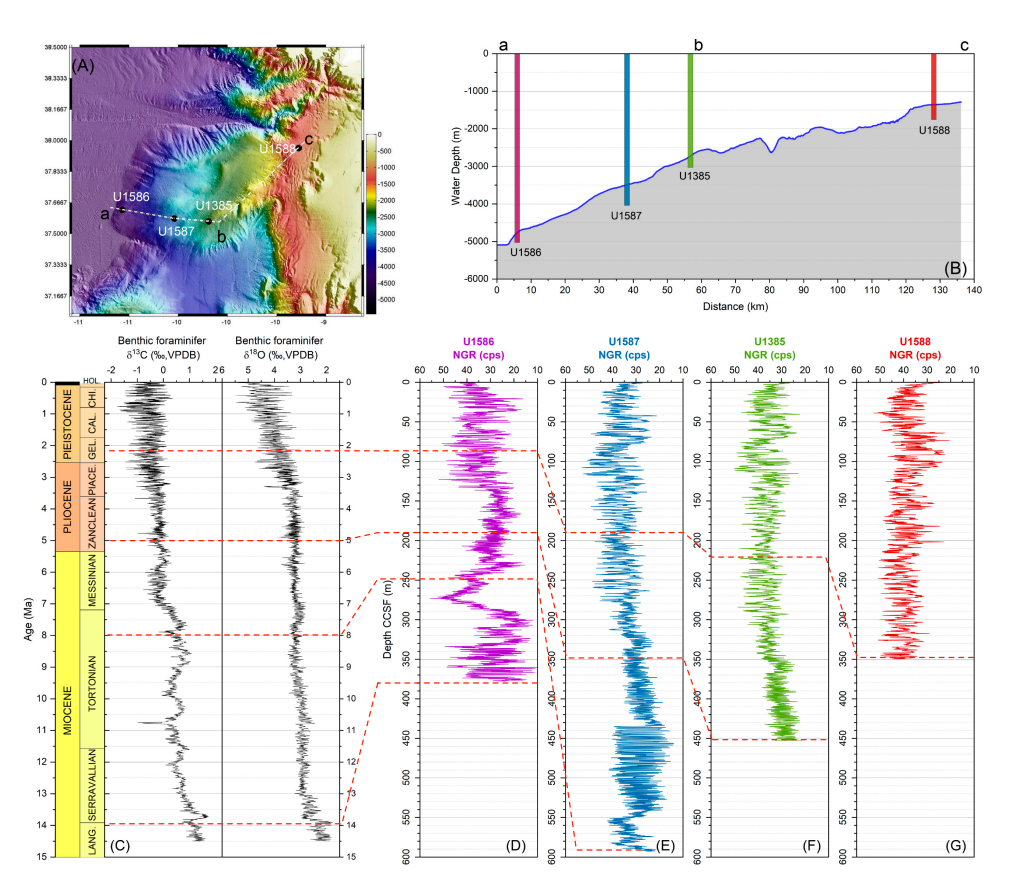


Figure F8. A–G. NGR data for each Expedition 397 site relative to the global stable isotope curves showing the depth transect of sites and relative age of the sequences. VPDB = Vienna Peedee belemnite, cps = counts per second.

will span the last 1.5 My. Figure $\mathbf{F9}$ shows the natural gamma radiation (NGR) records of all Expedition 397 sites along the bathymetric transect for the last ~ 1.5 My. With few exceptions, such as the slump at Site U1586, the records correlate peak-for-peak among the sites despite a nearly four-fold difference in sedimentation rates. These sites will serve as marine reference sections of Pleistocene climate variability and are important for linking to the polar ice cores and European terrestrial sequences.

Sediments at all sites show strong cyclic variations in physical properties (color, magnetic susceptibility (MS), and NGR) that are presumably related to changes in Earth's orbital cycles. Particularly notable are the precession cycles of the Pliocene that can be correlated peak-for-peak among sites (Figure F10) and the exceptional late Miocene cycles at Site U1587. These cyclic variations will be invaluable for deriving orbitally tuned timescales for Expedition 397 sites and correlating them with classic Mediterranean cyclostratigraphy. The cycles are also evident in the downhole logging NGR data of Site U1587, which will be important for core-log integration.

Although Expedition 397 was overall highly successful, no expedition is without its compromises, and Expedition 397 is no exception. We had planned to produce two complete stratigraphic splices at each site for sampling purposes, but this was impossible because of time lost to waiting on weather, which totaled 8 days (192 h) for the expedition (14.5% of operating days). Logging was successful at only two of the four sites because of problems with the tools becoming lodged in the drill pipe. Some slumps were encountered at Site U1586 that disturbed the continuity of the stratigraphic section. Site U1588 could only be drilled to 412.5 mbsf out of the planned 500 mbsf

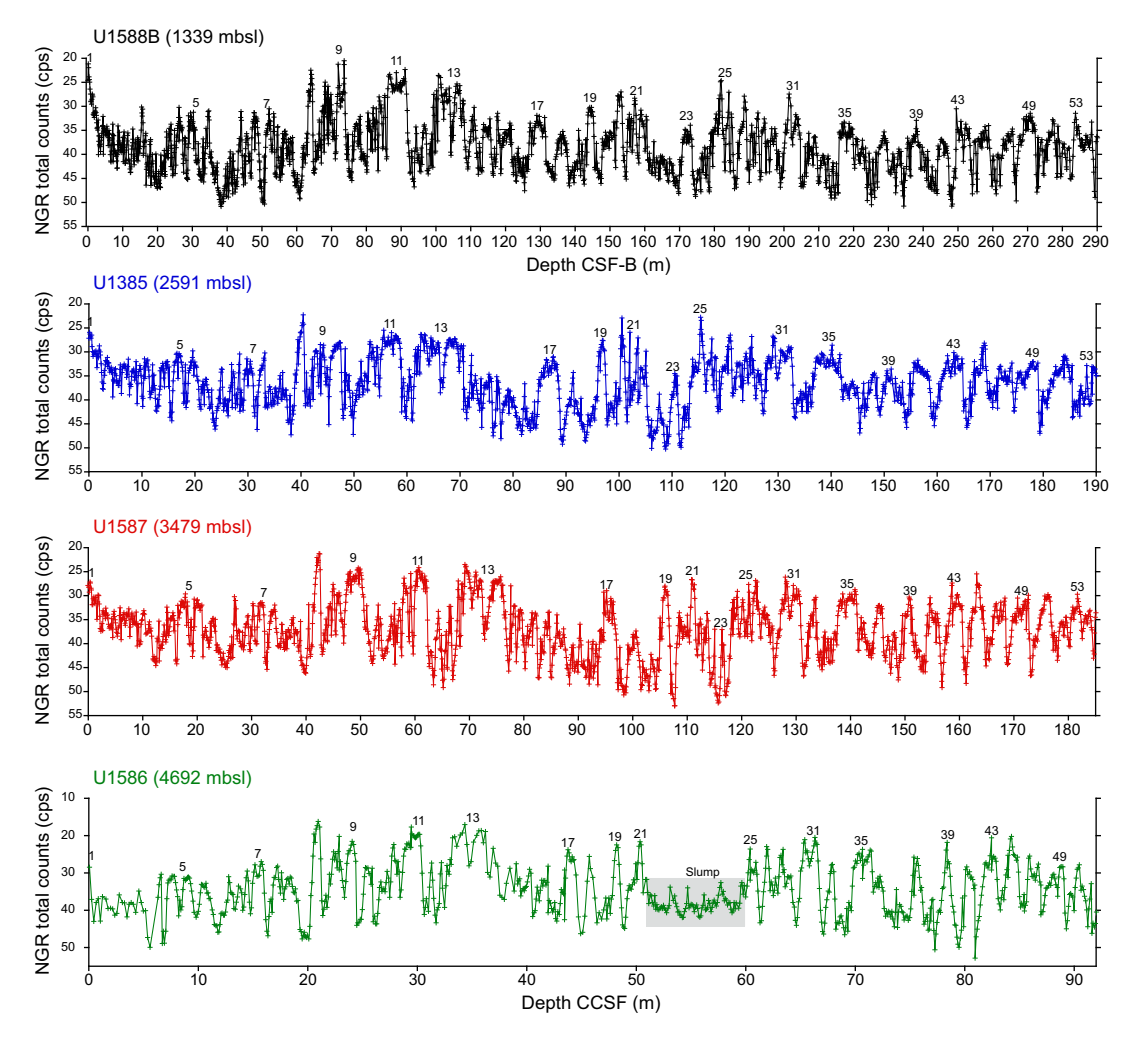


Figure F9. NGR data for each Expedition 397 site showing the approximate location of selected marine oxygen isotope stages. cps = counts per second. NGR data have been cleaned for outliers and spurious data at section ends.

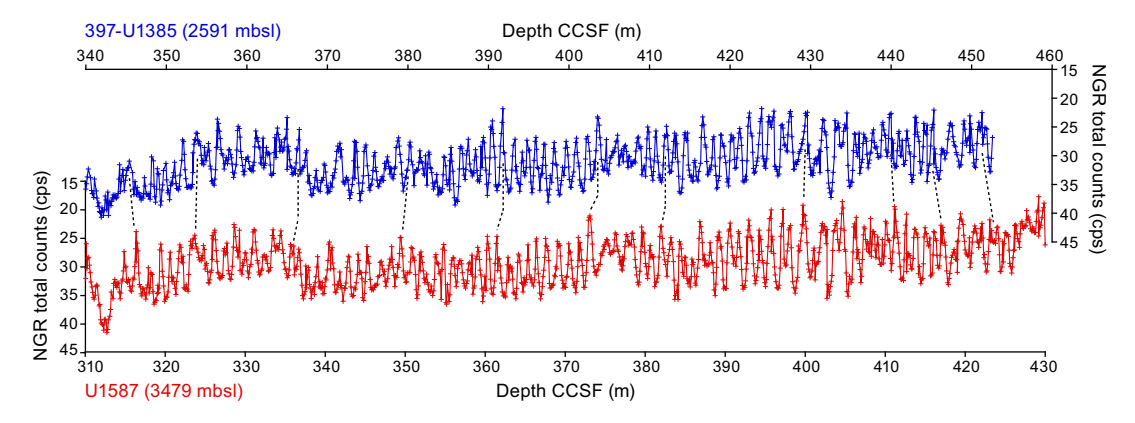


Figure F10. Correlation of Pliocene NGR cycles between Sites U1587 and U1385. cps = counts per second. NGR data have been cleaned for outliers and spurious data at section ends.

because of severe gas expansion of the sediment. The basal age of the cored section at Site U1588 is considerably younger (2.2 Ma) than the original objective of reaching the Pliocene. These relatively minor shortcomings do not detract from the invaluable >6 km sediment archive recovered from the Iberian margin that will provide the raw material needed for paleoclimate studies for generations to come.

3. Background

3.1. Geological setting

The Expedition 397 drill sites are located on a plateau, Promontório dos Príncipes de Avis (PPA), on the southwestern Iberian margin. The PPA protrudes from the continental shelf and slope and extends seaward toward the Tagus Abyssal Plain (Vanney and Mougenot, 1981) (Figure F1). The PPA is approximately 100 km long by 50 km wide with a bathymetric relief of 4 km above the abyssal plain (Figure F2). It is topographically isolated from the turbidites that are funneled to the Tagus Abyssal Plain via the bordering submarine canyons to the north and south.

Sites were selected for Expedition 397 by examining available seismic data. Geophysical coverage of the PPA is excellent with a dense network of multichannel seismic lines. Furthermore, a dedicated site survey cruise aboard the RSS *James Cook*, conducted in 2013, provided high-resolution seismic lines at each of the proposed site locations (Hodell et al., 2014). Piston cores, recovered during the same cruise, supplied evidence for hemipelagic sediments consisting of nannofossil muds and clays with varying proportions of biogenic carbonate and terrigenous components on the entire PPA (Abrantes et al., 1998; Baas et al., 1997; Expedition 339 Scientists, 2013a). High sedimentation rates, ranging 10–20 cm/ky, occur during both glacial and interglacial periods and are attributed to the copious pelagic sediment supply and lateral transport of sediment by bottom and contour currents. Enhanced lateral transport and deposition of finer sediments (i.e., clay and silt) on the Iberian margin are affected by an enhanced nepheloid layer associated with the MOW (Ambar et al., 2002; Abrantes et al., 2000; Magill et al., 2018). Detrital input from the Tagus and Sado Rivers are mainly channeled by turbidity currents through submarine canyon systems to the abyssal plains (Lebreiro et al., 1997, 2009) and have relatively little effect on open slope deposition.

3.2. Surface hydrography

The western Iberian margin is at the northern limit of the Canary Current/Northwest African eastern boundary upwelling system (Figure F11). Coastal upwelling driven by northerly winds occurs predominantly from late May/early June to late September/early October (Fiúza et al., 1998; Haynes et al., 1993). As a result, the current flow direction is equatorward with the offshore presence of the perennial Portugal Current (PC), the eastern boundary recirculation from the North Atlantic Drift, and the nearshore seasonal Portugal Coastal Current (PCC). The PC is centered at 10°W and slowly advects surface and subsurface waters equatorward (Pérez et al., 2001),

whereas the PCC is a jet-like slope current transporting the upwelled waters southward (Fiúza, 1984).

Eastern North Atlantic Central Water (ENACW) is the PC's subsurface component and forms by winter cooling in the eastern North Atlantic (Brambilla et al., 2008). The second major perennial current influencing the margin, especially the southwestern regions, is the Azores Current (AC). The AC, whose northern boundary is associated with the subtropical front, diverges from the Gulf Stream and flows as a jet with large meanders between 35 and 37°N across the North Atlantic. Although most of the AC recirculates southward, its eastern branch flows into the Gulf of Cádiz (Peliz et al., 2005). During the winter months, a northward bending of this subtropical front deflects it toward the SW Portuguese margin and feeds the Iberian Poleward Current (IPC) (Peliz et al., 2005). As the PC, the IPC's subsurface or undercurrent component also transports ENACW of subtropical origin. This subtropical ENACW flows poleward year round and is formed by strong evaporation and winter cooling along the Azores front (Rios et al., 1992); it is poorly ventilated and warmer and saltier than the PC's subpolar counterpart.

The oceanographic conditions along the western Iberian Peninsula have important implications for primary production, biodiversity and biogeochemical cycles in the region. Moreover, the upwelling fronts are not simple continuous features, but rather punctuated by mesoscale structures (filaments) that can extend 200 km offshore, generating a transition zone between the oligotrophic offshore water and the highly productive coastal region, where particle accumulation leads to biogeochemical and productivity hotspots (Woodson and Litvinb, 2015). This upwelling process leaves a clear imprint in the sediments covering the ocean bottom in the area, including physical properties, geochemistry, and diatom and planktonic foraminiferal assemblages (Abrantes, 1988; Abrantes and Moita, 1999; Salgueiro et al., 2008).

3.3. Subsurface hydrography

The flanks of the PPA intersect each of the major subsurface water masses of the North Atlantic and are ideal for the placement of a depth transect of sites (Figure F2). During Cruise JC089, 13 conductivity-temperature-depth (CTD) casts were made and subsurface water masses were recognized by their temperature-salinity characteristics (Figure F12). ENACW occupies the depth interval below the thermocline between ~50 and 500 m (van Aken, 2000). Between 500 and 1500 m, the warm, salty MOW dominates. MOW forms as warm, salty water from the Mediterranean flows over the Strait of Gibraltar into the Gulf of Cádiz and splits into two cores centered at ~800 and 1200 m (Ambar and Howe, 1979), flowing north along the western Iberian margin. Below 2000 m, recirculated Northeast Atlantic Deep Water (NEADW) prevails, representing a mixture of Labrador Sea Water, Iceland Scotland Overflow Water, Denmark Strait Overflow Water, and to a lesser extent MOW and Lower Deep Water (LDW) (van Aken, 2000). The deepest water mass is

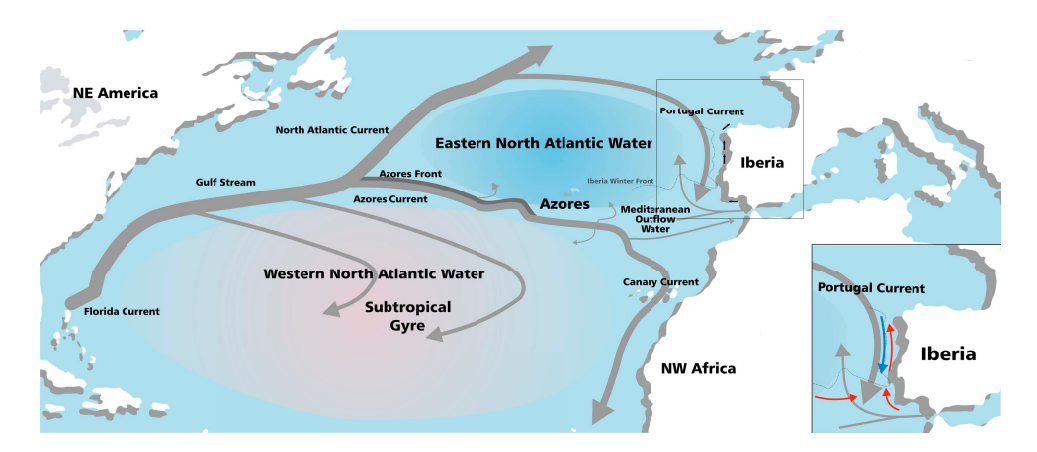


Figure F11. Gulf Stream and its relation to the Azores Current and Azores Front system and Portugal and Canary Currents. Also shown are the MOW, Iberian Winter Front, and the river plumes' flow direction (small arrows). Lower inset: more detail of the changing surface circulation on the western Iberian margin in summer (Portugal Coastal Current [PCC]; blue arrows) and winter (Iberian Poleward Current [IPC]; red arrows).

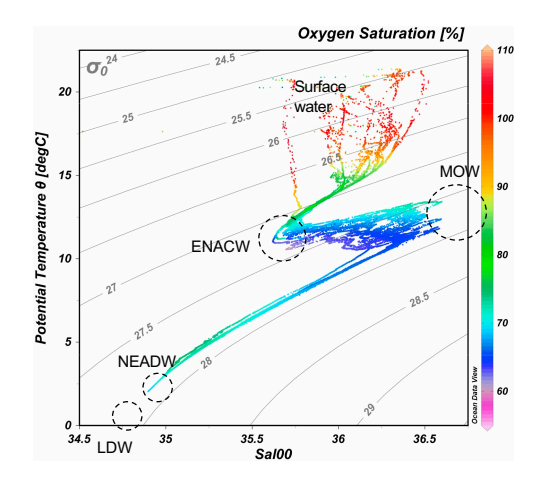


Figure F12. Temperature vs. salinity of CTD casts made during Cruise JC089 to the Iberian margin showing major subsurface water masses (Hodell et al., 2014). Color bar = percent oxygen saturation, contours = potential density.

southern-sourced LDW, which is modified Antarctic Bottom Water (AABW) that enters the eastern Atlantic Basin through the Vema Fracture Zone at 11°N (Saunders, 1987).

Jenkins et al. (2015) performed an optimum multiparameter analysis (OMPA) water mass analysis for the stations along the GEOTRACES North Atlantic transect. OMPA assesses the relative contributions of end-member water masses by a least-square optimization using input values for conservative properties. We used this analysis to identify the optimal site locations based on the relative contribution of end-member water masses at each of the proposed drill sites.

3.4. Paleo-conductivity-temperature-depth strategy

We employed a paleo-conductivity-temperature-depth (paleo-CTD) approach whereby the seabed is sampled beneath each of the major subsurface water masses. The PPA provides the bathymetric relief that in a limited area intersects all the principal water masses involved in the Atlantic thermohaline circulation (Figure F7). Water depths at the sites range 1339-4691 mbsl, permitting the sampling of paleowater mass properties of intermediate-water (Mediterranean Overflow) and deepwater masses (NEADW and LDW). The water depth range also complements those sites drilled during Expedition 339, which focused on the variability of MOW at five sites (U1386-U1390) in the Gulf of Cádiz at 566-980 mbsl and Site U1391 on the southwest Iberian margin at 1074 mbsl. Together with Expedition 339, the proposed sites constitute a complete depth transect from 566 to 4686 mbsl on the eastern margin of the North Atlantic Basin. Because the depth ranges of water masses differed in the past, it is important to sample the sediment column under a wide range of bathymetric and hydrographic conditions. The paleo-CTD approach permits a comprehensive reconstruction of past water mass variability in the North Atlantic, much of which appears to be related to spatial redistributions on both glacial-interglacial and millennial timescales. Understanding the role of the deep ocean in climate change is necessary to identify the underlying mechanisms of glacial-interglacial cycles and millennial-scale climate variation (Adkins, 2013).

4. Scientific objectives

The overall objective of the Expedition 397 drilling proposal is to recover the late Miocene–Pleistocene sediment archive located offshore Portugal in a range of water depths to document past changes in vertical water mass structure and its relation to global climate change. By producing multiproxy time series at each site and placing them on an integrated stratigraphy, these sediments provide the information needed to study MCV over the Pliocene–Pleistocene and understand its underlying causes and evolving contextuality.

Some of the specific scientific objectives include the following:

- Document the occurrence of MCV for older glacial cycles beyond the limit of Site U1385 (1.45 Ma) and how MCV evolved as glacial boundary conditions changed with the progressive intensification of Northern Hemisphere glaciation (NHG) since the late Pliocene.
- Derive a marine sediment proxy record for Greenland and Antarctic ice cores to examine the amplitude and pacing of MCV during the Quaternary.
- Determine interhemispheric phase relationships (leads/lags) by comparing the timing of proxy variables that monitor surface (Greenland) and deepwater (Antarctic) components of the climate system.
- Study how changes in orbital forcing and glacial boundary conditions affect the character of MCV and, in turn, how MCV interacts with orbital geometry to produce the observed glacial-to-interglacial patterns of climate change.
- Reconstruct the history of changing local dominance of northern-sourced versus southern-sourced deep water using the depth transect of Expedition 397 and 339 sites on orbital and suborbital timescales during the Quaternary.
- Develop orbitally tuned timescales for each of the sites and correlate them into the classic Mediterranean cyclostratigraphy.
- Document changes in the coastal upwelling system from the Miocene to the present, including its impact on productivity, carbon export, and biogeochemical cycling.
- Reconstruct the evolution of continental vegetation and hydroclimate using pollen and terrestrial biomarkers that are delivered to the deep-sea environment of the Iberian margin.
- Link terrestrial, marine, and ice core records by comparing proxy signals of different components of the Earth system that are coregistered in a single sediment archive.

A more comprehensive explanation of the scientific objectives follows.

4.1. Integrated global stratigraphy

Precise stratigraphy is the main factor limiting our ability to determine phase relationships (leads/lags) among various variables in the ocean-atmosphere system, which is essential for testing causal mechanisms of global climate change. A great strength of the Iberian margin sediment record is that it contains proxies of marine, atmospheric (ice core), and terrestrial signals coregistered in a single archive. It is thus possible to determine the relative phasing of changes in proxy variables that monitor different components of the ocean climate system in the same core (Shackleton et al., 2000, 2004). For example, temporal comparisons between marine stable isotope and pollen records in the same core have allowed the evaluation of phase relationships between global climate and European terrestrial change during the last 420 ky (Margari et al., 2010, 2014; Oliveira et al., 2020; Roucoux et al., 2001; Shackleton et al., 2000, 2003, 2002; Tzedakis et al., 2004). A similar strategy can be applied to the entire sequence recovered by Expedition 397, circumventing many problems associated with core-to-core correlation and developing age models on millennial timescales (Blaauw, 2012).

At Site U1385, variations in sediment color contain an eccentricity-modulated precession signal over the past 1.4 My (Hodell et al., 2013a, 2013b, preprint), and shipboard data indicates this cyclicity continues for older time periods. The modulation of precession by eccentricity provides a powerful tool for developing orbitally tuned age models (Shackleton et al., 1995). An astronomically tuned timescale will be developed at each of the Expedition 397 sites by correlating variations in physical properties to orbital target curves (e.g., Hodell et al., 2015). This also will allow the sites to be correlated to the classic Mediterranean cyclostratigraphy (Hilgen, 1991; Konijnendijk et al., 2015). In addition, the correlation of Iberian margin proxy records with European speleothems will provide a novel opportunity to tie marine records into a radiometrically dated chronology using U-Th and U-Pb isotopes (e.g., Tzedakis et al., 2018; Bajo et al., 2020).

4.2. Marine sediment analog to the polar ice cores

Ice cores offer the most detailed records available for reconstructing changes in climate and green-house gases in the latest Pleistocene. However, many of the mechanisms that control atmospheric composition and climate are rooted in the oceans. The answers to Pleistocene climate questions require a coupled ocean-atmosphere approach where ice core data are integrated with marine sed-

iment cores. In this regard, Iberian margin sediments are important for comparison to existing and future ice core records from Greenland and Antarctica (Nehrbass-Ahles et al., 2020; Wolff et al., 2022). Given that the Greenland ice core is limited to the last glacial cycle and the oldest ice core in Antarctica (EPICA Dome C) is limited to the last 800 ky, we must rely on marine sediment records to provide the longer term history of changes in polar climate.

If we assume the correlation between rapid temperature changes on the Iberian margin and over Greenland has held for older glacial periods, then sediment recovered during Expedition 397 can serve as a marine sediment proxy record for the Greenland ice core beyond the age of the oldest undisturbed ice (~122 ka). Comparing surface water signals from the Iberian margin with the synthetic Greenland reconstruction (Barker et al., 2011) has demonstrated a strong similarity for the last 400 ky (Hodell et al., 2013a). Similarly, millennial-scale variability in benthic δ^{18} O from the Iberian margin is similar to EPICA δ D for the last 800 ky (Hodell et al., preprint). Beyond the last three glacial cycles, the temporal resolution of the EPICA Dome C record diminishes because of compression and diffusion, which hinders clear detection of millennial to submillennial events for older glacial periods depending on sampling resolution (Jouzel et al., 2007; Pol et al., 2010). Problems of diffusion and compression will undoubtedly be more severe in older ice to be recovered by the BE-OI Project and COLDEX (Fischer et al., 2013; Bereiter et al., 2014; Wolff et al., 2022). Comparison of the ice core record from BE-OI and proxies measured in Expedition 397 sediment will allow an assessment of whether there has been significant loss of climate information at higher frequencies due to diffusion and migration in the ice core record.

4.3. Millennial-scale climate variability during the Pliocene-Pleistocene

Much progress has been made toward understanding the orbital effects on climate, but a complete theory of the ice ages remains elusive (Raymo and Huybers, 2008). Understanding how climate changes on shorter (i.e., suborbital) timescales and interacts with the effects of orbital forcing to produce the observed patterns of glacial-interglacial cycles through the Pleistocene may be the missing piece of the puzzle. For example, MCV may play an important role in longer term climate transitions, such as glacial terminations (Cheng et al., 2009; Denton et al., 2010; Wolff et al., 2009; Barker and Knorr, 2021). Studying the coevolution of orbital and suborbital variability requires a new caliber of sediment archives with a high level of chronological precision. With few exceptions, deep-sea sedimentary records generally lack the resolution needed to delineate such variability; however, exceptions do exist, such as those from the Iberian margin. MCV has been well documented for the last glacial cycle in the North Atlantic, but relatively little is known about similar variability during older glacial periods of the Pleistocene (de Abreu et al., 2003; Margari et al., 2010; Martrat et al., 2007; Rodrigues et al., 2011). Some marine records of MCV exist beyond the last glacial cycle (Alonso-Garcia et al., 2011; Barker et al., 2015, 2011; Hodell et al., 2008; Jouzel et al., 2007; Kawamura et al., 2007; Dome Fuji Ice Core Project Members, 2017; Margari et al., 2010; Martrat et al., 2007; McManus et al., 1999; Oppo et al., 1998; Rodrigues et al., 2017), but only a few extend beyond 800 ka into the early Pleistocene (Barker et al., 2021; Billups and Scheinwald, 2014; Birner et al., 2016; Hodell and Channell, 2016; Hodell et al., 2008, preprint; Mc Intyre et al., 2001; Raymo et al., 1998) and none for the Pliocene.

MCV is thought to be a pervasive feature of Quaternary climate change (Jouzel et al., 2007; Weirauch et al., 2008; Hodell et al., 2015; Sun et al., 2021), but its pacing and amplitude are likely to be influenced by changing orbital and ice sheet boundary conditions. MCV can exert an upscale influence on orbital timescales through its effect on ice sheet dynamics (Verbitsky et al., 2018) or atmospheric CO₂ by changing carbon storage in the deep sea. MCV is also a source of high-frequency variability (noise) on glacial–interglacial timescales that may affect the resonance of internal climate change with external orbital forcing. Sediments recovered during Expedition 397 will be important for documenting how orbital and millennial variability co-evolved through the Quaternary and Pliocene (Hodell et al., preprint).

4.4. Testing the thermal bipolar seesaw hypothesis

The leading cause to explain MCV recorded in Greenland and Antarctic ice cores during the last glacial period is the change in the strength of Atlantic Meridional Overturning Circulation (AMOC), which alters interhemispheric heat transport and results in opposite temperature responses in the two hemispheres. However, we know little about whether this bipolar seesaw was a persistent feature of older glacial climate states.

Determining phase relationships of MCV in glacial periods beyond the last climate cycle is challenging because absolute dating of marine cores is too imprecise to correlate and resolve small differences in the timing of paleoclimate signals (Blaauw, 2012; Andrews et al., 1999; Wunsch, 2006). An alternative approach is to determine the relative phasing of changes in proxy variables in the same core that monitor different components of the ocean climate system. A great strength of the Iberian margin sediment record is the fact that it contains signals of both Greenland and Antarctic ice cores in a single archive and it is possible to determine the relative phasing of polar climate by comparing planktonic and benthic δ^{18} O signals in the same core (Figure F1). Iberian margin sediments can be used to test whether similar phasing patterns existed in older glacial periods, consistent with the operation of a bipolar seesaw (e.g., Margari et al., 2010).

4.5. North Atlantic thermohaline circulation

The most widely invoked explanation of past abrupt climate variability and its asymmetrical interhemispheric (Greenland versus Antarctica) phasing is the occurrence of major perturbations to the AMOC (for a review, see Alley, 2007). Production of Northern Component Water is thought to have been stronger during the warmer, longer Greenland interstadials (e.g., IS 8, 12, and 14) and reduced during Greenland stadials, especially during Heinrich events (Hodell et al., 2010; Kissel et al., 2008; Piotrowski et al., 2008; Henry et al., 2016). Previous work using sediments from the Iberian margin has confirmed (with particularly firm chronostratigraphic constraints) the link between past interhemispheric climate change and perturbations to the deep Atlantic hydrography. Thus, changes in deepwater radiocarbon concentration (Skinner and Shackleton, 2004; Skinner et al., 2021), oxygenation (Martrat et al., 2007; Skinner et al., 2003; Thomas et al., 2022), temperature (Skinner et al., 2003, 2007), remineralized nutrient content (Shackleton et al., 2000; Skinner et al., 2007; Willamowski and Zahn, 2000), and lateral export rates (Gherardi et al., 2005) have all been linked to abrupt climatic changes that occurred in the recent geological past. These reconstructions have identified hydrographic changes on the Iberian margin as a highly sensitive gauge of changes in the deep overturning circulation, in particular because of their sensitivity to changes in the representation of northern- and southern-sourced deep waters in the northeast Atlantic (e.g., Martrat et al., 2007; Skinner et al., 2007). Indeed, it is precisely the tight connection between deepwater circulation on the Iberian margin and the bipolar seesaw that lies at the heart of Shackleton's initial observation of northern and southern signals recorded simultaneously in Core MD95-2042 (Shackleton et al., 2000).

Expedition 397 sites permit the types of reconstructions noted above, such as benthic $\delta^{13}C$ as a proxy for deepwater sourcing and ventilation (Thomas et al., 2022), to be extended beyond the 1.45 Ma of Site U1385. Furthermore, the range of water depths of the Expedition 397 sites (1339–4691 mbsl) allow the study of past changes in the overturning circulation with especially strong stratigraphic constraints.

The cores recovered during Expedition 397, together with those drilled during Expedition 339, provide the basis for marine reference sections of temporal water column variability in the northeast Atlantic. Postcruise studies of this material will prove invaluable for assessing the expression and impacts of abrupt ocean circulation change in the past, especially as this relates to interhemispheric climate phasing and glacial—interglacial climate evolution.

4.6. Terrestrial vegetation and hydroclimate changes

Marine archives recovered adjacent to the continents have the potential to link continental and marine climate records because they are influenced directly by continental inputs, such as sediment from rivers and winds. The western Iberian margin has emerged as a critical area for study-

ing continent-ocean connections because of the combined effects of major river systems and a narrow continental shelf that lead to the rapid delivery of terrestrial material (e.g., pollen and organic biomarkers) to the deep-sea environment (Margari et al., 2014, 2020; Oliveira et al., 2016, 2017, 2018, 2020; Rodrigues et al., 2017; Sánchez Goñi et al., 2016; Tzedakis et al., 2015). In the southern Portuguese margin, pollen enters the ocean mainly as particulate suspended matter through the Tagus and Sado rivers and upwelling filaments (Naughton et al., 2007). A comparison of modern marine and terrestrial samples along western Iberia has shown that the marine pollen assemblages provide an integrated picture of the regional vegetation on the adjacent continent. Moreover, modern biogeographical differences in the distribution of Atlantic and Mediterranean plant communities are reflected in the pollen signal of northern and southern marine pollen spectra, respectively (Naughton et al., 2007). Thus, the Portuguese margin provides a rare opportunity to (1) enhance the study of ocean-continent linkages by analyzing proxies for continental hydrology and vegetation (e.g., pollen, elemental ratio data in bulk sediments, and molecular and isotopic composition of leaf waxes) in marine sediment cores that can be precisely correlated to polar ice cores and (2) to construct the longest continuous record of late Miocene-Pleistocene vegetation changes available anywhere to date. A detailed pollen record from the Portuguese margin linked to the marine isotopic stratigraphy and record of millennial-scale variability will be a unique resource that can be used to place vegetation changes in the context of global and North Atlantic climate changes. Comparisons with terrestrial pollen reference sequences, such as Tenaghi Philippon, Greece (Tzedakis et al., 2006), and with International Continental Scientific Drilling Program (ICDP) sites from Lake Ohrid (Albania/Macedonia) and Lake Van (Turkey), will assess patterns of geographical variation. Furthermore, it will also allow us to investigate major vegetation changes throughout the Pliocene-Pleistocene with shifts in climatic regimes (e.g., intensification of NHG, mid-Pleistocene transition, etc.).

4.7. History of upwelling on the Portuguese margin

The Iberian margin is a coastal upwelling region where primary production increases in response to seasonal (May–September) wind intensity and direction coastal upwelling of nutrient-rich ENACW. Although upwelling centers are mainly coastal, upwelled water spreads seaward through filaments extending up to 200 km offshore depending on northerly wind intensity (Fiúza, 1984; Relvas et al., 2009). These nutrient-rich waters generate a transition zone between the oligotrophic water offshore and the highly productive area near the coast.

This upwelling process leaves a clear imprint in the sediments covering the ocean bottom in the area, including physical properties, geochemistry, diatom and planktonic foraminiferal assemblages, and their geographic distribution (Abrantes, 1988; Abrantes and Moita, 1999; Salgueiro et al., 2008). The past geological variability of the upwelling has been studied both at orbital and millennial timescales. At the glacial–interglacial scale, an increase in diatom accumulation rates, which is in good agreement with other independent productivity proxies, has been interpreted to represent an order of magnitude increase in productivity during the previous glacial periods, not only on the Portuguese margin but in both hemispheres of the eastern Atlantic (Abrantes, 1991, 2000). Abrantes et al. (1998) suggested increased primary production associated with Heinrich events off the Portuguese coast, whereas the high-resolution planktonic foraminiferal study of three sites along the Iberian margin indicates a more complex north–south pattern (Salgueiro et al., 2010). Primary productivity decreased markedly during stadials and Heinrich events on the northern margin but increased off Sines in the region of influence of the Cape da Roca filament and near the Expedition 397 sites.

Sites U1391 and U1385 are located in the area influenced by the Cape Sines and Cape St. Vicente filaments (Sousa and Bricaud, 1992) and constitute a transect across a productivity gradient, allowing for the investigation of the impact of climate variations on marine production and preservation. The investigation of the totality of those two cores revealed a mostly barren Site U1385, whereas Site U1391 has diatom abundance peaks during some deglaciation—early interglacial periods, such as MIS 2/MIS 1, MIS 10/MIS 9, and the mid-Pleistocene transition (MIS 22/MIS 21 to MIS 32/MIS 31) (Abrantes et al., 2017). In addition, increased values of upwelling-related species at the shallower and coastal location of Site U1391 support a coastal upwelling-related increase in primary production in accordance with the Northwest African ODP Site 658 Si/Al record (Meck-

ler et al., 2013). Furthermore, large oligotrophic warm water species at the base of MIS 25 at Sites U1391 and U1387 points to significantly different surface ocean circulation dynamics at the southern Portuguese coast during early MIS 25.

Expedition 397 sites will provide information about the regional coastal upwelling system and the biotic response to global climate change from the Miocene to the present. Additionally, it will elucidate how the upwelling system evolved with changing glacial boundary conditions during the late Pliocene and Quaternary.

4.8. Connections to the 2050 Scientific Framework

IODP Expedition 397 is highly relevant to many of the strategic objectives and initiatives proposed by the IODP 2050 Scientific Framework, including Themes 3 (Earth's Climate System), 4 (Feedback in the Earth System), and 5 (Tipping Points in Earth History). The sediment cores recovered during Expedition 397 and those of Expedition 339 from the same region constitute an invaluable sedimentary archive with which to study past climate variability at high temporal resolution. The Iberian margin sedimentary archive will be used to document orbital and suborbital variability in climate and AMOC and its relation to carbon storage in the deep ocean and atmospheric CO₂ changes, as recorded in Antarctic ice cores. The long continuity, high resolution, and precise chronology offered by Iberian margin cores will enhance our understanding of how Earth's climate system operates and responds to various forcing and feedback processes across a wide array of background states, including those warmer than today and with atmospheric CO₂ concentrations equal to or greater than at present. By comparing marine and ice core records with their European terrestrial counterparts, Expedition 397 research will document the response of European hydroclimate and vegetation to regional and global climate change. These outcomes will advance the IODP 2050 scientific framework's objective of "obtaining the data necessary to calibrate and improve numerical models to project future climate impacts and inform mitigation strategies.

5. Site summaries

5.1. Site U1586

5.1.1. Background and objectives

Site U1586 is the deepest (4692 mbsl) and farthest from shore of all the Expedition 397 sites. It is located at the toe of the PPA in a slightly elevated region protected from bottom currents and turbidite deposition (Figure F13). As the deepest site in the bathymetric transect, it is bathed by LDW that consists of AABW, which has been modified by mixing during its transit from the South Atlantic.

Because of relatively lower sedimentation rates at Site U1586 compared to other sites, drilling at this site represents our best opportunity to obtain the oldest sediment (Miocene) to be recovered

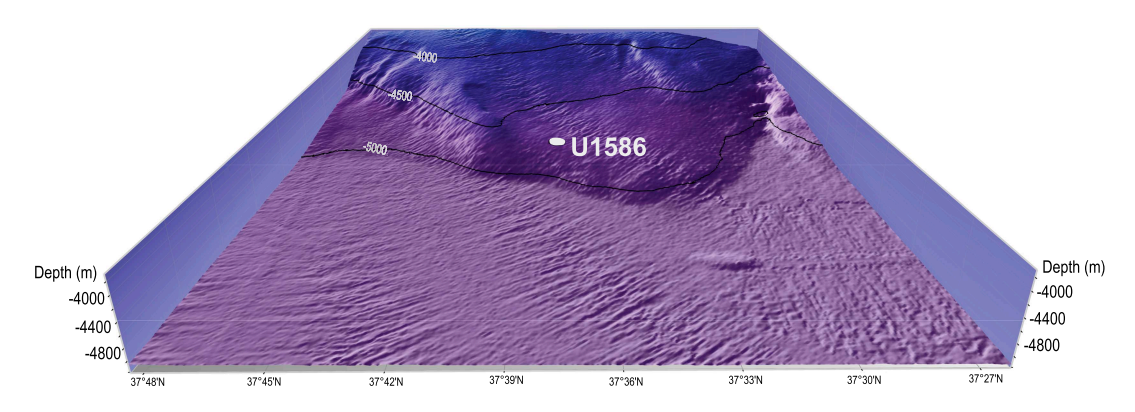


Figure F13. Location of Site U1586 at the toe of the PPA at a water depth of 4692 mbsl. See Figure F2 for broader bathymetric context.

during Expedition 397. The main drilling objective is to recover a high-resolution record of the late Miocene–Pleistocene with which to study the evolution of the surface and deepest water masses of the northeast Atlantic. Of specific interest are the time periods associated with (1) the water exchange between the Mediterranean and the Atlantic before, during, and following the Messinian Salinity Crisis (latest Miocene to the base of the Pliocene); (2) the mid-Pliocene warm period characterized by atmospheric CO_2 concentrations similar to present values (400 ppm); (3) the late Pliocene intensification of the NHG (~2.9 Ma); and (4) the Pleistocene (last 2.6 Ma) when MCV was superimposed upon glacial–interglacial cycles.

Site U1586 is positioned at Common Midpoint 1330 on Seismic Line 2 of Cruise JC089 in a region with good continuity of reflectors (Figure **F14**). The objective is to drill to the package of high-amplitude reflectors represented by the pink and green reflectors in Figure **F14**. A target drilling depth of 350 mbsf was approved by the EPSP.

5.1.2. Operations

Expedition 397 began on 11 October 2022 at 1045 h (UTC +1 h) upon the arrival of *JOIDES Resolution* at Rocha Pier in Lisbon, Portugal, at the end of Expedition 397T. On 16 October, *JOIDES Resolution* left port by 0830 h Portuguese time, reaching Site U1586 at 1834 h. A water depth reading with the ship's precision depth recorder (PDR) was taken as the vessel arrived on site, giving a seafloor depth of 4702.4 meters below rig floor (mbrf)/4691.4 mbsl.

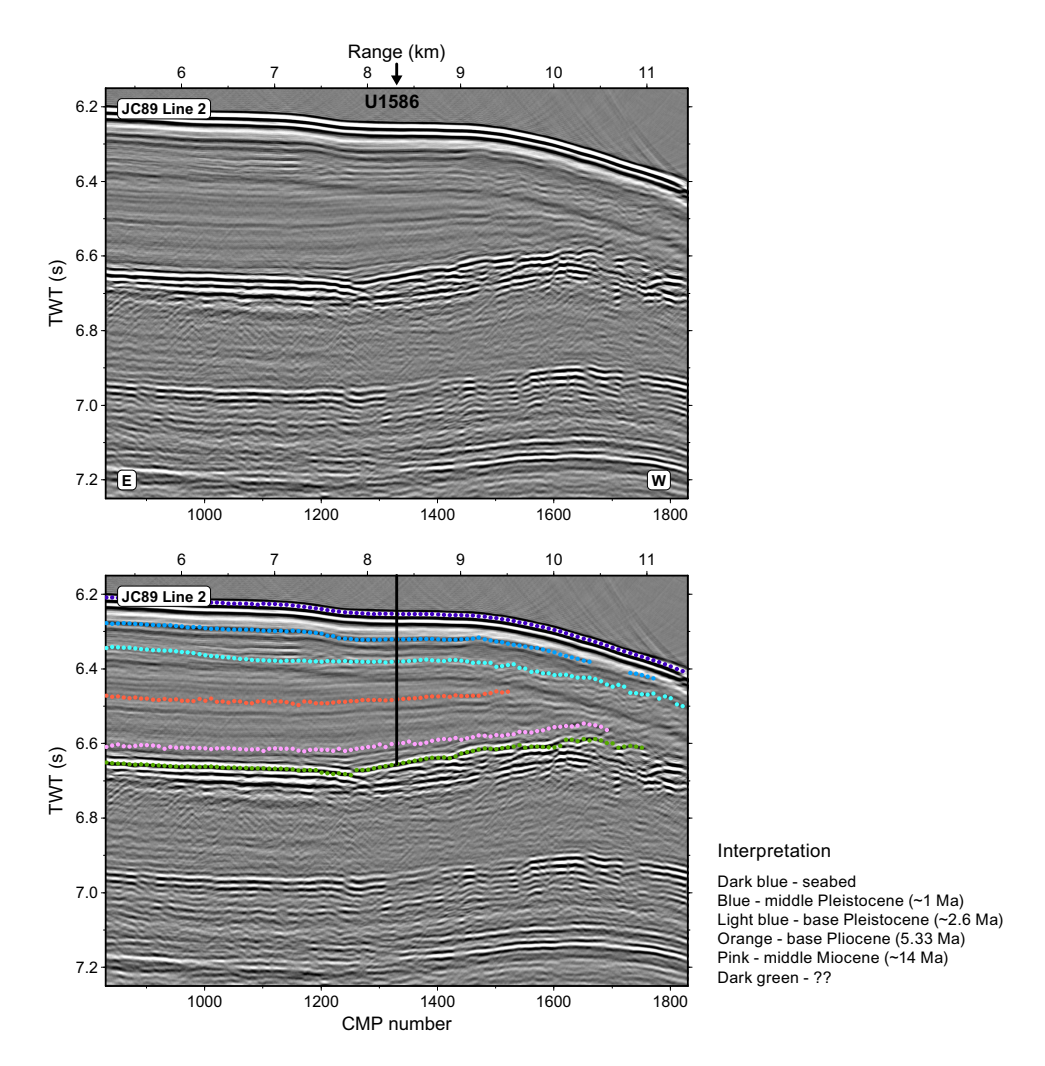


Figure F14. Original and interpreted seismic profile (JC89-2) showing the location of Site U1586 with penetration to 350 mbsf. The ages of the reflectors have been revised during the expedition to reflect the ages of the recovered sediment. TWT = two-way traveltime, CMP = common midpoint.

The plan for Site U1586 was to core five holes. Holes U1586A–U1586C were to be cored with the APC and half-length APC (HLAPC) to refusal (estimated to be approximately 250 mbsf) and then cored to a maximum depth of 350 mbsf using the XCB system. Holes U1586D and U1586E were to be cored to the APC/HLAPC refusal depth. Formation temperature measurements were planned for Hole U1586A using the advanced piston corer temperature (APCT-3) tool, and downhole wireline logging measurements were planned for Hole U1586C with the triple combo tool string.

Once on site, weather conditions and high seas caused ~48 h of delay over the planned 14.8 days of operations, and the coring strategy was adjusted. The high core quality obtained using the XCB system fitted with a PDC bit and cutting shoe in Hole U1586A allowed for it to be deployed earlier than normal in Holes U1586B–U1586D, eliminating the need to use the HLAPC system. Therefore, a revised plan was executed, using the APC system until the first partial stroke and then extending the hole to total depth using the XCB system. Site U1586 consisted of four holes to 350 mbsf (Figure F3). Hole U1586D was logged using the triple combo tool string. All APC and HLAPC cores used nonmagnetic core barrels, and APC cores were oriented using the Icefield orientation tool. In total, 1399.1 m were cored using the three coring systems with an overall recovery rate of 96%. Operations at Site U1586 took 349.5 h (14.6 days) to complete.

5.1.3. Principal results

Site U1586 yielded several significant findings and observations, some of which were unexpected:

- Operationally, the quality of the cores recovered using the XCB system was surprisingly good with high recovery and relatively minor disturbance (biscuiting), which is attributed to the use of a PDC bit and cutting shoe.
- A ~350 m Holocene-middle Miocene spliced sedimentary sequence (14 Ma) was recovered (Figure **F15**), nearly twice the age (7 Ma; late Miocene) predicted from the interpretation of the seismic profiles.
- The occurrence of convoluted banded sediment interpreted as slumps was found in all the holes at the same stratigraphic position, indicating slope instability associated with possible sea level fluctuations or tectonic activity. Slumped intervals were carefully noted by sedimentologists and can be recognized by the low-amplitude signal of physical properties measurements. Although the occurrence of slumps interrupts the stratigraphic section, many continuous intervals, suitable for paleoclimate studies, are identified (Figure F15).
- The Pliocene sequence at Site U1586 is remarkably complete and unaffected by slumping. Sediments are marked by very strong cyclic variations in color and other physical properties (MS and NGR), which are dominated by an apparent precession signal and offer much promise for developing an orbitally tuned age model and correlating to Mediterranean sequences (Figure F16).
- A serendipitous finding was an exceptionally high peak in MS that was detected at the same stratigraphic interval in all the holes. The sediments were found to contain abundant metallic particles, some of which are spherical and interpreted to be of cosmic origin. The estimated age of the layer is 3.6 Ma by correlation of the color reflectance signal to precession and the identification of the Gilbert-Gauss polarity reversal boundary.

At Site U1586, four holes (U1586A–U1586D) were drilled to 350 mbsf and a total of 1346.85 m of sediment was recovered. The primary lithology consisted of various proportions of nannofossil ooze and clay/silt. Very fine to coarse calcareous sands were found near the base of the holes below 310 mbsf (Figure F15) and may have resulted from sediment gravity flows (turbidites). Different types and intensities of drilling disturbance were observed in the cores, with the most common being up-arching, flow-in, soupy, and slurry in the APC cores and biscuiting and fall-in for the XCB cores. Bioturbation varied from absent to complete disturbance of sedimentary layers. Pyrite nodules filling burrows are commonly observed in X-ray images.

A well-constrained biostratigraphic age model was developed for Site U1586 based on analyses of calcareous nannofossils and planktonic foraminifera (Figure F17A). Overall, 51 calcareous nannofossils and planktonic foraminifera bioevents were identified. The integrated biostratigraphy suggests a reasonably complete sequence from Holocene to middle Miocene.

The magnetostratigraphy of Site U1586 was established based on the NRM by combining NRM (after 20 mT demagnetization) inclination and orientation-corrected declination data from archive-half core sections and stepwise NRM demagnetization (up to 50 or 80 mT) data from cubes. Identified polarity reversals include the Brunhes/Matuyama, Matuyama/Gauss, and Gauss/Gilbert boundaries and the following subchrons: Jaramillo, Olduvai, Cobb Mountain, Mammoth, Cochiti and Thyera (Figure F15).

Whole round samples (5–10 cm thick) were taken for IW from the base of every section for the uppermost 34 m and then from the penultimate section recovered from every core from Hole U1586A. IW analysis shows relatively constant salinity, sodium, and chloride throughout Hole U1586A, with values close to seawater, whereas potassium declines downhole with a relatively constant slope. Decreasing sulfate concentration is indicative of organic matter respiration via sul-

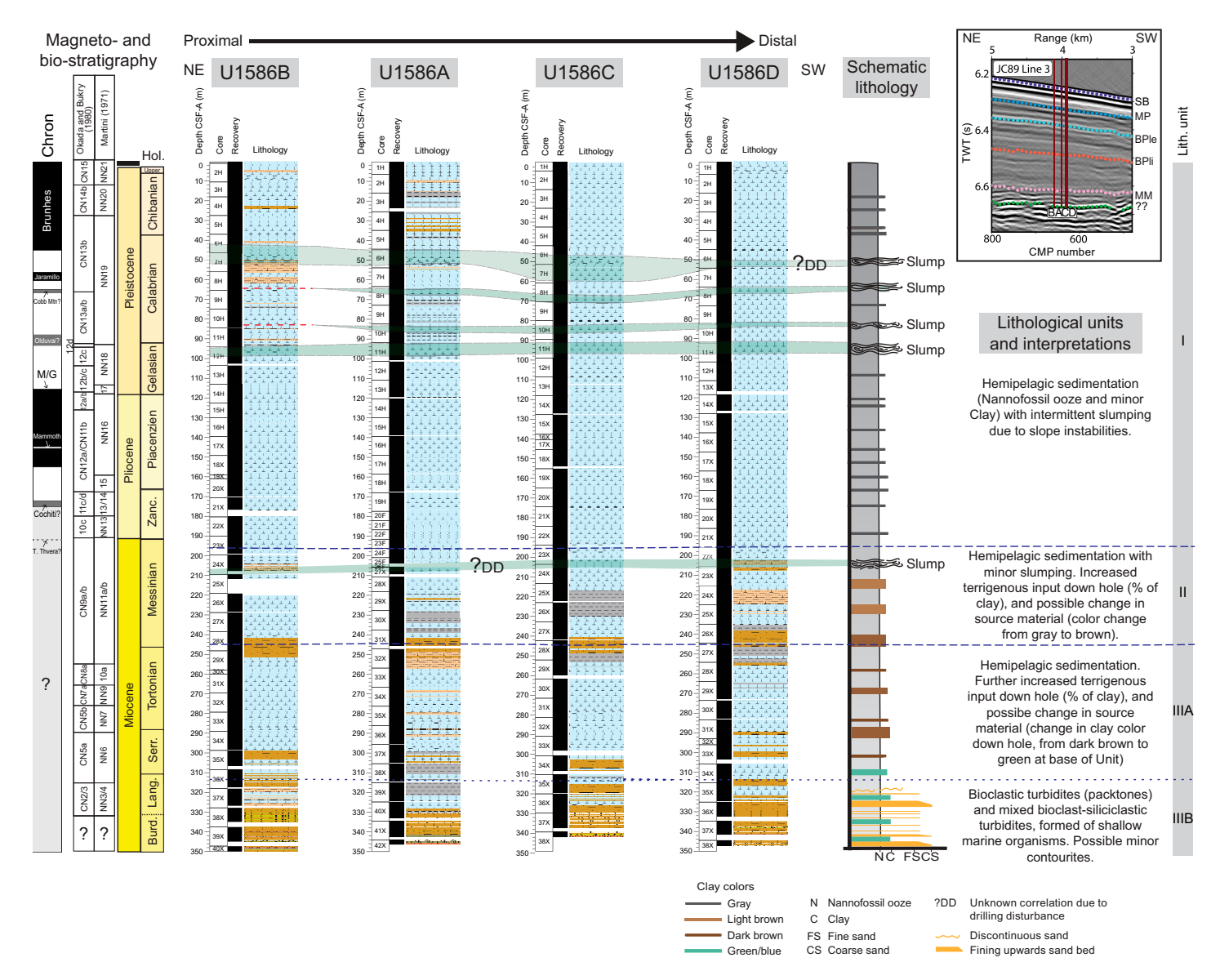


Figure F15. Lithologic summary, Site U1586. Left: chronostratigraphy and biostratigraphy (nannofossil biozones). M/G = Matuyama/Gauss, T.Thvera = Top Thvera, ? = uncertainty. Center: summary lithostratigraphic logs of Holes U1586A–U1586AD, ordered left to right from northeast to southwest (upslope to downslope). Blue dashed line = divisions of lithostratigraphic units, blue dotted line = division of subunits (not slump related), green overlay = correlation of slumped intervals (Subunits B, D, F, and H of Unit I and Subunit B of Unit II). Right: lithologic unit names and preliminary interpretations of depositional processes. Colors are based on visual description as well as L*a*b* values. Unit and subunit boundaries are primarily based on sedimentary structures as well as changes and color and banding thickness. Color is independent of lithology and is related to relative amounts of minor constituents such as pyrite and glauconite. Inset: cropped section of Seismic Line JC89 Line 3 showing location along transect and depth of Holes U1586A–U1586D. TWT = two-way traveltime, CMP = common midpoint, SB = seabed, MP = middle Pleistocene, BPIe = base Pleistocene, BPIi = base Pliocene, MM = middle Miocene.

fate reduction; however, sulfate never reaches zero and methane concentration never exceeds 15 ppmv (Figure F18). A decrease in calcium and magnesium in the upper 50 m reflects authigenic carbonate precipitation driven by high pore water alkalinity and associated with sulfate reduction. Peaks in redox-sensitive elements, such as iron and manganese, are similarly indicative of microbially mediated respiration reactions within the sediments. Below 200 mbsf, Ca, Sr, and Si concentrations increase while Mg decreases. Although dolomitization may explain the Mg, Ca and Sr profiles, by liberating Ca and Sr and using Mg, the high silicon concentration near the bottom of the hole indicates important Si dissolution within the silty clay layers of Lithostratigraphic Unit III. Mean $CaCO_3$ in Hole U1586A is 37.4 wt%, and values increase steadily but nonmonotonically with depth. Total organic carbon values in Hole U1586A are generally low (mean = 0.48 \pm 0.32 wt%), ranging 0–2.02 wt%; they are highest in the upper 50 m (0.57 \pm 0.21 wt%) and steadily decline with depth (0.33 \pm 0.27 wt% in the bottom 50 m). Methane is the only detectable gas, and its concentration ranges 0–14.10 ppmv with a peak between 100 and 150 mbsf.

Inductively coupled plasma–atomic emission spectroscopy (ICP-AES) data from bulk sediment analysis show strong correlations between SiO_2 , K_2O , Fe_2O_3 , MgO, and TiO_2 with Al_2O_3 , indicating the dominance of local detritus. Barium is weakly correlated with Al or Ca, likely due to barite in

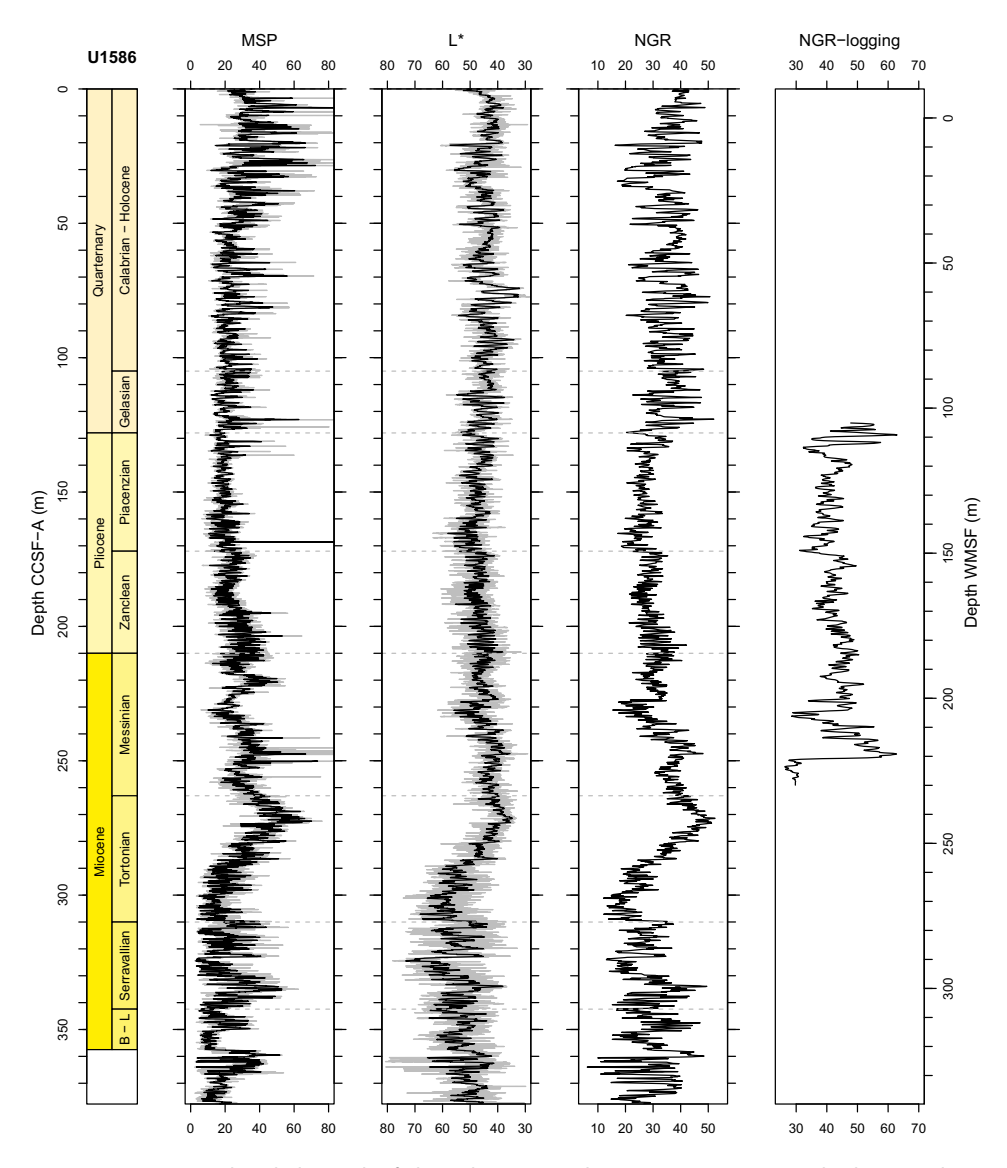


Figure F16. Core composite downhole trends of physical properties data, Site U1586. B-L = Burdigalian–Langhian. MSP = section-half point MS, NGR = whole-round NGR, NGR-logging = NGR data from the triple combo logging tool. WMSF = wireline log matched depth below seafloor. MSP and L* panels: a smoothed curve (black line; 20-point moving average) is shown over the original data (gray line). NGR panels: only the original data is shown.

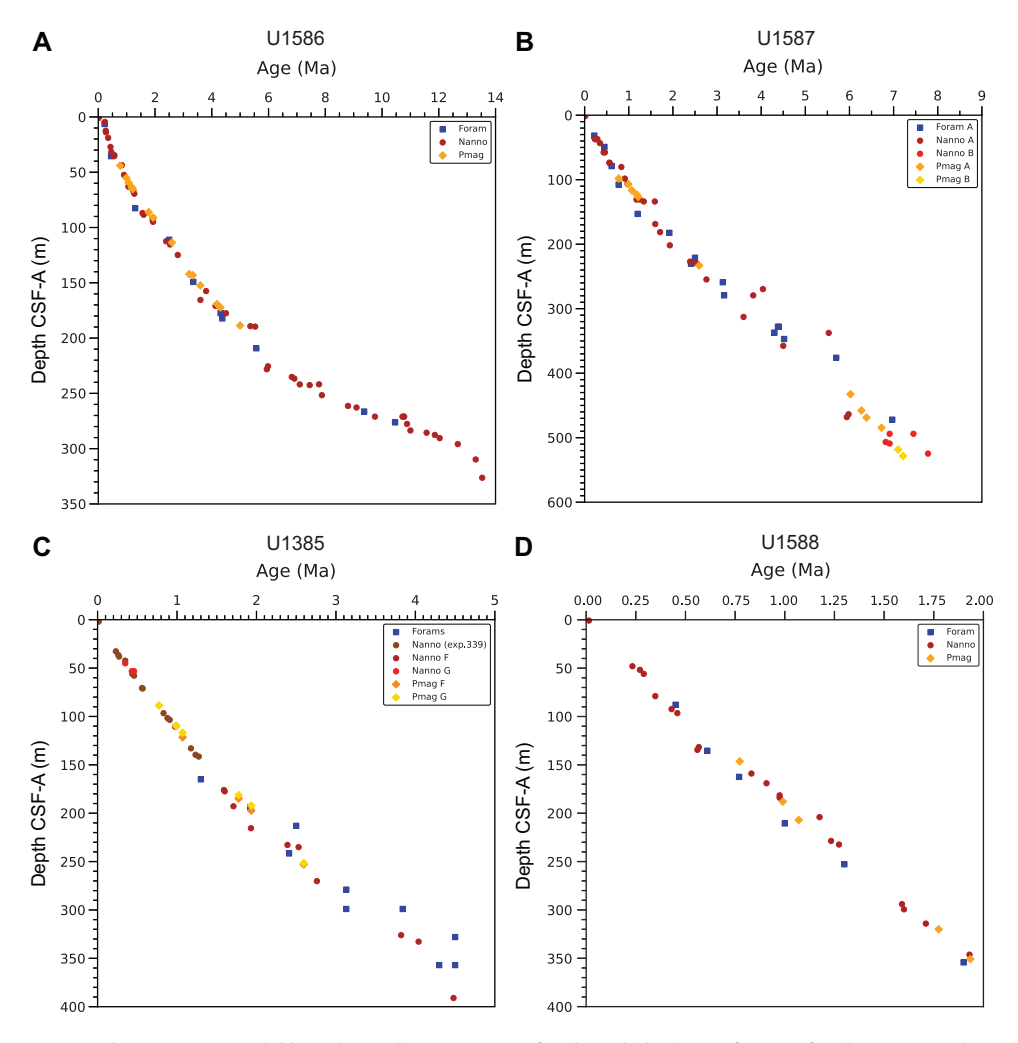


Figure F17. Preliminary age model based on calcareous nannofossils and planktonic foraminifera biostratigraphic events and magnetostratigraphic transitions for Sites (A) U1586, (B) U1587, (C) U1385, and (D) U1588.

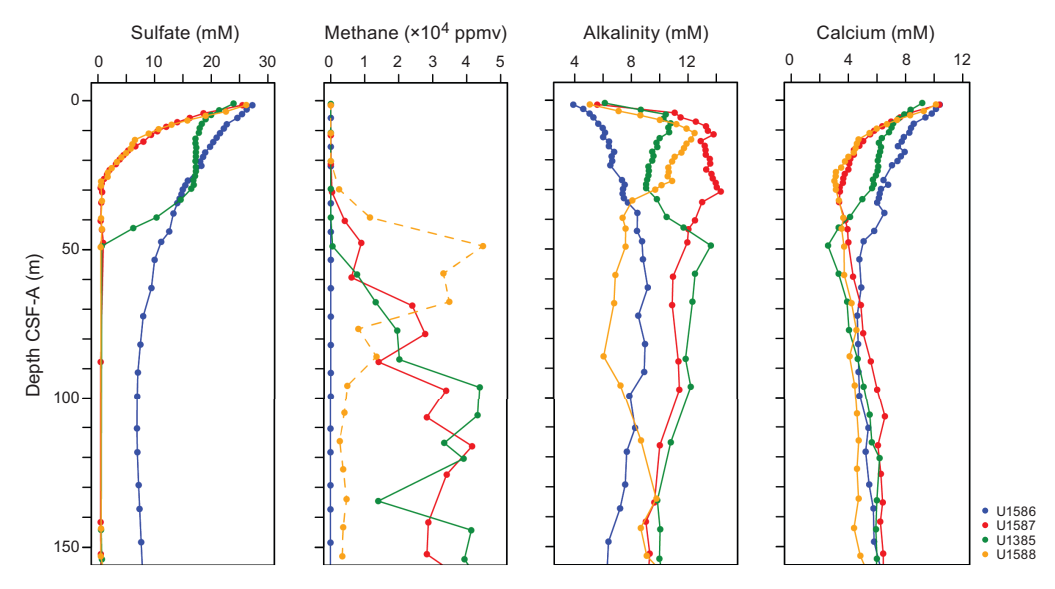


Figure F18. Comparison of IW sulfate, headspace methane, alkalinity, and calcium between Expedition 397 sites.

sediments. Elemental ratios of Si/Al, K,Al, Si/Al, Sr/Ca, and estimated biogenic Ba are highlighted as potential proxies for provenance, weathering, and productivity. Sediment physical properties data acquired from whole-round measurements for Site U1586 are generally in good agreement with those from split core measurements for gamma ray attenuation (GRA) and moisture and density (MAD) bulk densities, P-wave logger (PWL) and P-wave caliper (PWC) velocities, and MS loop and point count measurements. The cyclic variations in MS, NGR and L* color reflectance values are particularly distinct throughout all holes (Figure **F16**), showing lower MS and NGR values in carbonate-rich sediments with higher L* values, whereas higher MS and NGR values occur in clay-rich sediments with lower L* values. The gradual increasing trend of bulk densities, thermal conductivity, and P-wave velocities and decreasing trend of porosity are attributed to compaction of sediments with depth. Downhole changes in physical properties overall are coherent with the defined lithofacies based on sedimentological observations. MS gradually declines over the upper ~100 m, coinciding with a decrease in pore water sulfate. This reflects the reaction of fine-grained magnetite with hydrogen sulfide, produced by sulfate reduction, to form iron sulfides (e.g., pyrite).

Downhole logging was conducted in Hole U1586D with the triple combo tool string between 84.6 (bottom of the pipe) and 255.3 mbsf. Comparison of the processed logging and core physical properties data reveal a good correlation in the NGR (Figure **F16**) and less so for density and MS. Four downhole formation temperature measurements were made in Hole U1586A. The calculated in situ sediment temperatures ranged from 4.27°C at 34.9 mbsf to 5.77°C at 120.4 mbsf, resulting in a geothermal gradient of 26.9°C/km.

Stratigraphic correlation among holes at Site U1586 was accomplished using Correlator software. Tie points were established using L* color reflectance, MS, and the blue channel extracted from the color images (RGB-blue). A splice was constructed from 0 to 320 m CCSF-A using four holes (U1586A–U1586D). The splice is complete except for one potential small gap in the upper Pliocene where overlap is equivocal. Slump intervals noted by the sedimentologists were correlatable among all holes and have disturbed/removed variable amounts of intact stratigraphy. These include four in the middle to upper Pleistocene sequence and two in the upper Miocene. Gaps in core recovery were evident when offset holes were compared and appear to correlate with sea state. For example, gaps of up to 4 m were noted in the XCB section of Hole U1586B, which was drilled during heavy swells.

In summary, the preliminary age model based on biostratigraphy and magnetostratigraphy suggests that the sedimentary sequence recovered at Site U1586 spans the last 14 My. The combination of nearly continuous recovery, moderate sedimentation rates, clear cyclic variations in physical properties and sediment color, and a rich array of well-preserved calcareous microfossils suggest Site U1586 will provide an important record of North Atlantic surface and deepwater variability for the middle Miocene to Pleistocene.

5.2. Site U1587

5.2.1. Background and objectives

Site U1587 (proposed Site SHACK-14A) is positioned at 3480 mbsl (Figure **F19**) and bathed today by a mixture of 75% North Atlantic Deep Water (NADW) and 25% LDW sourced from the Southern Ocean (Jenkins et al., 2015). The mixing ratio of these water masses has changed in the past, as well as their vertical position in the water column, which has implications for ventilation and carbon storage in the deep Atlantic. Site U1587 is the second deepest site along the Expedition 397 bathymetric transect (paleo-CTD) and will be important for reconstructing changes in the physical and chemical properties of the deep eastern North Atlantic on both long and short timescales.

The upper Miocene to Quaternary sequence is expanded at Site U1587 and more than 500 m thick (Figure **F20**). Sedimentation rates are estimated to average \sim 10 cm/ky. We received permission from the EPSP to drill to 500 mbsf at this site but requested and were granted permission to drill an additional 50 m to extend the record well into the late Miocene.

Site U1587 was designed to recover an expanded sequence of late Miocene to Quaternary sediments with which to address several expedition objectives related to the history of MCV, orbital forcing of glacial–interglacial cycles, cyclostratigraphy, warm Pliocene climate, and the Messinian salinity crisis. The high sedimentation rates and long continuous record at Site U1587 will permit

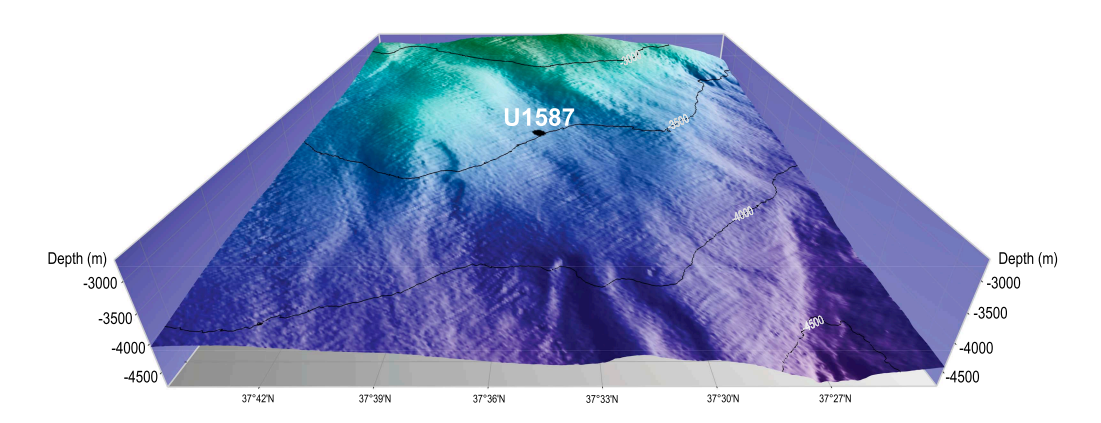


Figure F19. Location of Site U1587 on the PPA at a water depth of 3480 mbsl. See Figure F2 for broader bathymetric context.

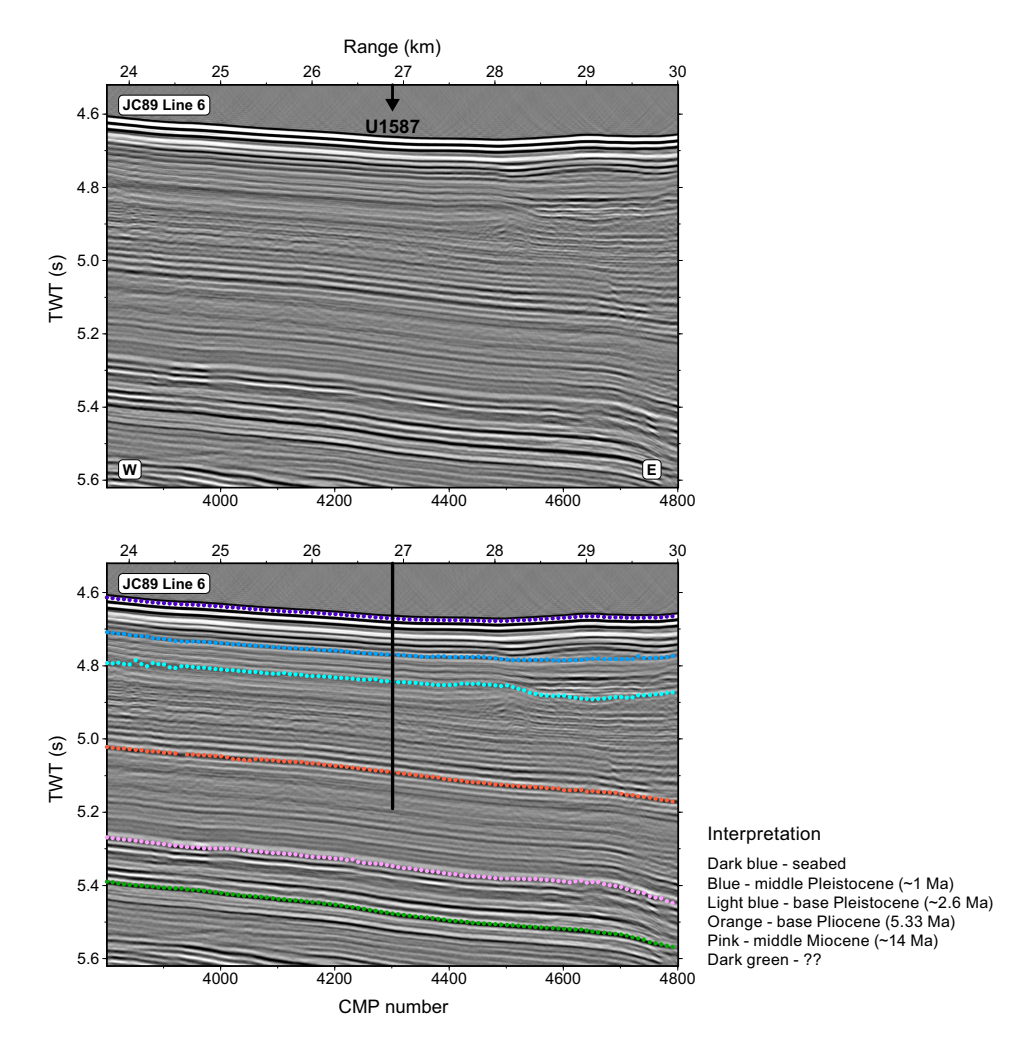


Figure F20. Original and interpreted seismic profile (JC89-6) showing the location of Site U1587 with penetration to 500 mbsf. The age of the reflectors have been revised to reflect the age of the recovered sediment. TWT = two-way traveltime, CMP = common midpoint,

paleoceanographic reconstruction at millennial resolution as the climate system evolved from the warm Pliocene, through the intensification of NHG in the late Pliocene, the obliquity-dominated "41-kyr world," the middle Pleistocene transition, and the Great Ice Ages of the "100-kyr world."

5.2.2. Operations

We arrived at Site U1587 at 1121 h on 1 November 2022 after completing the 16.9 nmi transit from Site U1586 with the thrusters down and the vessel heading controlled by dynamic positioning (DP). The drill crew made up an APC/XCB bottom-hole assembly (BHA) using the same APC/XCB PDC bit used at Site U1586.

The plan for Site U1587 was to core four holes with the APC and HLAPC systems to refusal (estimated to be approximately 250 mbsf), then core to a maximum depth of 500 mbsf using the XCB system. Formation temperature measurements were planned for the first hole using the APCT-3 tool and core orientation was planned for all APC cores. Downhole logging with the triple combo tool string was also planned for Hole U1587D.

Once on site, weather conditions and high seas caused some delays and the coring strategy was adjusted, removing the fourth hole from the plan after all site objectives had been met. Permission to deepen the site was asked for and approved by the EPSP while coring Hole U1587B. The site consisted of three holes. Hole U1587A was cored to 500 mbsf, Hole U1587B was cored to 547.8 mbsf, and Hole U1587C was cored to 567.9 mbsf. As at Site U1586, the drilling strategy consisted of using the APC system until the first partial stroke and extending the hole to total depth using the XCB system. Hole U1587C was successfully logged using the triple combo tool string to 558 mbsf, roughly 10 m above the total depth of the hole. The drill string was raised, clearing the seafloor at 0850 h on 15 November and ending Hole U1587C and the site. The bit was raised to 2484 mbrf, and at 1115 h, we started the transit to Site U1385 under DP navigation mode.

All APC cores used nonmagnetic core barrels and were oriented using the Icefield orientation tool. In total, 1615.7 m were cored at Site U1587 using the APC and XCB systems with a recovery rate of 97%. The site took 335.5 h (14.0 days) to complete.

5.2.3. Principal results

Principal results for Site U1587 are as follows:

- Recovery of a 567 m sequence ranging in age from the late Miocene (Tortonian, ~7.8 Ma) to Quaternary with sedimentation rates from 6.5 to 11 cm/ky (Figures **F17B**, **F21**).
- Continuous deposition and high sedimentation rates for the last 1.5 My are ideal for studying MCV and correlating Site U1587 to the polar ice core records (BE-OI and COLDEX Projects).
- Pliocene sediments contain very strong precession-scale cycles in color and other physical
 properties (MS, density, and NGR) (Figures F10, F22). Amplitude modulation of these precession cycles by eccentricity provides a powerful tool for developing an orbitally tuned timescale
 for Site U1587.
- Recovery of an apparently complete Messinian Stage (7.246–5.333 Ma) of the late Miocene with strong Milankovitch cyclicity consisting of alternating dark clay-rich sediments and lighter nannofossil ooze. This sequence will permit the study of the Messinian Salinity Crisis in an open ocean setting adjacent to the Mediterranean.
- Complete logging run from 81 to 558 mbsf showing cyclic variations in NGR that will be used for core-log integration (Figure F22).
- Expanded late Pliocene section documenting the intensification of NHG between 3.3 (MIS M2) and 2.6 Ma (MIS 100), including the mid-Pliocene warm period (3.3–3 Ma).

Coring in Holes U1587A, U1587B, and U1587C recovered a total of 1566 m of sediment. The dominant lithologies are nannofossil ooze and clay in varying proportions (Figure F21), which manifest as light and dark sediment layers reflected by changes in sediment physical properties. Pyrite nodules and infilled pyrite burrows are common throughout the sedimentary sequence. Bioturbation varies from slight to heavy. Drilling disturbance in a few APC cores include soupy/slurry sediments, mostly in Section 1, and slight up-arching toward the bottom of the APC interval. XCB cores are generally undisturbed, but biscuiting occurs mainly below 204 mbsf.

Nannofossils are extraordinarily abundant, and all calcareous microfossils, including ostracods, are present and well preserved. Planktonic foraminiferal preservation decreases with depth, and Miocene specimens are very small in size, recrystallized, and challenging to identify. A total of 51 biostratigraphic markers (37 nannofossils and 14 planktonic foraminifera) were recognized and suggest a continuous sequence from the late Miocene (Tortonian, 7.8 Ma) to Holocene. Nannofossil and planktonic foraminifera stratigraphic events are in good agreement with magnetostratigraphy (Figure F17B). Sedimentation rate varies between 11 and 6.5 cm/ky.

A large abundance of ichthyoliths accompanied by a high diversity of benthic foraminifera and a monospecific ostracod assemblage consisting of the genus *Xylocythere* were found in Sample 397-U1587A-22X-CC. *Xylocythere* is an ostracod genus known from chemosynthetic environments, such as hydrothermal vents, cold seeps, and fish and whale carcasses (Karanovic and Brandão, 2015; Tanaka et al., 2019), and they are also known to inhabit oligotrophic, deep-sea sediments (Steineck et al., 1990).

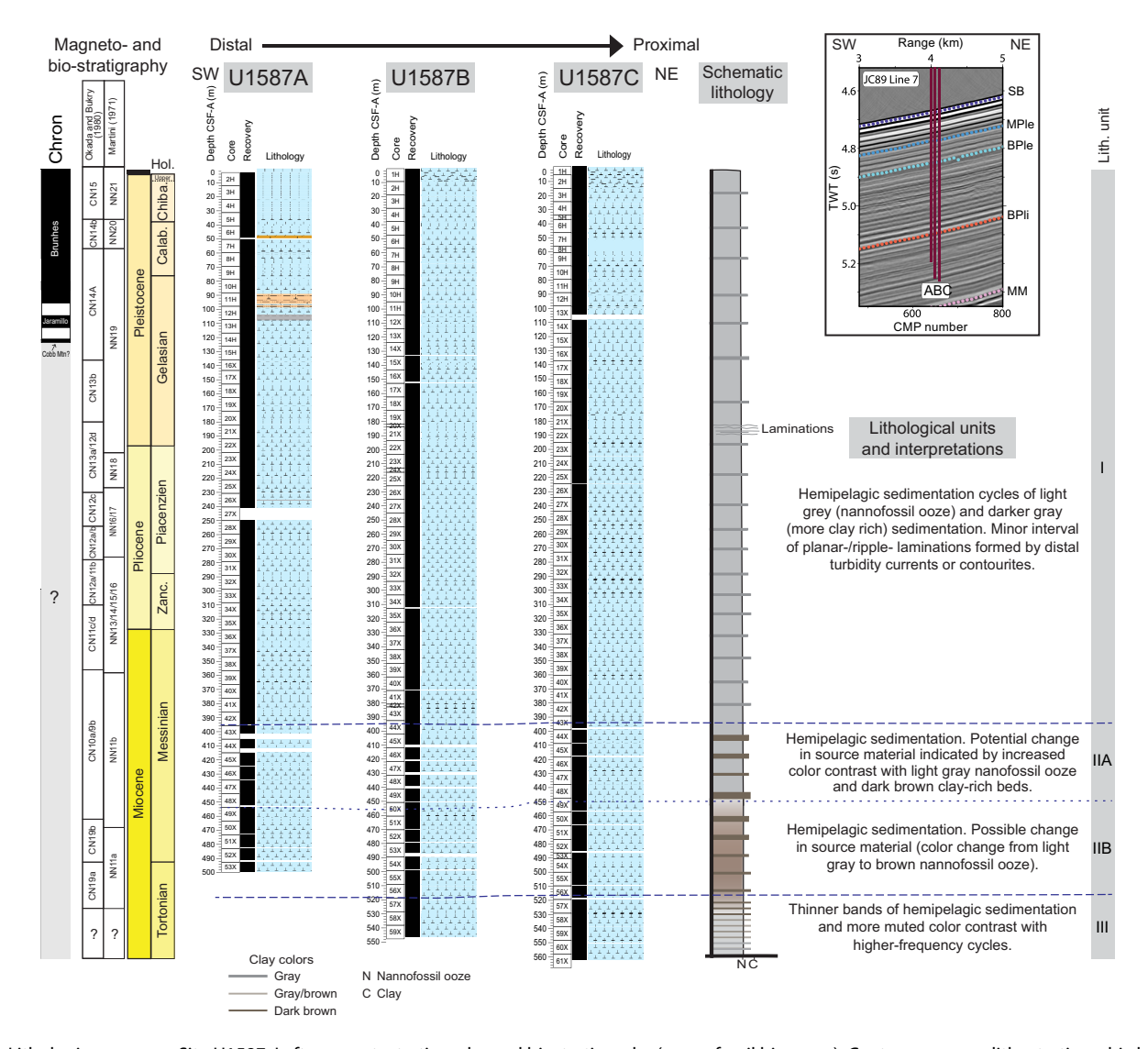


Figure F21. Lithologic summary, Site U1587. Left: magnetostratigraphy and biostratigraphy (nannofossil biozones). Center: summary lithostratigraphic logs of Holes U1587A–U1587C, ordered left to right from southwest to northeast (upslope to downslope). Blue dashed line = divisions of lithostratigraphic units, blue dotted line = division of subunits (not slump related). Right: lithologic unit names and preliminary interpretations of depositional processes. Colors are based on visual description as well as color (L*a*b*) values. Unit and subunit boundaries are primarily based on sedimentary structures as well as changes in color and banding thickness. Color is independent of lithology and is related to relative amounts of minor constituents such as pyrite and glauconite. Inset: cropped section of Seismic Line JC89 Line 7 showing location along transect and depth of the holes at the site. TWT = two-way traveltime, CMP = common midpoint, SB = seabed, MPle = middle Pleistocene, BPle = base Pleistocene, BPli = base Pliocene, MM = middle Miocene.

Paleomagnetic investigations of Site U1587 sediments focused on the measurement of NRM of archive-half core sections and a total of 142 cube samples taken from split cores and subject to stepwise alternating field (AF) demagnetization with peak fields up to 50 or 80 mT. Magnetostratigraphy of Site U1587 included the identification of the following polarity reversals and subchrons: the Brunhes/Matuyama boundary (0.773 Ma), the Matuyama/Gauss boundary (2.595 Ma), and the C3An.1n (6.023–6.272 Ma) and the C3An.2n (6.386–6.727 Ma) Subchrons. The Jaramillo (0.99–1.07 Ma) and possibly Cobb Mountain (1.18–1.215 Ma) Subchrons were identified in APC cores from Hole U1587A. The C3Bn Chron (7.104–7.214 Ma) could be recorded in Holes U1587B and U1587C, and the bottom ~20 m of sediments in Hole U1587C possibly records part of the C4n Chron (7.537–8.125 Ma).

IW samples show an increase in alkalinity, ammonium, and phosphate in the upper 50 m, whereas sulfate correspondingly decreases rapidly in the upper 30 m, indicating sulfate reduction and organic matter respiration (Figure F18). As sulfate reaches zero the concentration of methane begins to increase reaching about 40,000 ppmv at 125 mbsf. The decrease in calcium and magne-

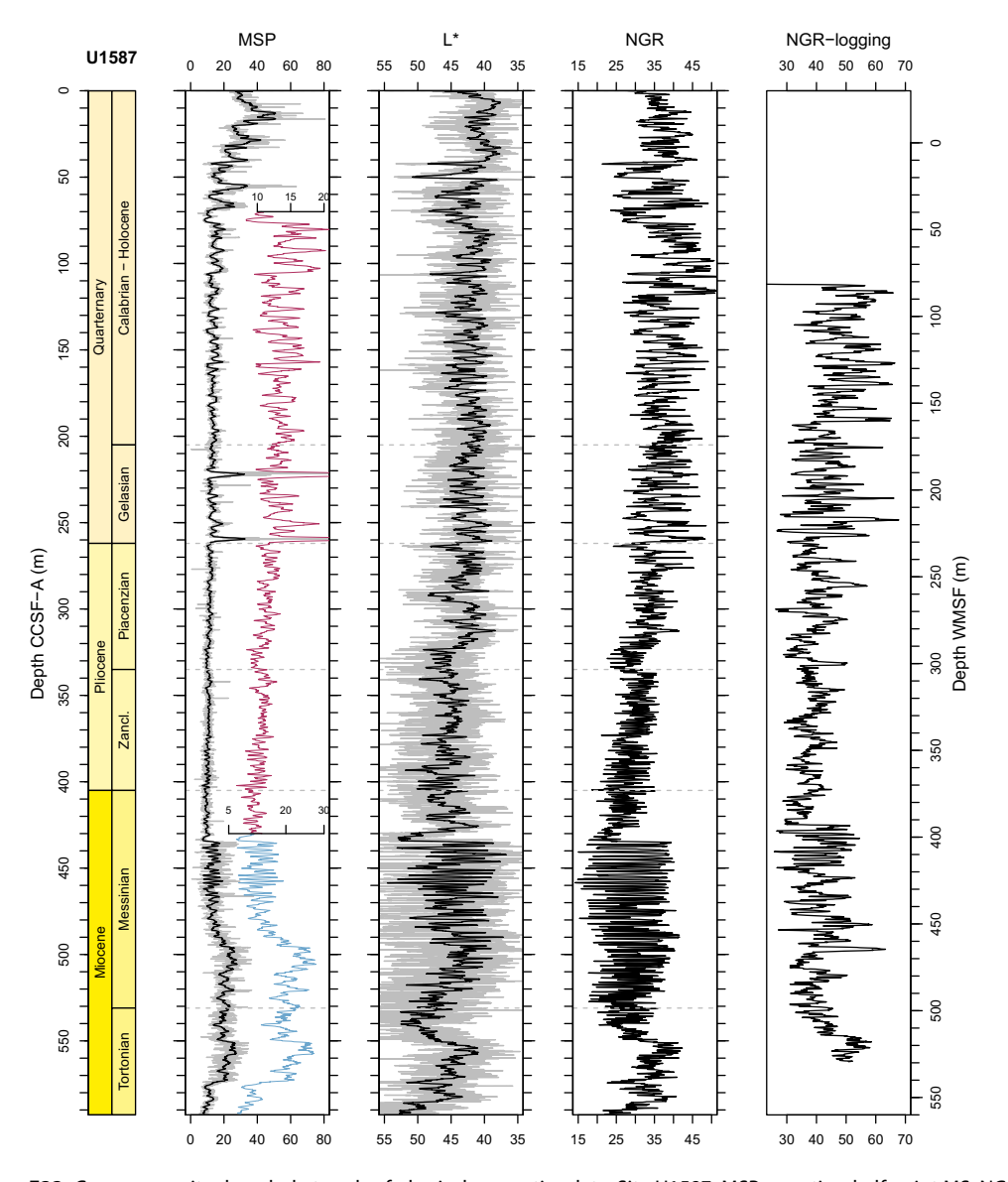


Figure F22. Core composite downhole trends of physical properties data, Site U1587. MSP = section-half point MS, NGR = whole-round NGR, NGR-logging = NGR data from the triple combo logging tool. WMSF = wireline log matched depth below seafloor. Inset MSP data (red and blue) are the same as the original signal but with an expanded scale to highlight the variability. MSP and L*: smoothed curve (black line; 50-point moving average) is shown over original data (gray line). NGR: only original data is shown.

sium in the upper 35 m reflects authigenic carbonate precipitation driven by high pore water alkalinity associated with sulfate reduction.

 $CaCO_3$ content in the sediments varies between 2.9 and 78.1 wt% with an average of 37.4 wt%. TOC, TN, and TS values are generally low, ranging within 0–2.02 wt% (mean = 0.48 wt%), 0–0.13 wt% (mean = 0.05 wt%), and 0–0.37 wt% (mean = 0.03 wt%), respectively. Organic carbon/nitrogen ratios (0–86.7; mean = 20.0) suggest that organic matter has marine and terrestrial sources.

ICP-AES data from the bulk sediment indicates elemental oxides of SiO_2 , K_2O , and TiO_2 are strongly and positively correlated to Al_2O_3 , reflecting the dominance of terrigenous detritus. The manganese and carbonate association in bulk sediment reinforces the IW indication of microbial mediated respiration reactions. Furthermore, elemental ratios of Ca/Ti, K/Al, Si/Al, Sr/Ca, and estimated biogenic Ba are potential proxies for provenance, weathering, and productivity.

Physical properties data show strong cyclic variations in MS, NGR, and color throughout the sedimentary succession retrieved at Site U1587, reflecting variations in relative proportion of carbonate and clay (Figure F22). MS and NGR show lower values in lighter carbonate-rich sediments, whereas MS and NGR values are higher in darker clay-rich sediments. MS decreases in the upper 40 m as sulfate reduction produces H₂S that reacts with magnetite to form iron sulfide minerals (e.g., pyrite). The X-ray images reveal the presence of pyrite nodules and burrow fill, diagenesis, and drilling disturbances. The gradual increasing trend of bulk densities, thermal conductivity, *P*-wave velocities, and the decreasing trend in porosity are attributed to the compaction of sediments with depth.

Following completion of drilling at Hole U1587C, the bit was pulled to 80.1 mbsf for downhole logging. The triple combo tool string was deployed into the hole to 558 mbsf. We conducted an upward pass with the caliper open at a pace of 274 m/h over the entire hole to achieve the maximum possible data resolution from the Hostile Environment Natural Gamma Ray Sonde (HNGS) of the triple combo tool string. Initial evaluation of the log from Hole U1587C looks promising for correlating many of the cyclic features seen in core physical property measurements (Figure F22).

A composite splice was constructed from 0 to 593 m CCSF-A using all three holes (U1587A–U1587C). A disturbed interval occurs from ~198 to 210 m CCSF-A, interrupting the sequence that is otherwise easy to correlate to late Pliocene and Pleistocene oxygen isotope stages. The disturbed interval appears to be in a similar stratigraphic position as the one identified at Site U1586 but removes much less section: the gap is equivalent to MIS 64–MIS 76. The late Miocene–Pliocene sequence is without apparent stratigraphic gaps, and the Pliocene sequence correlates cycle-for-cycle to Site U1586. An interval of expanded sedimentation with cycles ~1.5 m thick occupies the late Messinian. The cyclicity in sediment physical properties is remarkably strong at Site U1587 with a strong precession signal expressed throughout the late Miocene and Pliocene, which will be valuable for developing an astronomically tuned timescale.

5.3. Site U1385

5.3.1. Background and objectives

As a proof of concept for demonstrating the potential of the Iberian margin for providing long, continuous records of MCV, Site U1385 was first drilled during Expedition 339 in November 2011. As expected, a 1.45 My sequence with continuously high sedimentation rates was recovered at Site U1385 (Hodell et al., preprint). Postcruise studies demonstrated the great potential of the site to yield detailed records of MCV (Figure **F6**). On the basis of the success of Site U1385, Expedition 397 sought to extend the length of this remarkable sediment archive to 400 mbsf, spanning the entire Quaternary into the early Pliocene.

Expedition 397 Site U1385 is located \sim 1 km southwest of Expedition 339 Site U1385 (Figure **F1**) at 2592 mbsl, in the core of lower NEADW. It is the second shallowest site along the Expedition 397 bathymetric transect (paleo-CTD) (Figure **F23**), and it is positioned on Seismic Line JC089-9 (Figure **F24**). The site was designed to provide a marine reference section from the core of NEADW. During glacial periods, Site U1385 was influenced by a relatively greater proportion of deep water sourced from the Southern Ocean.

The overall objective of Expedition 397 Site U1385 is to recover a Pliocene–Pleistocene sediment sequence that can serve as a marine reference section for reconstructing the long-term history of orbital- and millennial-scale climate variability. Isotope and XRF records from Expedition 339 Site U1385 have demonstrated that MCV was a persistent feature of glacial climates over the past 1.45 My (Hodell et al., preprint). But does similar MCV persist during glacial periods beyond 1.5 Ma throughout the entire Quaternary? How does the nature (intensity, duration, and pacing) of MCV

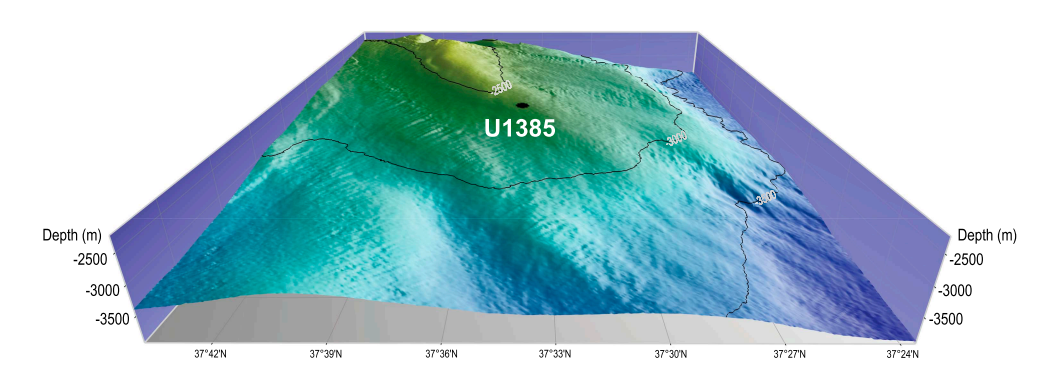


Figure F23. Location of Site U1385 on the PPA at a water depth of 2592 mbsl. See Figure F2 for broader bathymetric context.

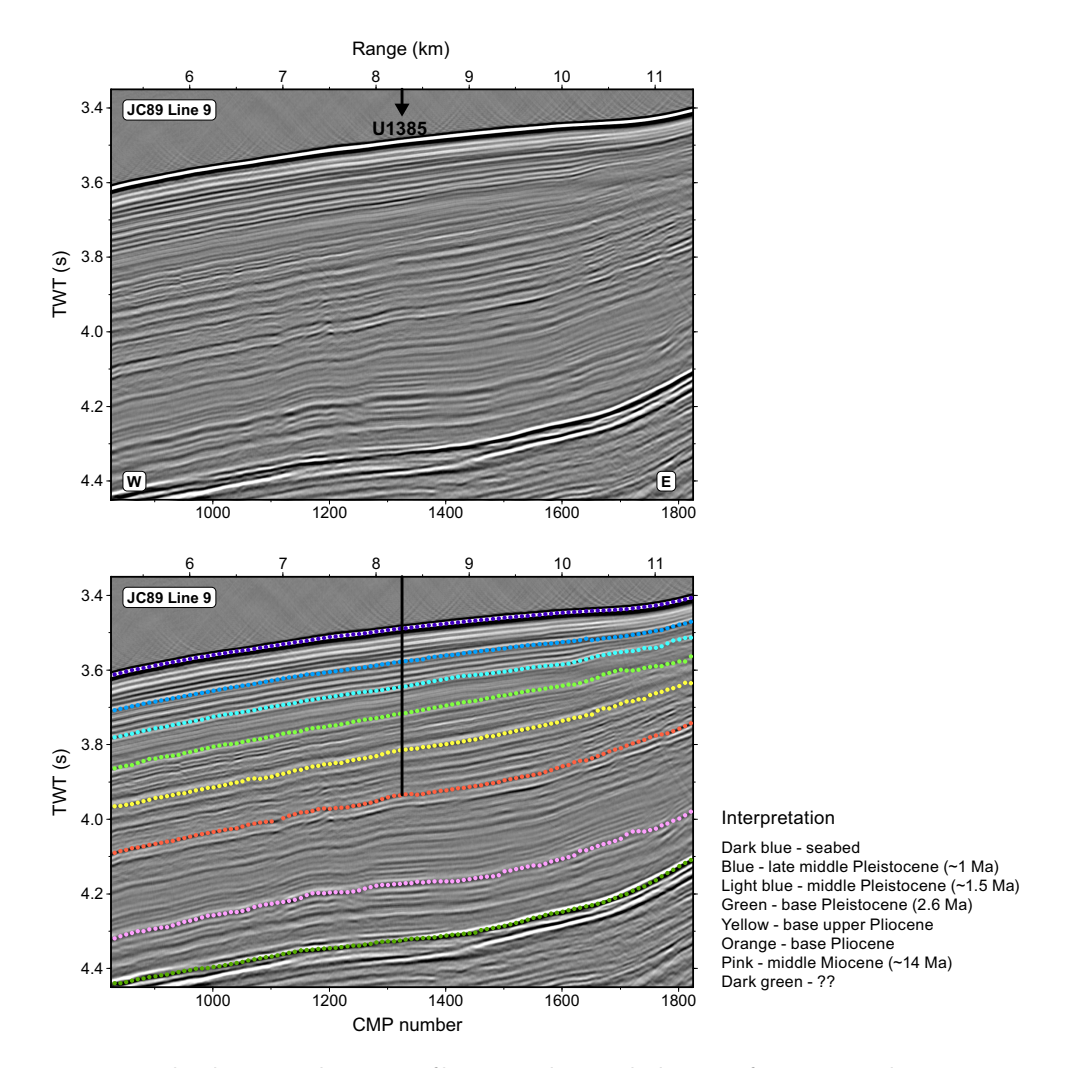


Figure F24. Original and interpreted seismic profile (JC89-9) showing the location of Site U1385 with penetration to 400 mbsf. The age of the reflectors have been revised to reflect the age of the recovered sediment. TWT = two-way traveltime, CMP = common midpoint.

change with orbital configuration and climate background state throughout the Quaternary? How did MCV change with the intensification of NHG during the late Pliocene? Was MCV suppressed during the warm Pliocene prior to the intensification of NHG as it was during most interglacial stages of the Pleistocene? How did millennial climate change interact with the effects of orbital forcing to produce the observed patterns of glacial–interglacial cycles through the Pliocene–Pleistocene? How did the relative importance of obliquity and precession evolve in the Pliocene–Pleistocene? What was responsible for the strong precession cycle observed in sediment color throughout the record? These are some of the questions that will be addressed by collaborative postcruise investigations among Expedition 397 scientists.

5.3.2. Operations

The vessel made the transit to Site U1385 with the thrusters deployed in DP mode between 15 and 16 November 2022. The move took 12.75 h with the vessel arriving on site at 0220 h on 16 November.

Site U1385 was previously occupied during Expedition 339 when five holes were cored. Expedition 397 began operations in Hole U1385F. The plan for the reoccupation of Site U1385 was to core four new holes with the APC system to refusal (estimated to be at \sim 135 mbsf) and then core to 400 mbsf using the XCB system. Orientation was planned for all APC cores in all four holes. Downhole measurements with the triple combination (triple combo) tool string were also planned for Hole U1385I.

Once on site, weather conditions and high seas caused some delays, and the coring strategy was adjusted to take full advantage of all operational time to achieve the best possible core quality. Five holes were eventually cored. Two holes were drilled ahead without coring (Hole U1385F to 96.9 mbsf and Hole U1385H to 114.6 mbsf) to allow for XCB coring in the lower section of the holes to the total depth (400 mbsf). In the other three holes, the APC system was deployed from the seafloor until the first partial stroke was registered and then the holes were extended to 400 mbsf using the XCB system. Logging was attempted in Hole U1385J using the triple combo tool string, but a portion of a bow spring centralizer on the tool broke and wedged in the lockable float valve, trapping the tool string inside the pipe, and logging was abandoned.

All APC cores used nonmagnetic core barrels and were oriented using the Icefield MI-5 core orientation tool. In total, 1537.5 m was cored using both the APC and XCB systems with an overall core recovery of 99%. Site U1385 took 336.0 h (14.0 days) to complete, including 101.0 h (4.2 days) waiting on weather.

5.3.3. Principal results

Principal results for Site U1385 are as follows:

- Drilling at Site U1385 recovered a continuous 4.5 My record of hemipelagic sediments to the early Pliocene with an average sedimentation rate between 11 and 9 cm/ky (Figures F17C, F25).
- A complete spliced section was constructed to 453 m core composite depth below seafloor (CCSF) using five holes (U1385F–U1385J).
- We reproduced the upper 158 mbsf of the sequence recovered previously at Expedition 339
 Site U1385, which provides additional sediment for sampling of these high-demand cores. We
 also recovered a more complete record of MIS 11 than was previously recovered at the site,
 which was partially missing in a hiatus at Expedition 339 Site U1385.
- Extension of the Site U1385 record beyond the last 1.45 My (MIS 47) permits the study of MCV for the earlier part of the Quaternary and late Pliocene, prior to the intensification of NHG, including linkages and phase relationship with the polar ice core and European terrestrial records.
- Variations in sediment color and other physical properties at Site U1385 display very strong cyclicity throughout the Pliocene and Pleistocene (Figure F26), permitting the development of an orbitally tuned timescale and correlation to Mediterranean cyclostratigraphy. The cycles can be matched one-for-one between Site U1385 and Sites U1586 and U1587 (Figure F10), providing a powerful cross check of the completeness of the stratigraphic sections.

• Complete recovery of Pliocene sediments to 4.5 Ma permits studies of variability under warmer climate conditions and atmospheric CO₂ concentrations similar to today.

A total of 1515.2 m of sediment was recovered at Site U1385 in five holes (U1385F, U1385G, U1385H, U1385I, and U1385J), four of which were drilled to a total depth of 400 mbsf. One lithostratigraphic unit was defined that primarily consists of nannofossil ooze with varying amounts of clay, indicating the dominance of hemipelagic sedimentation. Cyclic color banding is evident throughout all cores. Drilling disturbance is present in many cores from all holes, ranging from slight to severe, which varies with the drilling system, operation conditions (ship heave), and gas (methane) content of the sediments.

On the basis of 15 nannofossil and 11 planktonic foraminifera bioevents, the $\sim\!400$ m thick sedimentary succession at Site U1385 ranges in age from the Pleistocene to the early Pliocene ($\sim\!4.5$ Ma). Both nannofossils and foraminifera show good preservation and are very abundant to common throughout the section. The zonal schemes of the two microfossil groups are in good agreement and consistent with previous biostratigraphy of Expedition 339 Site U1385 for the upper 150 mbsf.

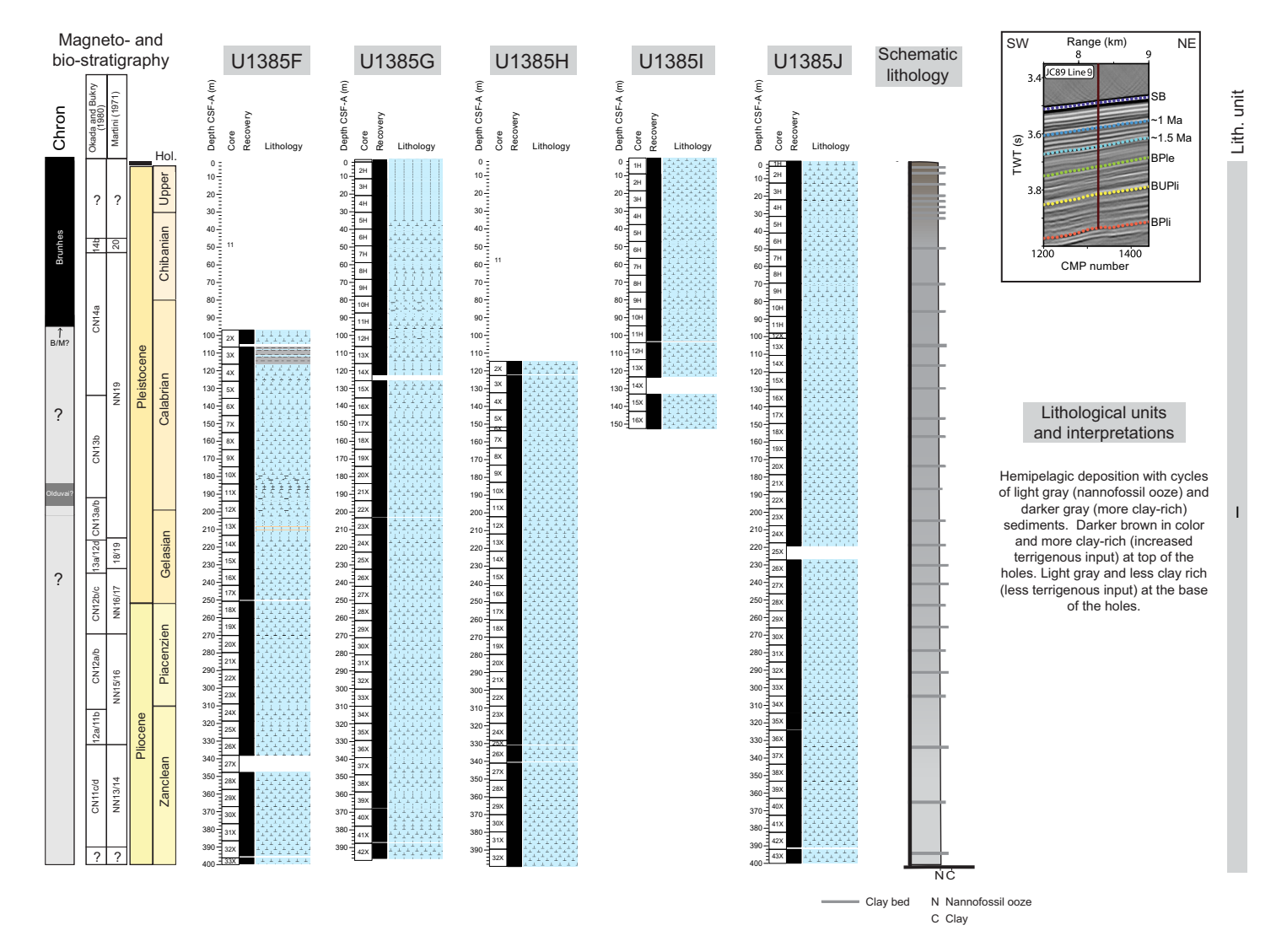


Figure F25. Lithologic summary, Site U1385. Left: chronostratigraphy and biostratigraphy (nannofossil biozones). Paleomagnetic horizons labeled with a question mark (?) are uncertain. Center: summary lithostratigraphic logs of Holes U1385F–U1385J. Right: lithologic unit names and preliminary interpretations of depositional processes. Colors are based on visual description as well as L*a*b* values. Color is independent of lithology and is related to relative amounts of minor constituents such as pyrite and glauconite. Inset: cropped section of Seismic Line JC89 Line 9 showing location along transect and depth of Holes U1385F–U1385J. TWT = two-way traveltime, CMP = common midpoint.

Magnetostratigraphy of Site U1385 was established based on the natural remanent magnetization (NRM) after 20 mT demagnetization using inclination and orientation-corrected declination data from archive-half core sections and stepwise NRM demagnetization data from discrete cube samples. The Brunhes/Matuyama boundary (0.773 Ma) is identified in APC cores from Holes U1385G, U1385I, and U1385J. The Jaramillo Subchron is recorded in XCB cores from Holes U1385F, U1385G, U1385I, and U1385J. The Olduvai Subchron (1.775–1.934 Ma) and the Matuyama/Gauss boundary (2.595 Ma) are recorded in XCB cores from Holes U1385F, U1385G, U1385H, and U1385J. The magnetostratigraphy and biostratigraphy are generally in good agreement, and sedimentation rates vary between 11 and 9 cm/ky (Figure F17C).

In the upper 150 m CSF-A, the interstitial water (IW) chemistry of Expedition 397 Site U1385 is very similar to that of Expedition 339 Site U1385 (Expedition 339 Scientists, 2013b). Sulfate shows a two-step decrease before reaching values of zero by 48.8 m CSF-A (Figure F18). The first step represents organoclastic sulfate reduction, and the second represents anaerobic oxidation of methane (Turchyn et al., 2016). Once sulfate reaches zero, methane increases, reaching maximum values of \sim 35,000 between 100–280 m CSF-A. Alkalinity, ammonium, and phosphate also increase

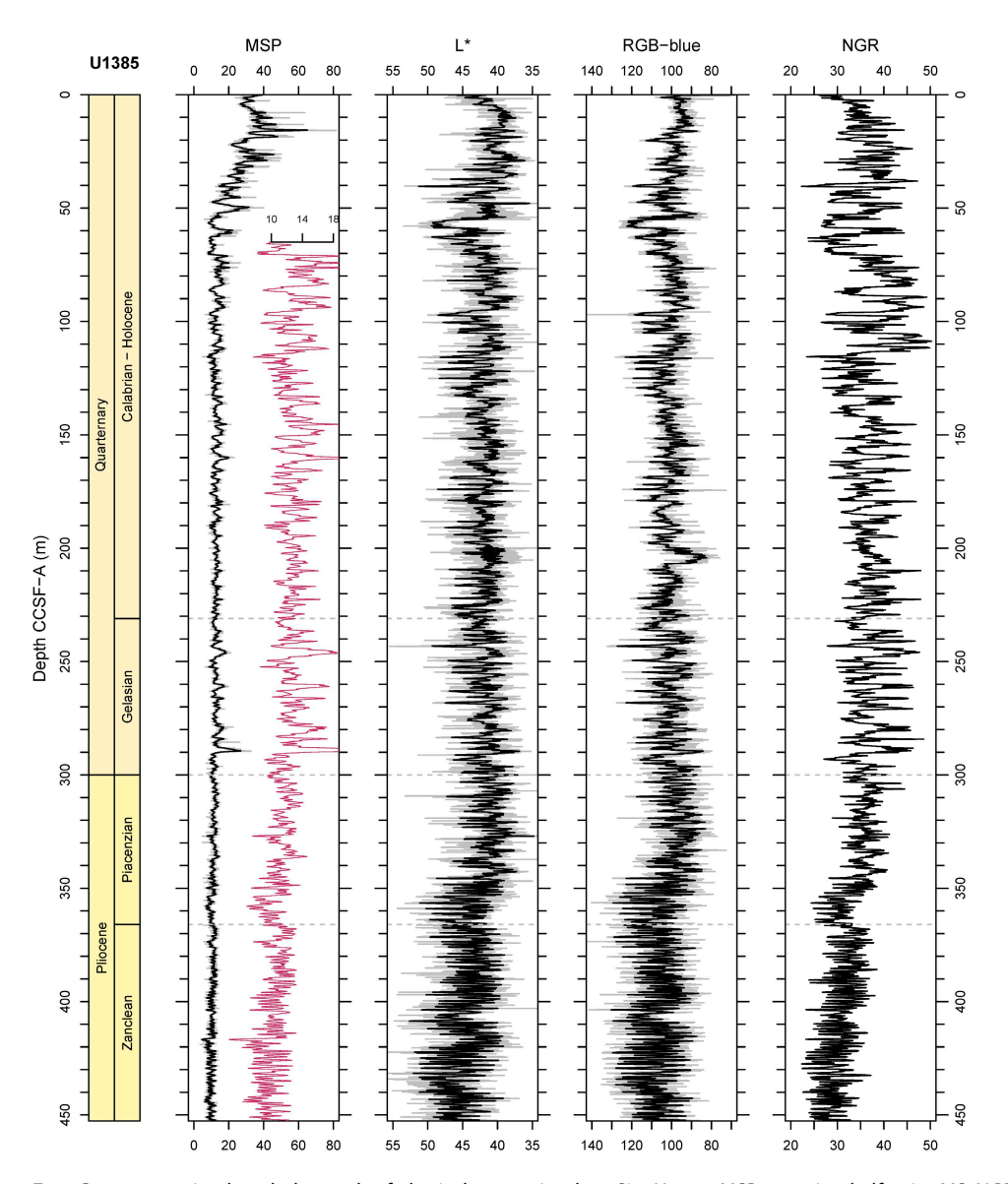


Figure F26. Core composite downhole trends of physical properties data, Site U1385. MSP = section-half point MS, NGR = whole-round NGR. The red MSP data are the same as the original signal but with an expanded scale to emphasize the cyclic variability. MSP, L*, and RGB-blue: smoothed curve (black line; 20-point moving average) is shown over original data (gray line). NGR: only original data is shown.

in the upper 50 m CSF-A in conjuction with sulfate reduction. Calcium declines in two steps in the upper 50 m, likely reflecting authigenic precipitation of carbonate as a consequences of increased alkalinity associated with the two-step change in sulfate reduction.

The calcium carbonate ($CaCO_3$) content of the sediment averages 38.8 wt%, varies between 15.2% and 63.3%, and is positively correlated with L* reflectance and negatively correlated with NGR. Total organic carbon (TOC), total nitrogen (TN) and total sulfur (TS) values at Site U1385 are generally low with a mean value of 0.48, 0.005, and 0.115 wt%, respectively. Organic C/N ratios (mean = 20.2) suggest that organic matter is marine dominated with higher terrestrial input in the upper 75 m CSF-A.

Bulk sediment geochemistry suggests that Ca is primarily biogenic carbonate, and because of the incorporation of Sr into biogenic carbonates, both elements show an inverse relationship with Al. Barium is weakly correlated with Al or Ca, likely due to the presence of barite. Manganese seems to be mainly associated with carbonate. Elemental ratios of Ca/Ti, Si/Al, Ti/Al, Zr/Al, K/Al, Sr/Ca, and estimated biogenic Ba are suggested as potential proxies of provenance, weathering, and productivity.

Physical properties data acquired from whole-round measurements follow those from split core measurements. A decline in MS in the upper 50 m follows sulfate reduction in the sediment pore waters, suggesting that H_2S from sulfate reduction reacts with Fe in magnetite to produce iron monosulfides and pyrite. The cyclic variations in MS, NGR, and L^* color reflectance parameter values are particularly strong throughout all holes at Site U1385 (Figure F26), showing lower MS and NGR values in carbonate-rich sediments with higher L^* values and higher MS and NGR values in clay-rich sediments with lower L^* values. The gradual increasing trend of bulk densities, thermal conductivity, and P-wave velocity and the decreasing trend in porosity are attributed to the compaction of sediments with depth. The X-ray images reveal the presence of pyritized burrows, authigenic minerals, gas expansion, and drilling disturbance.

Stratigraphic correlation between holes at Site U1385 were accomplished using Correlator software (version 4.0.1). Tie points were established using the L* color reflectance parameter, whole-round MS, and the blue color channel extracted from the core images (RGB-blue). We constructed a splice from 0 to 452.7 m CCSF-A using all five of the newly drilled holes at the site (U1385F–U1385J). The data from Site U1385 will be integrated postcruise with Expedition 339 Holes U1385A–U1385E to produce a common splice. The Pliocene sequence correlates cycle-for-cycle to Sites U1586 and U1587 (Figure **F10**).

5.4. Site U1588

5.4.1. Background and objectives

Site U1588 (proposed Site SHACK-10B) is the closest to the coast and the shallowest of the proposed depth transect (1339 mbsl) (Figures F1, F2, F27). The site is on a drift deposit formed under the influence of the lower MOW (Hernández-Molina et al., 2014). It lies on the broad, gently

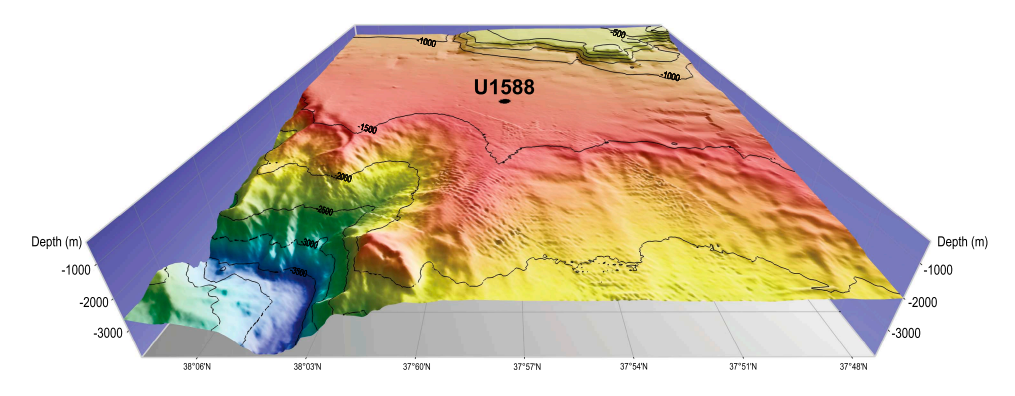


Figure F27. Location of Site U1588 on the PPA at a water depth of 1339 mbsl. See Figure F2 for broader bathymetric context.

inclined middle-slope region of the PPA, where the seismic data indicate an extensive plastered drift deposit located on the distal part of the contourite system (Figure F28). The water depth of Site U1588 complements the sites drilled during Expedition 339 in the Gulf of Cádiz (Sites U1386–U1390) and along the Portuguese margin (Site U1391) at intermediate water depths (560–1073 mbsl) to study past variations in the depth and intensity of the MOW.

Our objective at Site U1588 was to drill multiple holes to 500 mbsf to recover a continuous and complete Pliocene–Pleistocene sedimentary succession (Figure F28). Sedimentation rates at Site U1588 are the highest (±20 cm/ky) of the four sites drilled during Expedition 397 (Figure F4), which provides a marine reference section for reconstructing climate variability at high temporal resolution (millennial to submillennial) and studying how the MOW has varied on orbital and millennial timescales.

5.4.2. Operations

The operational plan for Site U1588 was to core five holes with the APC/XCB systems. The first three were to be cored to 500 mbsf, and the final two holes were to be cored to 250 mbsf. Downhole logging measurements were to be conducted in Hole U1588D. Because of time constraints toward the end of the expedition and unexpectedly high methane gas content in the formation, the coring plan was shortened to three holes to approximately 350 mbsf and a fourth hole cored as

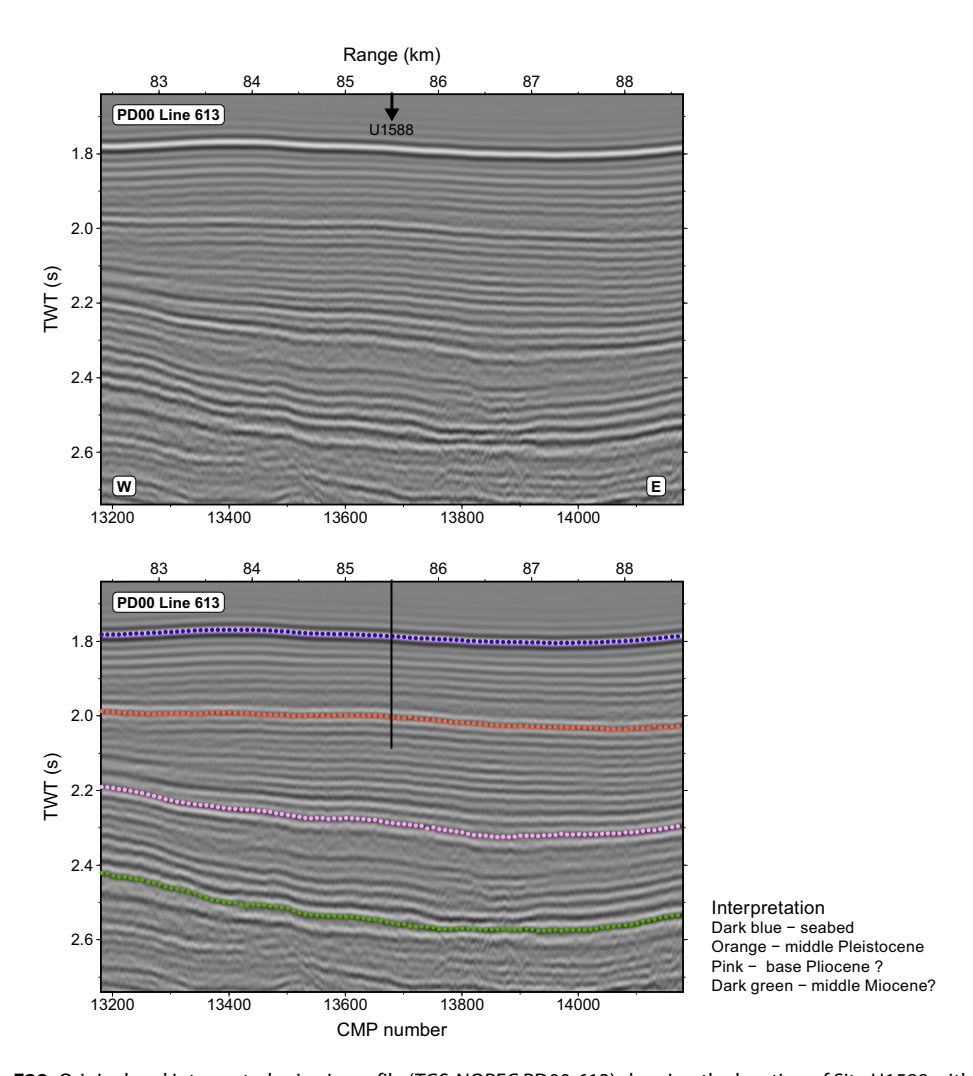


Figure F28. Original and interpreted seismic profile (TGS-NOPEC PD00-613) showing the location of Site U1588 with penetration to ~400 mbsf. The depth of penetration and age of the reflectors have been revised to reflect the actual depth and age of the recovered sediment (data courtesy of TGS-NOPAC Geophysical Company ASA). TWT = two-way traveltime, CMP = common midpoint.

deep as possible with the remaining time, reaching a final depth of 412.5 mbsf. Downhole logging was canceled.

Significant core expansion and curatorial difficulties encountered in Hole U1588A due to high methane gas content in the sediment led to a change in the XCB coring strategy starting on Core 397-U1588A-25X and followed at all subsequent holes at the site. XCB cores were taken using half advances, giving cores room to expand inside the core liners as gas was released.

Holes U1588A, U1588B and U1588D were APC cored to 154.2, 81.8, and 90.5 mbsf, respectively, and then XCB cored to their final depths. Because of increasing seas, APC coring was dropped in Hole U1588C in favor of drilling ahead to 92.0 mbsf before starting to XCB core the lower section.

A total of 242 cores were taken at the site, 37 APC and 205 XCB. All APC cores used nonmagnetic core barrels and were oriented using the Icefield orientation tool. In total, 1377.1 m were cored, recovering 1748.93 m (127%). Formation temperature measurements were done with the APCT-3 tool in Hole U1588A on Cores 4H, 7H, 10H, and 13H. Site U1588 took 186.75 h (7.8 days) to complete.

5.4.3. Principal results

Principal results for Site U1588 are as follows:

- Successful demonstration of an alternative coring method for gassy sediment involving half advances of the XCB, thereby allowing the core to expand into the empty part of the liner.
- Recovery of an expanded 412.5 m sequence spanning the last 2.3 My with sedimentation rates averaging 18 cm/ky (Figures F17D, F29).
- Recovery of a marine reference section for studying Quaternary climate variability at very high temporal resolution (millennial to submillennial), including changes across the mid-Pleistocene transition.
- Proxy signals of surface temperature (e.g., alkenones, planktonic $\delta^{18}O$) will constitute a marine sediment analog for the Greenland ice core.
- Contourite sedimentation under the influence of the lower MOW will, in conjunction with other Expedition 339 sites, provide a detailed history of the response of the MOW to orbital and millennial climate change.

At Site U1588, because of the significant core expansion, all depths of the scientific results are reported in meters on the core depth below seafloor, Method B (m CSF-B), scale hereafter. The CSF-B depth scale corrects for core expansion by uniformly compressing the recovery to the advance of the bit (driller's depth).

The ~412.5 m thick sedimentary succession drilled at Site U1588 consists of one lithostratigraphic unit (Figure F29). Most sediments are from Lithofacies 1 and consist primarily of nannofossil ooze, with varying amounts of inorganic/detrital/recrystallized calcium carbonate of indeterminate origin (hereafter termed "carbonate") and clay. The abundance of nannofossil ooze with substantial amounts of clay and carbonate indicates the persistence of hemipelagic sedimentation and an indeterminate (recrystallized or detrital) source of carbonate at Site U1588 through the Pleistocene. Foraminifera, diagenetic features (dark patches and pyrite), and rare, subtle color banding are disseminated throughout the cores. Bioturbation varies from absent to heavy and generally increases downhole. Deformational sedimentary structures are rare and, when present, are at a decimeter scale. Drilling disturbance is present within most cores in all holes, varies from slight to severe, and is influenced by the drilling type, operation conditions (ship heave), and methane gas contents of sediments.

Site U1588 ranges in age from the Holocene to the early Pleistocene (~2.2 Ma) based on calcareous nannofossils (21 bioevents) and planktonic foraminifera (6 bioevents) biostratigraphy. The zonal schemes of calcareous nannofossils and planktonic foraminifera generally agree, indicating an average sedimentation rate of 18 cm/ky (Figure F17D).

The site revealed excellent preservation for all microfossils, including biogenic Si, mainly in the form of diatoms, sponge spicules, silicoflagellates, and radiolarians at specific depth intervals that

are associated with some glacial terminations (e.g., Terminations XII, V, and VI). The occurrence of biogenic silica at these terminations is in good agreement with observations from Expedition 339 Site U1391 (Abrantes et al., 2017). All calcareous microfossils, including coccoliths, planktonic and benthic foraminifera, and ostracods, are abundant to common and are generally well distributed throughout the succession. Excellent preservation is also indicated by the presence of pteropods. Ostracod diversity increases toward the top of the sequence, and variations in planktonic foraminifera species composition throughout the Pleistocene are likely associated with glacial—interglacial or even millennial-scale climate fluctuations. Benthic foraminifera assemblages suggest variability in organic flux and/or oxygen conditions relative to changes in surface productivity and bottom water oxygenation.

The magnetostratigraphy of Site U1588 was established based on the NRM (after 20 mT demagnetization) inclination and (orientation-corrected) declination data from archive-half core sections and stepwise NRM demagnetization data from discrete cube samples. The Brunhes/Matuyama boundary (0.773 Ma) is identified in APC cores from Hole U1588A and XCB cores from Holes U1588B–U1588D. The Jaramillo Subchron and the top of Olduvai Subchron (1.775 Ma) appear to be recorded in XCB cores from all four holes. However, the bottom of Olduvai Subchron (1.934 Ma) is only recorded in XCB cores recovered in the deepest Hole U1588D (below 350 m CSF-B).

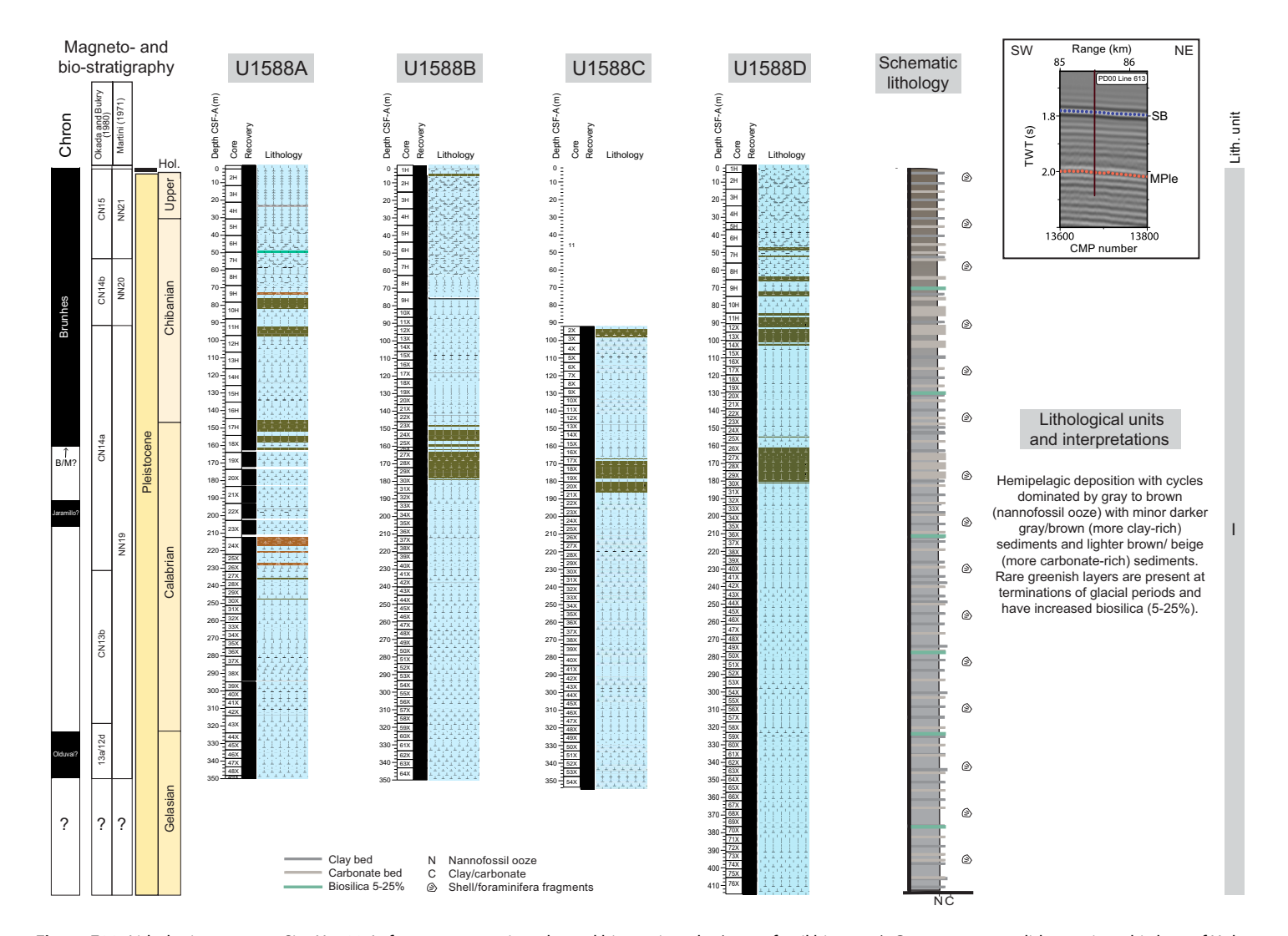


Figure F29. Lithologic summary, Site U1588. Left: magnetostratigraphy and biostratigraphy (nannofossil biozones). Center: summary lithostratigraphic logs of Holes U1588A–U1588D. Right: lithologic unit name and preliminary interpretation of depositional processes. Colors are based on visual description as well as L*a*b* values. Inset: cropped section of Seismic Line JC89 Line PD00-613 showing location along transect and depth of the holes at the site. TWT = two-way traveltime, CMP = common midpoint.

Geochemistry of IW samples show that alkalinity, ammonium, and phosphate increase in the upper 50 m, whereas sulfate shows a two-step decrease in the upper 50 m (Figure F18), indicating organic matter respiration. At this site, the sulfate reaches zero and stays low. Methane levels increase to about 45,000 ppmv at 50 m CSF-B but decline to \sim 5,000 ppmv by 100 m to the bottom of the hole. Given the consistently high degassing of sediment below 50 m CSF-B, it is likely the decrease in methane concentrations measured in headspace samples does not accurately reflect the sediment gas content, which is supported by very high methane concentrations measured in void gas.

 $CaCO_3$ content varies between 16.0% and 53.6% and averages 30.2 wt%. The $CaCO_3$ content determined by coulometric titration shows consistent results with stoichiometric $CaCO_3$ calculated from the Ca concentrations measured by ICP-AES, and both are positively correlated with L* reflectance and negatively correlated with NGR, TOC, TN, and TS. TOC, TN, and TS values at Site U1588 are generally low, ranging 0.30–1.89 wt% (mean = 0.74 wt%), 0.042–0.189 wt% (mean = 0.085 wt%), and 0–3.18 wt% (mean = 0.291 wt%), respectively. Organic C/N ratios (3.04–16.5; mean = 8.97) suggest that organic matter is marine dominated.

Bulk sediments SiO_2 , K_2O , and TiO_2 show strong positive correlations with Al_2O_3 , indicating the dominance of terrigenous detritus. Relatively weak correlations are observed for Fe_2O_3 , MgO, Na_2O , MnO, and Ba against Al_2O_3 due to the widespread presence of authigenic and biogenic phases such as pyrite, dolomite and/or Mg-bearing calcite, halite (NaCl) precipitated from seawater, Mn hydroxides, and barite, respectively. Bulk sediment Ca primarily represents biogenic carbonate ($CaCO_3$), and because of the incorporation of Sr into biogenic carbonates, both elements show an inverse relationship with Al. Elemental ratios of Ca/Ti, Si/Al, Ti/Al, Zr/Al, K/Al, Sr/Ca, and estimated biogenic Ba are potentially useful proxies for provenance, weathering, and productivity.

Physical properties data acquired from whole-round core measurements for Site U1588 are in good agreement with measurements carried out on split core and discrete samples. A decrease in MS at shallower depths follows sulfate reduction in sediment pore waters. The cyclic variations in MS, NGR, and L* values are distinct throughout all holes (Figure F30), showing lower NGR and MS values in carbonate-rich sediments with higher L* values, whereas higher MS and NGR values occur in clay-rich sediments with lower L* values. The gradually increasing values of bulk density, thermal conductivity, *P*-wave velocity, and a decreasing trend in porosity are attributed to the compaction of sediments with increasing depth. X-ray imaging of the core sections revealed the presence of authigenic minerals and burrows, further evidence of gas expansion, and drilling disturbance.

Downhole temperature measurements (APCT-3) were made in Hole U1588A at 30.7, 56.2, 87.7, and 116.2 m CSF-B. The calculated in situ sediment temperatures ranged from 12.12°C at 30.7 m CSF-B to 14.88°C at 116.2 m CSF-B, resulting in a geothermal gradient of 33.2°C/km. This value is slightly lower than that measured at Site U1385 during Expedition 397 and the published value for the region.

Stratigraphic correlation between holes at Site U1588 was accomplished using Correlator software (version 4.0.1). Tie points were established using MS from the Whole-Round Multisensor Logger (WRMSL) as well as NGR. A splice was constructed from 0 to 366 m CCSF-B using four holes (U1588A–U1588D). The drilling and correlation strategies were unique at this site due to the severely expanded cores. A mixture of APC, full-advanced XCB, and half-advanced XCB coring was used for different levels of core expansion at each hole. Instead of the CSF-A scale, the CSF-B scale was used for correlation. Considering the high-quality XCB cores and the high sedimentation rate at this site, the composite section was nearly complete with only one possible small gap.

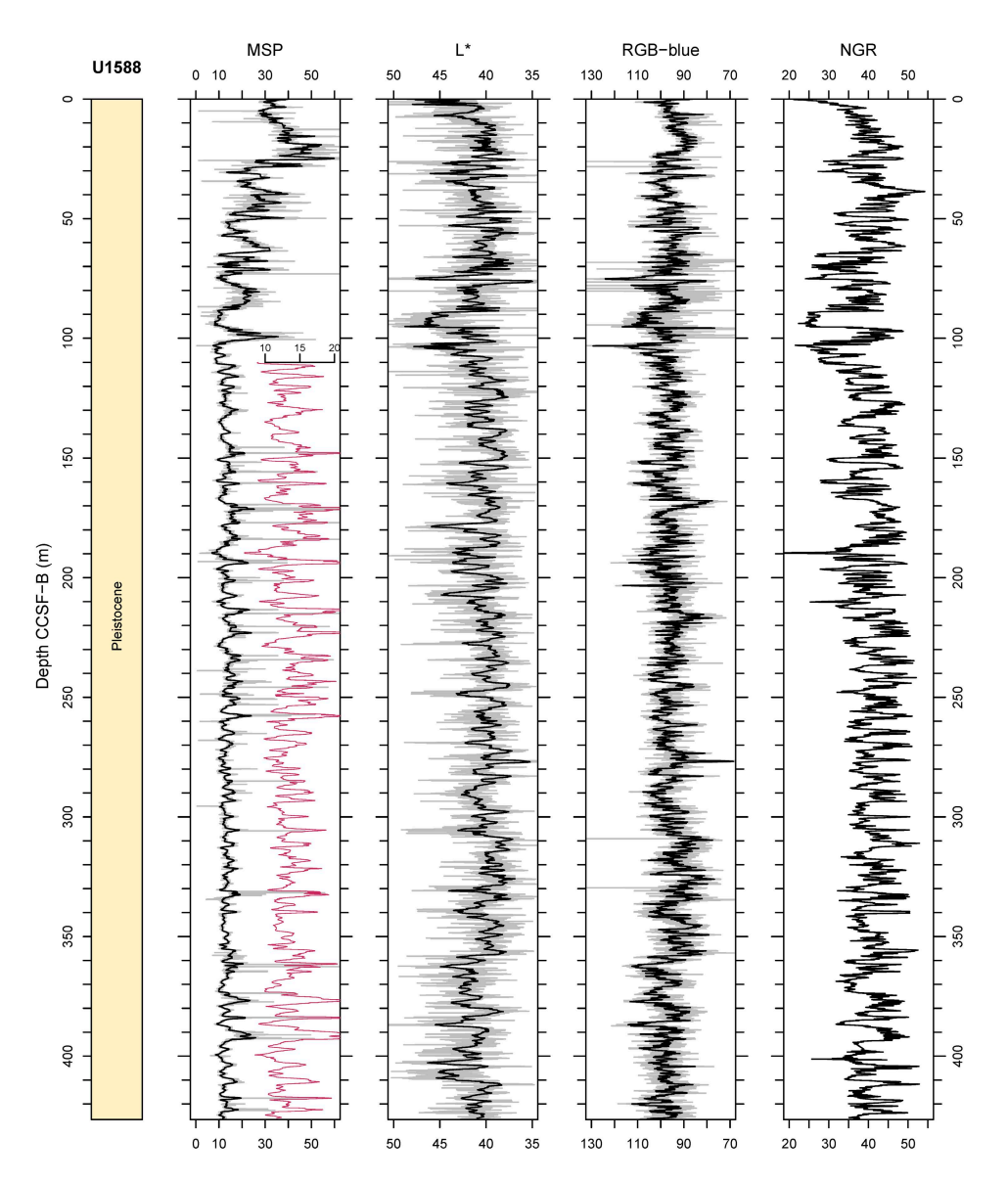


Figure F30. Core composite downhole trends of physical properties data, Site U1588. MSP = section-half point MS, NGR = whole-round NGR. The red MSP data are the same as the original signal but with an expanded scale to emphasize the cyclic variability. MSP, L*, and RGB-blue: smoothed curve (black line; 20-point moving average) is shown over original data (gray line). NGR: only original data is shown.

6. Education and outreach

Expedition 397 had two Education and Outreach Officers: Amy Mayer, a reporter, producer, photographer, and storyteller based out of California, USA, who conducted outreach from aboard *JOIDES Resolution*; and Maya Pincus, a high school teacher from New York, USA, who carried out education activities onshore in Portugal. The officers communicated the science objectives of the expedition to students and the general public across the world through several diverse platforms, including live ship-to-shore events, webinars, social media, videos, radio pieces, blog posts, and in-person activities. The onshore officer also developed curriculum and educational materials for students in primary and secondary school in English and Portuguese.

6.1. Ship-to-shore connections

The onboard Education and Outreach Officer hosted live ship-to-shore video tours over Zoom to interact with formal and informal groups all over the world. These events introduced students and

members of the general public to the goals, methods, and scientific findings of Expedition 397 and the broader history and significance of scientific ocean drilling.

The typical broadcast began with an introduction to IODP, *JOIDES Resolution*, and Expedition 397. The scientific context and objectives of the expedition were translated into language appropriate for each specific audience. In many cases, a scientist who shared a non-English language with the audience cohosted the tour. Participants then received a tour of the ship that included (depending on daylight and weather conditions) the lifeboats, bridge, derrick, rig floor, catwalk, and laboratories. Viewers learned about the core flow process from scientists in each laboratory, as well as how physical properties analyses, core description, paleomagnetism, biostratigraphy, and geochemistry contribute to the research and goals of the expedition. Tours ended with extensive question and answer sessions with scientists and the outreach officer.

Over the course of the expedition, the onboard Education and Outreach officer facilitated 86 Zoom tours to 64 different institutions, including primary and secondary schools, colleges and universities, conferences, museums, after school programs, informal public groups, and some special productions such as the IODP Germany annual Geo Show. Student audiences ranged from Pre-K to graduate university level. The Expedition Project Manager, both Co-Chief scientists and 18 members of the science party assisted with the tours and many of the scientists recruited tour audiences in their home countries. Two Chinese scientists worked with IODP China to arrange a live tour with six high schools. That connection was facilitated by the Xinhua official Chinese news agency, which livestreamed the event, reaching an audience of approximately 3.5 million people in China.

Tours were conducted in eight different languages and reached over 3,505,000 people across four continents, in Australia, Belgium, Canada, China, France, Germany, India, Japan, Portugal, Spain, Sweden, the United Kingdom, and the United States of America. Broadcasts in America reached 13 states: Alabama, California, Illinois, Indiana, Iowa, Massachusetts, New Mexico, New York, Ohio, Oregon, Pennsylvania, Texas, and Washington. Demand for broadcasts was very high, with two to four taking place on most weekdays.

Participants were provided with educational materials and useful links from https://joidesresolution.org as well as custom-made Expedition 397 resources prior to their scheduled event. In a follow-up email after the tour, teachers or coordinators were asked for feedback and attendance numbers.

At times, scheduling broadcasts was a challenge. The sole onboard outreach officer was responsible for interacting with groups in many different time zones, leading to broadcasts at all hours of the day. Members of the science party supported this effort by leading broadcasts to their home countries when they were available. Broadcasts were also affected by an inconsistent internet connection at sea. Multiple broadcasts had to be rescheduled after two extended (12 and 14 h) internet disruptions. The broadcasts that did take place were wholly successful, with positive feedback from event organizers. Below are some reactions from teachers:

- "It was great to get a live peek into the world of a working research vessel—as a sedimentologist, it is always super exciting to see a good core pulled out. Thank you so much for the tour/discussion! I'll definitely do it again with future classes!"
- "The students were very excited when I told them what was going to happen—this was a surprise to them as we'd just finished talking about IODP in the lecture, so they only knew we were doing this 5 minutes before we started! They really appreciated seeing around the ship."
- "The timing of going outside just as a core came up was great! It was like you planned it that way for us! We had looked at some IODP core photos, so the students recognized the calcareous ooze when they saw it. I was proud of them."

6.2. Expedition activities

While at sea, the education and outreach priority was to learn more about the science of Expedition 397, as well as the people involved in it. This included shadowing scientists, technicians, and

crew members; conducting interviews; participating in scientific meetings and discussions; and documenting science and daily life by photograph and sound.

A total of 11 blog posts were written for the *JOIDES Resolution* website. These blogs covered topics including the scientific objectives and methods of the expedition, life at sea, and geographic history of the drilling locations. Throughout the expedition, 28,000 users visited the *JOIDES Resolution* website over 32,000 sessions, which is 5.9% higher than the previous 60 days. In the second half of the expedition, sessions increased by 12% and website page views were up 7%.

The onboard outreach officer conducted short interviews with 12 of the scientists and combined these with a few photos to package up audiograms (short snippets of sound about science). In addition to 12 audiograms in English, six of the scientists repeated their stories in one or two additional languages. The Education and Outreach Officer shared the audiograms on Twitter and Facebook and then collected them all into two blog posts so they would be available in one place in the future. Most English audiograms included captions to increase accessibility.

The onboard outreach officer also filed a radio and web story for The Public's Radio in Providence, Rhode Island, featuring the two scientists from Brown University and presenting the paleoclimate objectives of the Expedition. The Public's Radio shared that story in a Twitter thread as well. An additional story is planned for WHYY's The Pulse, a radio show and podcast distributed nationally in the United States. The Children's Hour, a radio show that airs on 135 stations and in six countries, joined a live ship-to-shore and plans to use the audio from the tour and the Q&A in a production that will air in February and will also be available as a podcast.

6.3. Social media

The Education and Outreach Officers maintained four websites during the expedition: Twitter, Facebook, Instagram, and the *JOIDES Resolution* Expedition 397 webpage. From October 13 to December 11, over 70 posts were made to Twitter, resulting in over 208,000 impressions, 6,000 engagements, 2,900 likes, 500 retweets, and 60 replies. The Twitter account gained almost 700 new followers. More than 50 posts were made to Facebook, reaching over 44,000 people and resulting in over 2,500 engagements. The Facebook account gained 56 new followers. Over 30 posts were made to Instagram, reaching almost 6,000 people and garnering almost 1,500 engagements. The Instagram account gained 68 new followers.

6.4. Onshore outreach

With the goal of expanding education and outreach activities to engage a broader audience, Expedition 397 piloted a new format for onshore outreach. Given that this expedition departed from the port of Lisbon, all drilling sites were located not far off the coast of Portugal, and one of the Co-Chief Scientists works in Portugal, significant consideration was dedicated to outreach in Portugal. From October 11 through October 28, the onshore Education and Outreach Officer traveled to ten schools (nine secondary schools and one primary school) around the country, interacting with over 1100 students and teachers. School visits consisted of an introductory presentation in Portuguese, teaching participants about the International Ocean Discovery Program, *JOIDES Resolution*, and Expedition 397, followed by hands-on activities in which students learned about lithology, micropaleontology, and scientific ocean drilling procedures. All materials were provided in Portuguese and were adapted to fit the specific needs of each group.

Additionally, the onshore Education and Outreach Officer hosted two webinars for teachers affiliated with the Associação Portuguesa de Geólogos, reaching a total of approximately 60 educators around the country. Onshore outreach efforts resulted in over 30 ship-to-shore events that connected the *JOIDES Resolution* to students in Portugal.

6.5. Educational materials

To provide enduring access to Expedition 397 science, the onshore Education and Outreach Officer is developing a series of digital resources to be used in formal and informal educational settings, based on the activities that were provided during in-school visits in Portugal. The goal of

these materials is not only to immerse students in the science of the expedition, but to make science accessible for students historically underrepresented in the field. These resources include lessons to help students develop fundamental science skills and inquiry-based investigations to engage students in an authentic process of science. The lessons will be fully digital, which will allow teachers to modify them as necessary to fit their students' needs, and will be appropriate for the postpandemic classroom.

References

- Abrantes, F., 1988. Diatom assemblages as upwelling indicators in surface sediments off Portugal. Marine Geology, 85(1):15–39. https://doi.org/10.1016/0025-3227(88)90082-5
- Abrantes, F., 1991. Increased upwelling off Portugal during the last glaciation: diatom evidence. Marine Micropaleontology, 17(3–4):285–310. https://doi.org/10.1016/0377-8398(91)90017-Z
- Abrantes, F., and Moita, T., 1999. Water column and recent sediment data on diatoms and coccolithophorids, off Portugal, confirm sediment record of upwelling events. Oceanologica Acta, 22:319–336. https://doi.org/10.1016/S0399-1784(99)90007-5
- Abrantes, F., 2000. 200,000 yr diatom records from Atlantic upwelling sites reveal maximum productivity during LGM and a shift in phytoplankton community structure at 185 000 yr. Earth and Planetary Science Letters, 176(1):7–16. https://doi.org/10.1016/S0012-821X(99)00312-X
- Abrantes, F., Rodrigues, T., Ventura, C., Santos, C., Roell, U., Voelker, A., and Hodell, D., 2017. Past productivity conditions off SW Iberia at the transition from the 41 ky to the 100 ky world: the record of IODP Sites U1385 and U1391. Geophysical Research Abstracts, 19:EGU2017-9743.
 - https://meetingorganizer.copernicus.org/EGU2017/EGU2017-9743.pdf
- Abrantes, F., Baas, J., Haflidason, H., Rasmussen, T., Klitgaard, D., Loncaric, N., and Gaspar, L., 1998. Sediment fluxes along the northeastern European margin: inferring hydrological changes between 20 and 8 kyr. Marine Geology, 152(1–3):7–23. https://doi.org/10.1016/S0025-3227(98)00062-0
- Adkins, J.F., 2013. The role of deep ocean circulation in setting glacial climates. Paleoceanography and Paleoclimatology, 28(3):539–561. https://doi.org/10.1002/palo.20046
- Alley, R.B., 2003. Raising paleoceanography. Paleoceanography and Paleoclimatology, 18(4):1085. https://doi.org/10.1029/2003PA000942
- Alley, R.B., 2007. Wally was right: predictive ability of the North Atlantic "conveyor belt" hypothesis for abrupt climate change. Annual Review of Earth and Planetary Sciences, 35(1):241–272. https://doi.org/10.1146/annurev.earth.35.081006.131524
- Alonso-Garcia, M., Sierro, F.J., and Flores, J.A., 2011. Arctic front shifts in the subpolar North Atlantic during the mid-Pleistocene (800–400 ka) and their implications for ocean circulation. Palaeogeography, Palaeoclimatology, Palaeoecology, 311(3):268–280. https://doi.org/10.1016/j.palaeo.2011.09.004
- Ambar, I., and Howe, M.R., 1979. Observations of the Mediterranean outflow—II. The deep circulation in the vicinity of the Gulf of Cadiz. Deep Sea Research, Part A: Oceanographic Research Papers, 26(5):555–568. https://doi.org/10.1016/0198-0149(79)90096-7
- Ambar, I., Serra, N., Brogueira, M.J., Cabeçadas, G., Abrantes, F., Freitas, P., Gonçalves, C., and Gonzalez, N., 2002. Physical, chemical and sedimentological aspects of the Mediterranean outflow off Iberia. Deep Sea Research, Part II: Topical Studies in Oceanography, 49(19):4163–4177. https://doi.org/10.1016/S0967-0645(02)00148-0
- Andrews, J., Barber, D., and Jennings, A., 1999. Errors in generating time-series and in dating events at Late Quaternary millenial (radiocarbon) time-scales: examples from Baffin Bay, NW Labrador Sea, and east Greenland. In Clark, P.U., Webb, R.S., and Keigwin, L.D. (Eds.), Mechanisms of Global Climate Change at Millennial Time Scales. Geophysical Monograph, 112: 23–33. https://doi.org/10.1029/GM112p0023
- Baas, J.H., Mienert, J., Abrantes, F., and Prins, M.A., 1997. Late Quaternary sedimentation on the Portuguese continental margin: climate-related processes and products. Palaeogeography, Palaeoclimatology, Palaeoecology, 130(1–4):1–23. https://doi.org/10.1016/S0031-0182(96)00135-6
- Bajo, P., Drysdale, R.N., Woodhead, J.D., Hellstrom, J.C., Hodell, D., Ferretti, P., Voelker, A.H.L., Zanchetta, G., Rodrigues, T., Wolff, E., Tyler, J., Frisia, S., Spötl, C., and Fallick, A.E., 2020. Persistent influence of obliquity on ice age terminations since the middle Pleistocene transition. Science, 367(6483):1235–1239. https://doi.org/10.1126/science.aaw1114
- Barker, S., Chen, J., Gong, X., Jonkers, L., Knorr, G., and Thornalley, D., 2015. Icebergs not the trigger for North Atlantic cold events. Nature, 520(7547):333–336. https://doi.org/10.1038/nature14330
- Barker, S., and Knorr, G., 2021. Millennial scale feedbacks determine the shape and rapidity of glacial termination. Nature Communications, 12(1):2273. https://doi.org/10.1038/s41467-021-22388-6
- Barker, S., Knorr, G., Edwards, R.L., Parrenin, F., Putnam, A.E., Skinner, L.C., Wolff, E., and Ziegler, M., 2011. 800,000 years of abrupt climate variability. Science, 334(6054):347–351. https://doi.org/10.1126/science.1203580
- Barker, S., Zhang, X., Jonkers, L., Lordsmith, S., Conn, S., and Knorr, G., 2021. Strengthening Atlantic inflow across the mid-Pleistocene transition. Paleoceanography and Paleoclimatology, 36(4):e2020PA004200. https://doi.org/10.1029/2020PA004200
- Bereiter, B., Fischer, H., Schwander, J., and Stocker, T.F., 2014. Diffusive equilibration of N₂, O₂ and CO₂ mixing ratios in a 1.5-million-years-old ice core. The Cryosphere, 8(1):245–256. https://doi.org/10.5194/tc-8-245-2014
- Billups, K., and Scheinwald, A., 2014. Origin of millennial-scale climate signals in the subtropical North Atlantic. Pale-oceanography and Paleoclimatology, 29(6):612–627. https://doi.org/10.1002/2014PA002641

- Birner, B., Hodell, D.A., Tzedakis, P.C., and Skinner, L.C., 2016. Similar millennial climate variability on the Iberian margin during two early Pleistocene glacials and MIS 3. Paleoceanography and Paleoclimatology, 31(1):203–217. https://doi.org/10.1002/2015PA002868
- Blaauw, M., 2012. Out of tune: the dangers of aligning proxy archives. Quaternary Science Reviews, 36:38–49. https://doi.org/10.1016/j.quascirev.2010.11.012
- Blunier, T., and Brook, E.J., 2001. Timing of millennial-scale climate change in Antarctica and Greenland during the last glacial period. Science, 291(5501):109–112. https://doi.org/10.1126/science.291.5501.109
- Brambilla, E., Talley, L.D., Robbins, P.E., 2008. Subpolar mode water in the northeastern Atlantic: 2. Origin and transformation. J. Geophys. Res. 113. https://doi.org/10.1029/2006JC004063
- Cheng, H., Edwards, R.L., Broecker, W.S., Denton, G.H., Kong, X., Wang, Y., Zhang, R., and Wang, X., 2009. Ice age terminations. Science, 326(5950):248–252. https://doi.org/10.1126/science.1177840
- de Abreu, L., Shackleton, N.J., Schönfeld, J., Hall, M., and Chapman, M., 2003. Millennial-scale oceanic climate variability off the western Iberian margin during the last two glacial periods. Marine Geology, 196(1–2):1–20. https://doi.org/10.1016/S0025-3227(03)00046-X
- Denton, G.H., Anderson, R.F., Toggweiler, J.R., Edwards, R.L., Schaefer, J.M., and Putnam, A.E., 2010. The last glacial termination. Science, 328(5986):1652–1656. https://doi.org/10.1126/science.1184119
- Dome Fuji Ice Core Project Members, 2017. State dependence of climatic instability over the past 720,000 years from Antarctic ice cores and climate modeling. Science Advances, 3(2):e1600446. https://doi.org/10.1126/sciadv.1600446
- Expedition 339 Scientists, 2013a. Expedition 339 summary. In Stow, D.A.V., Hernández-Molina, F.J., Alvarez Zarikian, C.A., and the Expedition 339 Scientists, Proceedings of the Integrated Ocean Drilling Program. 339: Tokyo (Integrated Ocean Drilling Program Management International, Inc.). https://doi.org/10.2204/iodp.proc.339.101.2013
- Expedition 339 Scientists, 2013b. Site U1385. In Stow, D.A.V., Hernández-Molina, F.J., Alvarez Zarikian, C.A., and the Expedition 339 Scientists, Proceedings of the Integrated Ocean Drilling Program. 339: Tokyo (Integrated Ocean Drilling Program Management International, Inc.). https://doi.org/10.2204/iodp.proc.339.103.2013
- Fischer, H., Severinghaus, J., Brook, E., Wolff, E., Albert, M., Alemany, O., Arthern, R., Bentley, C., Blankenship, D., Chappellaz, J., Creyts, T., Dahl-Jensen, D., Dinn, M., Frezzotti, M., Fujita, S., Gallee, H., Hindmarsh, R., Hudspeth, D., Jugie, G., Kawamura, K., Lipenkov, V., Miller, H., Mulvaney, R., Parrenin, F., Pattyn, F., Ritz, C., Schwander, J., Steinhage, D., van Ommen, T., and Wilhelms, F., 2013. Where to find 1.5 million yr old ice for the IPICS "oldest-ice" ice core. Climate of the Past, 9(6):2489–2505. https://doi.org/10.5194/cp-9-2489-2013
- Fiúza, A., 1984. Hidrologia e Dinâmica das Águas Costeiras de Portugal [PhD dissertation]. Universidade de Lisboa, Portugal.
- Fiúza, A.F.G., Hamann, M., Ambar, I., Díaz del Río, G., González, N., and Cabanas, J.M., 1998. Water masses and their circulation off western Iberia during May 1993. Deep Sea Research, Part I: Oceanographic Research Papers, 45(7):1127–1160. https://doi.org/10.1016/S0967-0637(98)00008-9
- Gherardi, J.-M., Labeyrie, L., McManus, J.F., Francois, R., Skinner, L.C., and Cortijo, E., 2005. Evidence from the northeastern Atlantic Basin for variability in the rate of the meridional overturning circulation through the last deglaciation. Earth and Planetary Science Letters, 240(3–4):710–723. https://doi.org/10.1016/j.epsl.2005.09.061
- Haynes, R., Barton, E.D., Pilling, I., 1993. Development, persistence and variability of upwelling filaments off the Atlantic coast of Iberian Peninsula. J. Geophys. Res. 98, 22681–22692.
- Henry, L.G., McManus, J.F., Curry, W.B., Roberts, N.L., Piotrowski, A.M., and Keigwin, L.D., 2016. North Atlantic ocean circulation and abrupt climate change during the last glaciation. Science, 353(6298):470–474. https://doi.org/10.1126/science.aaf5529
- Hernández-Molina, F.J., Stow, D.A.V., Alvarez-Zarikian, C.A., Acton, G., Bahr, A., Balestra, B., Ducassou, E., Flood, R., Flores, J.-A., Furota, S., Grunert, P., Hodell, D., Jimenez-Espejo, F., Kim, J.K., Krissek, L., Kuroda, J., Li, B., Llave, E., Lofi, J., Lourens, L., Miller, M., Nanayama, F., Nishida, N., Richter, C., Roque, C., Pereira, H., Sanchez Goñi, M.F., Sierro, F.J., Singh, A.D., Sloss, C., Takashimizu, Y., Tzanova, A., Voelker, A., Williams, T., and Xuan, C., 2014. Onset of Mediterranean outflow into the North Atlantic. Science, 344(6189):1244–1250. https://doi.org/10.1126/science.1251306
- Hilgen, F.J., 1991. Astronomical calibration of Gauss to Matuyama sapropels in the Mediterranean and implication for the Geomagnetic Polarity Time Scale. Earth and Planetary Science Letters, 104(2–4):226–244. https://doi.org/10.1016/0012-821X(91)90206-W
- Hodell, D., Crowhurst, S., Lourens, L., Margari, V., Nicolson, J., Rolfe, J.E., Skinner, L.C., Thomas, N., Tzedakis, P.C., Mleneck-Vautravers, M.J., and Wolff, E.W., preprint. A 1.5-million-year record of orbital and millennial climate variability in the North Atlantic. Climate of the Past, 2022. https://doi.org/10.5194/cp-2022-61
- Hodell, D., Crowhurst, S., Skinner, L., Tzedakis, P.C., Margari, V., Channell, J.E.T., Kamenov, G., Maclachlan, S., and Rothwell, G., 2013a. Response of Iberian margin sediments to orbital and suborbital forcing over the past 420 ka. Paleoceanography and Paleoclimatology, 28(1):185–199. https://doi.org/10.1002/palo.20017
- Hodell, D. A., Elderfield, H., Greaves, M., McCave, I. N., Skinner, L., Thomas, A., & White, N., 2014. The JC089 scientific party, JC089 cruise report—IODP site survey of the Shackleton sites, SW Iberian margin, British ocean data Centre.
- Hodell, D., Lourens, L., Crowhurst, S., Konijnendijk, T., Tjallingii, R., Jiménez-Espejo, F., Skinner, L., Tzedakis, P.C., and the Shackleton Site Project Members, 2015. A reference time scale for Site U1385 (Shackleton Site) on the SW Iberian Margin. Global and Planetary Change, 133:49–64. https://doi.org/10.1016/j.gloplacha.2015.07.002
- Hodell, D.A., Lourens, L., Stow, D.A.V., Hernández-Molina, F. Javier, and Alvarez-Zarikian, C.A., 2013b. The "Shackleton Site" (IODP Site U1385) on the Iberian Margin. Scientific Drilling, 16:13–19. https://doi.org/10.5194/sd-16-13-2013

- Hodell, D.A., and Channell, J.E.T., 2016. Mode transitions in Northern Hemisphere glaciation: co-evolution of millennial and orbital variability in Quaternary climate. Climate of the Past, 12(9):1805–1828. https://doi.org/10.5194/cp-12-1805-2016
- Hodell, D.A., Channell, J.E.T., Curtis, J.H., Romero, O.E., and Röhl, U., 2008. Onset of "Hudson Strait" Heinrich events in the eastern North Atlantic at the end of the middle Pleistocene transition (~640 ka)? Paleoceanography and Paleoclimatology, 23(4):PA4218. https://doi.org/10.1029/2008PA001591
- Hodell, D.A., Evans, H.F., Channell, J.E.T., and Curtis, J.H., 2010. Phase relationships of North Atlantic ice-rafted debris and surface-deep climate proxies during the last glacial period. Quaternary Science Reviews, 29(27–28):3875–3886. https://doi.org/10.1016/j.quascirev.2010.09.006
- Jenkins, W.J., Smethie, W.M., Boyle, E.A., and Cutter, G.A., 2015. Water mass analysis for the U.S. GEOTRACES (GA03) North Atlantic sections. Deep Sea Research, Part II: Topical Studies in Oceanography, 116:6–20. https://doi.org/10.1016/j.dsr2.2014.11.018
- Jouzel, J., Masson-Delmotte, V., Cattani, O., Dreyfus, G., Falourd, S., Hoffmann, G., Minster, B., Nouet, J., Barnola, J.M., Chappellaz, J., Fischer, H., Gallet, J.C., Johnsen, S., Leuenberger, M., Loulergue, L., Luethi, D., Oerter, H., Parrenin, F., Raisbeck, G., Raynaud, D., Schilt, A., Schwander, J., Selmo, E., Souchez, R., Spahni, R., Stauffer, B., Steffensen, J.P., Stenni, B., Stocker, T.F., Tison, J.L., Werner, M., and Wolff, E.W., 2007. Orbital and millennial Antarctic climate variability over the past 800,000 years. Science, 317(5839):793–796. https://doi.org/10.1126/science.1141038
- Karanovic, I., and Brandão, S.N., 2015. Biogeography of deep-sea wood fall, cold seep and hydrothermal vent Ostracoda (Crustacea), with the description of a new family and a taxonomic key to living Cytheroidea. Deep Sea Research Part II: Topical Studies in Oceanography, Volume 111. https://doi.org/10.1016/j.dsr2.2014.09.008
- Kawamura, K., Parrenin, F., Lisiecki, L., Uemura, R., Vimeux, F., Severinghaus, J.P., Hutterli, M.A., Nakazawa, T., Aoki, S., Jouzel, J., Raymo, M.E., Matsumoto, K., Nakata, H., Motoyama, H., Fujita, S., Goto-Azuma, K., Fujii, Y., and Watanabe, O., 2007. Northern Hemisphere forcing of climatic cycles in Antarctica over the past 360,000 years. Nature, 448(7156):912–916. https://doi.org/10.1038/nature06015
- Kissel, C., Laj, C., Piotrowski, A.M., Goldstein, S.L., and Hemming, S.R., 2008. Millennial-scale propagation of Atlantic deep waters to the glacial Southern Ocean. Paleoceanography and Paleoclimatology, 23(2):PA2102. https://doi.org/10.1029/2008PA001624
- Konijnendijk, T.Y.M., Ziegler, M., and Lourens, L.J., 2015. On the timing and forcing mechanisms of late Pleistocene glacial terminations: insights from a new high-resolution benthic stable oxygen isotope record of the eastern Mediterranean. Quaternary Science Reviews, 129:308–320. https://doi.org/10.1016/j.quascirev.2015.10.005
- Lebreiro, S.M., McCave, I.N., and Weaver, P.P.E., 1997. Late Quaternary turbidite emplacement on the Horseshoe abyssal plain (Iberian margin). Journal of Sedimentary Research, 67(5):856–870. https://doi.org/10.1306/D4268658-2B26-11D7-8648000102C1865D
- Lebreiro, S.M., Voelker, A.H.L., Vizcaino, A., Abrantes, F.G., Alt-Epping, U., Jung, S., Thouveny, N., and Gràcia, E., 2009. Sediment instability on the Portuguese continental margin under abrupt glacial climate changes (last 60 kyr). Quaternary Science Reviews, 28(27–28):3211–3223. https://doi.org/10.1016/j.quascirev.2009.08.007
- Lisiecki, L.E., and Raymo, M.E., 2005. A Pliocene-Pleistocene stack of 57 globally distributed benthic δ^{18} O records. Paleoceanography, 20(1):PA1003. https://doi.org/10.1029/2004PA001071
- Magill, C.R., Ausín, B., Wenk, P., McIntyre, C., Skinner, L., Martínez-García, A., Hodell, D.A., Haug, G.H., Kenney, W., and Eglinton, T.I., 2018. Transient hydrodynamic effects influence organic carbon signatures in marine sediments. Nature Communications, 9(1):4690. https://doi.org/10.1038/s41467-018-06973-w
- Margari, V., Skinner, L.C., Hodell, D.A., Martrat, B., Toucanne, S., Grimalt, J.O., Gibbard, P.L., Lunkka, J.P., and Tzedakis, P.C., 2014. Land-ocean changes on orbital and millennial time scales and the penultimate glaciation. Geology, 42(3):183–186. https://doi.org/10.1130/G35070.1
- Margari, V., Skinner, L.C., Menviel, L., Capron, E., Rhodes, R.H., Mleneck-Vautravers, M.J., Ezat, M.M., Martrat, B., Grimalt, J.O., Hodell, D.A., and Tzedakis, P.C., 2020. Fast and slow components of interstadial warming in the North Atlantic during the last glacial. Communications Earth & Environment, 1(1):6. https://doi.org/10.1038/s43247-020-0006-x
- Margari, V., Skinner, L.C., Tzedakis, P.C., Ganopolski, A., Vautravers, M., and Shackleton, N.J., 2010. The nature of millennial-scale climate variability during the past two glacial periods. Nature Geoscience, 3(2):127–131. https://doi.org/10.1038/ngeo740
- Martrat, B., Grimalt, J.O., Shackleton, N.J., Abreu, L.d., Hutterli, M.A., and Stocker, T.F., 2007. Four climate cycles of recurring deep and surface water destabilizations on the Iberian margin. Science, 317(5837):502–507. https://doi.org/10.1126/science.1139994
- Mc Intyre, K., Delaney, M.L., and Ravelo, A.C., 2001. Millennial-scale climate change and oceanic processes in the late Pliocene and early Pleistocene. Paleoceanography and Paleoclimatology, 16:535–543. https://doi.org/10.1029/2000PA000526
- McManus, J.F., Oppo, D.W., and Cullen, J.L., 1999. A 0.5-million-year record of millennial-scale climate variability in the North Atlantic. In Science. 5404, 283: 971–975. https://doi.org/10.1126/science.283.5404.971
- Meckler, A.N., Sigman, D.M., Gibson, K.A., Françoise, R., Martínez-García, A., Jaccard, S.L., Röhl, U., Peterson, L.C., Tiedermann, R., and Haug G.H., 2013. Deglacial pulses of deep-ocean silicate into the subtropical North Atlantic Ocean. Nature, 495, pp. 495-498
- Naughton, F., Costas, S., Gomes, S.D., Desprat, S., Rodrigues, T., Sanchez Goñi, M.F., Renssen, H., Trigo, R., Bronk-Ramsey, C., Oliveira, D., Salgueiro, E., Voelker, A.H.L., and Abrantes, F., 2019. Coupled ocean and atmospheric changes during Greenland stadial 1 in southwestern Europe. Quaternary Science Reviews, 212:108–120. https://doi.org/10.1016/j.quascirev.2019.03.033

- Naughton, F., Sanchez Goñi, M.F., Desprat, S., Turon, J.L., Duprat, J., Malaizé, B., Joli, C., Cortijo, E., Drago, T., and Freitas, M.C., 2007. Present-day and past (last 25000 years) marine pollen signal off western Iberia. Marine Micropaleontology, 62(2):91–114. https://doi.org/10.1016/j.marmicro.2006.07.006
- Nehrbass-Ahles, C., Shin, J., Schmitt, J., Bereiter, B., Joos, F., Schilt, A., Schmidely, L., Silva, L., Teste, G., Grilli, R., Chappellaz, J., Hodell, D., Fischer, H., and Stocker, T.F., 2020. Abrupt CO₂ release to the atmosphere under glacial and early interglacial climate conditions. Science, 369(6506):1000–1005. https://doi.org/10.1126/science.aay8178
- Oliveira, D., Desprat, S., Rodrigues, T., Naughton, F., Hodell, D., Trigo, R., Rufino, M., Lopes, C., Abrantes, F., and Sánchez Goñi, M.F., 2016. The complexity of millennial-scale variability in southwestern Europe during MIS 11. Quaternary Research, 86(3):373–387. https://doi.org/10.1016/j.yqres.2016.09.002
- Oliveira, D., Desprat, S., Yin, Q., Naughton, F., Trigo, R., Rodrigues, T., Abrantes, F., and Sánchez Goñi, M.F., 2018. Unraveling the forcings controlling the vegetation and climate of the best orbital analogues for the present interglacial in SW Europe. Climate Dynamics, 51(1):667–686. https://doi.org/10.1007/s00382-017-3948-7
- Oliveira, D., Desprat, S., Yin, Q., Rodrigues, T., Naughton, F., Trigo, R.M., Su, Q., Grimalt, J.O., Alonso-Garcia, M., Voelker, A.H.L., Abrantes, F., and Sánchez Goñi, M.F., 2020. Combination of insolation and ice-sheet forcing drive enhanced humidity in northern subtropical regions during MIS 13. Quaternary Science Reviews, 247:106573. https://doi.org/10.1016/j.quascirev.2020.106573
- Oliveira, D., Sánchez Goñi, M.F., Naughton, F., Polanco-Martinez, J.M., Jimenez-Espejo, F.J., Grimalt, J.O., Martrat, B., Voelker, A.H.L., Trigo, R., Hodell, D., Abrantes, F., and Desprat, S., 2017. Unexpected weak seasonal climate in the western Mediterranean region during MIS 31, a high-insolation forced interglacial. Quaternary Science Reviews, 161:1–17. https://doi.org/10.1016/j.quascirev.2017.02.013
- Oppo, D.W., McManus, J.F., and Cullen, J.L., 1998. Abrupt climate events 500,000 to 340,000 years ago: evidence from subpolar North Atlantic sediments. Science, 279(5355):1335–1338. https://doi.org/10.1126/science.279.5355.1335
- Peliz, A., Dubert, J., Santos, A.M.P., Oliveira, P.B., Le Cann, B., 2005. Winter upper ocean circulation in the Western Iberian Basin—fronts, eddies and poleward flows: an overview. Deep-Sea Res. I Oceanogr. Res. Pap. 52, 621–646.
- Pérez, M.E., Lin, H.-L., Lange, C.B., Schneider, R., 2001. Pliocene—Pleistocene opal records off southwest Africa, sites 1082 and 1084: a comparison of analytical techniques. In: Wefer, G., Berger, W.H., Richter, C., Proceedings of the ODP Science Results. Ocean Drilling Program. College Station, TX, pp. 1–16.
- Piotrowski, A.M., Goldstein, S.L., Hemming, S.R., Fairbanks, R.G., and Zylberberg, D.R., 2008. Oscillating glacial northern and southern deep water formation from combined neodymium and carbon isotopes. Earth and Planetary Science Letters, 272(1–2):394–405. https://doi.org/10.1016/j.epsl.2008.05.011
- Pol, K., Masson-Delmotte, V., Johnsen, S., Bigler, M., Cattani, O., Durand, G., Falourd, S., Jouzel, J., Minster, B., Parrenin, F., Ritz, C., Steen-Larsen, H.C., and Stenni, B., 2010. New MIS 19 EPICA Dome C high resolution deuterium data: hints for a problematic preservation of climate variability at sub-millennial scale in the "oldest ice". Earth and Planetary Science Letters, 298(1):95–103. https://doi.org/10.1016/j.epsl.2010.07.030
- Raymo, M.E., Ganley, K., Carter, S., Oppo, D.W., and McManus, J., 1998. Millennial-scale climate instability during the early Pleistocene epoch. Nature, 392(6677):699–702. https://doi.org/10.1038/33658
- Raymo, M.E., and Huybers, P., 2008. Unlocking the mysteries of the ice ages. Nature, 451(7176):284–285. https://doi.org/10.1038/nature06589
- Relvas, P., Luís, J., and Santos, A.M.P., 2009. Importance of the mesoscale in the decadal changes observed in the northern Canary upwelling system. Geophysical Research Letters, 36(22):L22601. http://dx.doi.org/10.1029/2009GL040504
- Rios, A.F., Perez, F.F., Fraga, F., 1992. Water masses in the Upper and Middle North-Atlantic Ocean east of the Azores. Deep Sea Res. Part A 39, 645–658.
- Rodrigues, T., Alonso-Garcia, M., Hodell, D.A., Rufino, M., Naughton, F., Grimalt, J.O., Voelker, A.H.L., and Abrantes, F., 2017. A 1-Ma record of sea surface temperature and extreme cooling events in the North Atlantic: a perspective from the Iberian Margin. Quaternary Science Reviews, 172:118–130. https://doi.org/10.1016/j.quascirev.2017.07.004
- Rodrigues, T., Voelker, A.H.L., Grimalt, J.O., Abrantes, F., and Naughton, F., 2011. Iberian margin sea surface temperature during MIS 15 to 9 (580–300 ka): glacial suborbital variability versus interglacial stability. Paleoceanography and Paleoclimatology, 26(1):PA1204. https://doi.org/10.1029/2010PA001927
- Roucoux, K.H., Shackleton, N.J., de Abreu, L., Schönfeld, J., and Tzedakis, P.C., 2001. Combined marine proxy and pollen analyses reveal rapid Iberian vegetation response to North Atlantic millennial-scale climate oscillations. Quaternary Research, 56(1):128–132. https://doi.org/10.1006/qres.2001.2218
- Salgueiro, E., Voelker, A., Abrantes, F., Meggers, H., Pflaumann, U., Lončarić, N., González-Álvarez, R., Oliveira, P., Bartels-Jónsdóttir, H.B., Moreno, J., and Wefer, G., 2008. Planktonic foraminifera from modern sediments reflect upwelling patterns off Iberia: insights from a regional transfer function. Marine Micropaleontology, 66(3–4):135–164. https://doi.org/10.1016/j.marmicro.2007.09.003
- Salgueiro, E., Voelker, A.H.L., de Abreu, L., Abrantes, F., Meggers, H., and Wefer, G., 2010. Temperature and productivity changes off the western Iberian margin during the last 150 ky. Quaternary Science Reviews, 29(5–6):680–695. https://doi.org/10.1016/j.quascirev.2009.11.013
- Sánchez Goñi, M.F., Eynaud, F., Turon, J.L., and Shackleton, N.J., 1999. High resolution palynological record off the Iberian margin: direct land-sea correlation for the Last Interglacial complex. Earth and Planetary Science Letters, 171(1):123–137. https://doi.org/10.1016/S0012-821X(99)00141-7
- Sánchez Goñi, M.F., Llave, E., Oliveira, D., Naughton, F., Desprat, S., Ducassou, E., Hodell, D.A., and Hernández Molina, F.J., 2016. Climate changes in south western Iberia and Mediterranean Outflow variations during two con-

- trasting cycles of the last 1 myrs: MIS 31-MIS 30 and MIS 12-MIS 11. Global and Planetary Change, 136:18–29. https://doi.org/10.1016/j.gloplacha.2015.11.006
- Sánchez Goñi, M.F., Turon, J.-L., Eynaud, F., and Gendreau, S., 2000. European climatic response to millennial-scale changes in the atmosphere—ocean system during the last glacial period. Quaternary Research, 54(3):394–403. https://doi.org/10.1006/qres.2000.2176
- Saunders, P.M., 1987. Flow through Discovery Gap. Journal of Physical Oceanography, 17(5):631–643. https://doi.org/10.1175/1520-0485(1987)017%3C0631:FTDG%3E2.0.CO;2
- Shackleton, N.J., Hall, M.A., and Pate, D., 1995. Pliocene stable isotope stratigraphy of Site 846. In Pisias, N.G., Mayer, L.A., Janecek, T.R., Palmer-Julson, A., and van Andel, T.H. (Eds.), Proceedings of the Ocean Drilling Program, Scientific Results. 138: College Station, TX (Ocean Drilling Program), 337–355. https://doi.org/10.2973/odp.proc.sr.138.117.1995
- Shackleton, N.J., Chapman, M., Sánchez-Goñi, M.F., Pailler, D., and Lancelot, Y., 2002. The classic Marine Isotope Substage 5e. Quaternary Research, 58(1):14–16. https://doi.org/10.1006/qres.2001.2312
- Shackleton, N.J., Fairbanks, R.G., Chiu, T.-c., and Parrenin, F., 2004. Absolute calibration of the Greenland time scale: implications for Antarctic time scales and for Δ¹⁴C. Quaternary Science Reviews, 23(14–15):1513–1522. https://doi.org/10.1016/j.quascirev.2004.03.006
- Shackleton, N.J., Hall, M.A., and Vincent, E., 2000. Phase relationships between millennial-scale events 64,000–24,000 years ago. Paleoceanography and Paleoclimatology, 15(6):565–569. https://doi.org/10.1029/2000PA000513
- Shackleton, N.J., Sánchez-Goñi, M.F., Pailler, D., and Lancelot, Y., 2003. Marine Isotope Substage 5e and the Eemian interglacial. Global and Planetary Change, 36(3):151–155. https://doi.org/10.1016/S0921-8181(02)00181-9
- Skinner, L.C., and Elderfield, H., 2007. Rapid fluctuations in the deep North Atlantic heat budget during the last glacial period. Paleoceanography and Paleoclimatology, 22(1):PA1205. https://doi.org/10.1029/2006PA001338
- Skinner, L.C., Elderfield, H., and Hall, M., 2007. Phasing of millennial climate events and northeast Atlantic deep-water temperature change since 50 Ka Bp. In Schmittner, A., Chiang, J.C.H., and Hemming, S.R. (Eds.), Ocean Circulation: Mechanisms and Impacts—Past and Future Changes of Meridional Overturning. Geophysical Monograph, 173: 197–208. https://doi.org/10.1029/173GM14
- Skinner, L.C., Freeman, E., Hodell, D., Waelbroeck, C., Vazquez Riveiros, N., and Scrivner, A.E., 2021. Atlantic Ocean ventilation changes across the last deglaciation and their carbon cycle implications. Paleoceanography and Paleoclimatology, 36(2):e2020PA004074. https://doi.org/10.1029/2020PA004074
- Skinner, L.C., and Shackleton, N.J., 2004. Rapid transient changes in northeast Atlantic deep water ventilation age across Termination I. Paleoceanography and Paleoclimatology, 19(2):PA2005. https://doi.org/10.1029/2003PA000983
- Skinner, L.C., and Shackleton, N.J., 2006. Deconstructing Terminations I and II: revisiting the glacioeustatic paradigm based on deep-water temperature estimates. Quaternary Science Reviews, 25(23–24):3312–3321. https://doi.org/10.1016/j.quascirev.2006.07.005
- Skinner, L.C., Shackleton, N.J., and Elderfield, H., 2003. Millennial-scale variability of deep-water temperature and δ¹⁸O_{dw} indicating deep-water source variations in the northeast Atlantic, 0–34 cal. ka BP. Geochemistry, Geophysics, Geosystems, 4(12):1098. https://doi.org/10.1029/2003GC000585
- Sousa, F.M., and Bricaud, A., 1992. Satellite-derived phytoplankton pigment structures in the Portuguese upwelling area. Journal of Geophysical Research: Oceans, 97(C7):11343–11356. https://doi.org/10.1029/92JC00786
- Steineck, P.L., Maddocks, R.F., Coles, G.P., and Whatley, R.C., 1990. Xylophile ostracoda in the deep sea. 307–319. In Whatley, R.C. and Maybury, C. (eds). Ostracoda and global events. Chapman and Hall, London, 621 pp
- Suc, J.P., 1984. Origin and evolution of the Mediterranean vegetation and climate in Europe. Nature, 307(5950):429–432. https://doi.org/10.1038/307429a0
- Suc, J.-P., and Popescu, S.-M., 2005. Pollen records and climatic cycles in the North Mediterranean region since 2.7 Ma. In Head, M.J., and Gibbard, P.L. (Eds.), Early-Middle Pleistocene Transitions: The Land-Ocean Evidence. Geological Society Special Publication, 247: 147–158. https://doi.org/10.1144/GSL.SP.2005.247.01.08
- Sun, Y., McManus, J.F., Clemens, S.C., Zhang, X., Vogel, H., Hodell, D.A., Guo, F., Wang, T., Liu, X., and An, Z., 2021. Persistent orbital influence on millennial climate variability through the Pleistocene. Nature Geoscience, 14(11):812–818. https://doi.org/10.1038/s41561-021-00794-1
- Tanaka, H., Lelièvre, Y. & Yasuhara, M., 2019. Xylocythere sarrazinae, a new cytherurid ostracod (Crustacea) from a hydrothermal vent field on the Juan de Fuca Ridge, northeast Pacific Ocean, and its phylogenetic position within Cytheroidea. Mar. Biodivers. 49, 2571–2586. https://doi.org/10.1007/s12526-019-00987-3
- Thomas, N.C., Bradbury, H.J., and Hodell, D.A., 2022. Changes in North Atlantic deep-water oxygenation across the Middle Pleistocene Transition. Science, 377(6606):654–659. https://doi.org/10.1126/science.abj7761
- Thurow, J., Peterson, L.C., Harms, U., Hodell, D.A., Cheshire, H., Brumsack, H.J., Irino, T., Schulz, M., Masson-Delmotte, V., and Tada, R., 2009. Acquiring high to ultra-high resolution geological records of past climate change by scientific drilling. Scientific Drilling, 8:46–56. https://doi.org/10.2204/iodp.sd.8.08.2009
- Turchyn A. V., Antler G., Byrne D., Miller M., Hodell D. A., 2016. Microbial sulfur metabolism evidenced from pore fluid isotope geochemistry at Site U1385. Glob. Planet. Change 141 82–90. https://doi.org/10.1016/j.gloplacha.2016.03.004
- Tzedakis, P.C., 2007. Seven ambiguities in the Mediterranean palaeoenvironmental narrative. Quaternary Science Reviews, 26(17):2042–2066. https://doi.org/10.1016/j.quascirev.2007.03.014
- Tzedakis, P.C., Drysdale, R.N., Margari, V., Skinner, L.C., Menviel, L., Rhodes, R.H., Taschetto, A.S., Hodell, D.A., Crowhurst, S.J., Hellstrom, J.C., Fallick, A.E., Grimalt, J.O., McManus, J.F., Martrat, B., Mokeddem, Z., Parrenin, F., Regattieri, E., Roe, K., and Zanchetta, G., 2018. Enhanced climate instability in the North Atlantic and southern Europe during the last interglacial. Nature Communications, 9(1):4235. https://doi.org/10.1038/s41467-018-06683-3

- Tzedakis, P.C., Frogley, M.R., Lawson, I.T., Preece, R.C., Cacho, I., and de Abreu, L., 2004. Ecological thresholds and patterns of millennial-scale climate variability: the response of vegetation in Greece during the last glacial period. Geology, 32(2):109–112. https://doi.org/10.1130/G20118.1
- Tzedakis, P.C., Hooghiemstra, H., and Pälike, H., 2006. The last 1.35 million years at Tenaghi Philippon: revised chronostratigraphy and long-term vegetation trends. Quaternary Science Reviews, 25(23–24):3416–3430. https://doi.org/10.1016/j.quascirev.2006.09.002
- Tzedakis, P.C., Margari, V., and Hodell, D.A., 2015. Coupled ocean-land millennial scale changes 1.26 million years ago, recorded at Site U1385 off Portugal. Global and Planetary Change, 135:83–88. https://doi.org/10.1016/j.gloplacha.2015.10.008
- Tzedakis, P.C., Pälike, H., Roucoux, K.H., and de Abreu, L., 2009. Atmospheric methane, southern European vegetation and low-mid latitude links on orbital and millennial timescales. Earth and Planetary Science Letters, 277(3–4):307–317. https://doi.org/10.1016/j.epsl.2008.10.027
- van Aken, H.M., 2000. The hydrography of the mid-latitude Northeast Atlantic Ocean: II: the intermediate water masses. Deep Sea Research, Part I: Oceanographic Research Papers, 47(5):789–824. https://doi.org/10.1016/S0967-0637(99)00112-0
- Vanney, J.-R., and Mougenot, D., 1981. La plate-forme continentale du Portugal et les provinces adjacentes: analyse geomorphologique. Mem. Serv. Geol. Portugal, 28.
- Verbitsky, M. Y., Crucifix, M., and Volobuev, D. M., 2018. A theory of Pleistocene glacial 1908 rhythmicity, Earth System Dynamics, 9, 1025–1043.
- WAIS Divide Project Members, 2015. Precise interpolar phasing of abrupt climate change during the last ice age. Nature, 520(7549):661–665. https://doi.org/10.1038/nature14401
- Weirauch, D., Billups, K., and Martin, P., 2008. Evolution of millennial-scale climate variability during the mid-Pleistocene. Paleoceanography and Paleoclimatology, 23(3):PA3216. https://doi.org/10.1029/2007PA001584
- Willamowski, C., and Zahn, R., 2000. Upper ocean circulation in the glacial North Atlantic from benthic foraminiferal isotope and trace element fingerprinting. Paleoceanography and Paleoclimatology, 15(5):515–527. https://doi.org/10.1029/1999PA000467
- Wolff, E.W., Fischer, H., and Röthlisberger, R., 2009. Glacial terminations as southern warmings without northern control. Nature Geoscience, 2(3):206–209. https://doi.org/10.1038/ngeo442
- Wolff, E.W., Fischer, H., van Ommen, T., and Hodell, D.A., 2022. Stratigraphic templates for ice core records of the past 1.5 million years. Climate of the Past: Discussions.
- Wunsch, C., 2006. Abrupt climate change: an alternative view. Quaternary Research, 65(2):191–203. https://doi.org/10.1016/j.yqres.2005.10.006
- Zitellini, N., Gràcia, E., Matias, L., Terrinha, P., Abreu, M.A., DeAlteriis, G., Henriet, J.P., Dañobeitia, J.J., Masson, D.G., Mulder, T., Ramella, R., Somoza, L., and Diez, S., 2009. The quest for the Africa–Eurasia plate boundary west of the Strait of Gibraltar. Earth and Planetary Science Letters, 280(1–4):13–50. https://doi.org/10.1016/j.epsl.2008.12.005